

Analysis of a load frequency control implementation in Swedish run-of-river hydropower stations

Andreas Westberg



UPPSALA
UNIVERSITET

**Teknisk- naturvetenskaplig fakultet
UTH-enheten**

Besöksadress:
Ångströmlaboratoriet
Lägerhyddsvägen 1
Hus 4, Plan 0

Postadress:
Box 536
751 21 Uppsala

Telefon:
018 – 471 30 03

Telefax:
018 – 471 30 00

Hemsida:
<http://www.teknat.uu.se/student>

Abstract

Analysis of a load frequency control implementation in Swedish run-of-river hydropower stations

Andreas Westberg

The total amount of frequency deviations have during the last decade increased exponentially in the Nordic synchronous power system. The transmission system operators have therefore decided to implement load frequency control as a new automatic control system to stem these frequency deviations.

The aim of this feasibility study is to analyse the effects of an LFC implementation in Swedish hydropower stations by using a more dynamic river governing. The method chosen to analyse the effects of LFC-governing was to create a Matlab Simulink hydropower station library including dynamic modules for rivers and turbine governors. The library is then used to create a river reach that is implemented in an ENTSO-E model for the Nordic frequency reserves. The governing of the river uses economical dispatch theory to optimally distribute a LFC setpoint signal from the ENTSO-E model to the different hydropower stations.

Results show that the developed method has a future potential to create more frequency controlled reserves. By creating a central governing unit it was possible to govern frequency controlled reserves over an entire river reach under certain scenarios, but there are still many obstacles to overcome before an actual implementation. The method does however show both the possibilities and drawback of frequency controlled reserves in cascade coupled hydropower systems.

Key words: Hydropower, power system, frequency controlled reserves, load frequency control, Matlab Simulink

Handledare: Niklas Dahlbäck
Ämnesgranskare: Urban Lundin
Examinator: Kjell Pernestål
ISSN: 1650-8300, UPTEC ES12004

Populärvetenskaplig sammanfattning

Ansvar att upprätthålla effektbalansen i det nordiska synkrona elnätet har tilldelats till Svenska Kraftnät och dess nordiska motsvarigheter. Denna balansreglering sker kontinuerligt genom primärreglering i olika vattenkraftsstationer runtom i nordens. En direkt återkoppling på hur väl detta sköts kan ses genom den elektriska frekvensen i elnäten som är intimt sammankopplad med effektbalansen i näten.

Under det senaste decenniet har de ackumulerade avvikelserna från den nominella frekvensen 50 Hz ökat exponentiellt från 200 minuter/månad till 1000 minuter/månad. Detta tillförs att kraven på reglerförmågan inte har reviderats de senaste tio åren medan elmarknaden och resterande kraftsystem har utvecklats enormt. Med den fortsatta utvecklingen av elmarknaden och kraftsystemet med mer intermittent produktion (främst vind, våg, sol) och fler HVDC-kopplingar till kontinenten tros detta bli än värre. Ett projekt tillsattes därför inom *European Network for Transmission System Operators for Electricity (ENTSO-E)* för att utreda hur reglerförmågan skall utvecklas. En slutsats i projektet var att införandet Load Frequency Control (LFC) reglering kan vara en framtida möjlighet för att stävja frekvensavvikelserna. (ENTSO-E 2011a)

Projektmålet från Svenska Kraftnät blev därmed att som en förstudie analysera om LFC, som automatisk reserv, kan åläggas på svenska vattenkraftverk? För detta krävs en mer dynamisk driftläggning, speciellt i älvsträckor innehållandes vattenkraftverk med små reglermöjligheter i dess magasin.

Metoden som använts är att genom att skapa ett vattenkraftsbibliotek i *Matlab Simulink* kan en älvsträcka byggas upp och sedan implementeras som en genereringsmodul i en ENTSO-E modell för den nordiska reglerförmågan. Därefter utvecklades en regulator för att fördela ett externt reglerbehov genom att vikta effekttreglering mot vattenansamling i system. Denna regulator behövs för att samreglera alla kraftverk i älvsträckan på en mycket kortare tidsskala än vad som görs i dagsläget och på det viset ha bättre kontroll över de vattenmassor som rör sig i systemet. Genom en implementering i ENTSO-E modellen har den aktuella älvsträckan kunnat simuleras för att se hur den kan bidra till effektbalansen och frekvenshållningen.

Resultaten visar att genom att skapa den överliggande regulatorn, som fördelar en central reglersignal, skulle älvsträckor som idag ej bidrar med frekvenshållande reserver kunna göra det i framtiden. Mycket kvarstår att förbättra innan systemet kan bli operativt men den övergripande metoden visar både på möjligheterna och problemen med kaskadkopplade kraftverk.

Trevlig läsning.

Contents

- 1 Introduction..... 5
 - 1.1 Project aim 5
 - 1.2 Method 5
 - 1.3 Limitation in scope 5
- 2 Background..... 7
 - 2.1 Energy markets..... 7
 - 2.2 Frequency quality 7
 - 2.3 Frequency regulation reserves 9
 - 2.4 Hydropower..... 10
- 3 Theory..... 13
 - 3.1 Hydropower..... 13
 - 3.2 Frequency control systems..... 18
- 4 Method and Model development 21
 - 4.1 ENTSO-E model..... 22
 - 4.1 Hydro Power station..... 24
 - 4.2 LFC – distribution module 32
 - 4.3 Economical gains and losses from LFC sales 39
- 5 Simulations 40
 - 5.1 River reaches 40
 - 5.2 Simulation setup..... 41
 - 5.3 Results 42
- 6 Discussion 53
 - 6.1 Model implementation 53
 - 6.2 Results 57
 - 6.3 Project aim..... 60
- 7 Conclusions..... 61
- References 62
- Appendix..... 64
 - A – Model Modules 64
 - B – Initiation files/values 71
 - C – Simulation results..... 81

1 Introduction

The Nordic transmission system operators (TSOs) have defined the acceptable frequency operational band as 50.00 +/- 0.100 Hz. The accumulated frequency deviation's outside this range have during the last decade increased drastically and are threatening the operational stability of the system. The Nordic TSOs have therefore initiated studies to analyze the possibilities of increasing the reserve capabilities in the synchronous system. This is made by partly studying if the total amount of MW's of the current automatic frequency controlled reserves should be increased or if different time constants can be used within in the turbine governors. In addition, a new type of automatic reserve, load frequency control (LFC) is also studied to see if it can be implemented in the Nordic synchronous system.

1.1 Project aim

The project aim is to study the effects of how automatic LFC will affect the governing of a river reach with hydropower. This shall be done by studying a river's dynamic behaviour with respect to future needs of more automatic reserves by addressing the overall question:

-Can more reserves be created by using a more dynamic river governing?

The project shall also:

- Demonstrate the effects of LFC regulation on a river reach, by creating examples where the overall governing of the river remains unchanged.
- Analyse hydropower station's capacity to maintain frequency controlled reserves if more frequency restoration reserves are put on the hydropower system during low load operation.
- Analyse if any general requirements can be made for hydropower stations of a certain size to be able to contribute to the automatic LFC system.

1.2 Method

In this project a *Matlab Simulink library* consisting of a hydropower station will be created. This shall be used to create models for different river reaches that will be implemented in a model for the Nordic frequency reserves created by the *European Network for Transmission System Operators for Electricity (ENTSO-E)*. The ENTSO-E model will create a LFC setpoint signal for the river reach that is then optimally distributed to the different hydropower stations of the river reach. The results are specifically to be used to analyze differences during operation with and without the LFC system.

It's the intent to use a simulation environment to both create examples and answer the questions raised in the project aim.

1.3 Limitation in scope

To fulfil the project aim and method within the required time limit some general limitations have been imposed on the study. These were coordinated with Svenska Kraftnät (SvK) as the project owner and Vattenfall as the project supervisor with the following result. These limitations and their consequences will be discussed in 6.1.1 Assumptions and restrictions.

- 1 The system will only analyze hydropower stations connected in series, not in parallel.

- 2 Only incoming water flow from a hydropower station upstream will be used as incoming flow for the next hydropower station. Thereby all other flows are treated as non-existent.
- 3 Only a static discharge plan per hydropower station and simulation will be used.
- 4 The reservoir is treated as a rectangular box, without wave properties, where only the stored water volume is of interest.
- 5 All turbines and generators within a hydropower station are aggregated to one turbine-generator with the overall characteristics from each turbine-generator within the station.
- 6 On aspects concerning the power grid and power flows, only active power flows will be analysed. Thereby other influences such as reactive power and bottle neck effects are omitted.
- 7 The hydropower stations in the river reach will only place LFC bids of a total of +/- 10 MW and will always plays the cheapest regulation bid.

2 Background

This master's thesis was initiated as a result from the project *Analysis and Review of Requirements for Automatic Reserves in the Nordic Synchronous System*, in which future automatic frequency control reserves are investigated by the Nordic TSOs. One conclusion from this project was that implementation of 400 MW *LFC reserves* would be more efficient in increasing the frequency quality than another 400 MW of *frequency controlled normal reserves*. (ENTSO-E 2011a, sec.2.4)

With the conclusion that the power system can benefit from 400 MW LFC reserves, it was decided that it was in the interest of the TSOs and hydropower owners to see what the effects would be on river reaches containing hydropower stations with small reservoir regulation capacities and volumes, so called *run-of-river* hydropower stations.

The following sections will now give a brief description of factors influencing the grid frequency and also a general outlay of hydropower stations.

2.1 Energy markets

The Nordpool energy market was opened on January 1st 1996 for trading with electrical energy in Sweden and Norway. Following this Finland, Denmark and Estonia were also included later on. Trading on Nordpool is made through two different markets; one financial and one physical. The physical market is then also subdivided between day-ahead trading (Nordpool Spot market) and intra-day trading (Nordpool Elbas market). Both of these markets trade energy in blocks of MWh/h, energy is thus traded hour by hour.(Nordpool AS 2011)

During the operational hour, the Nordic TSOs have the judicial responsibility for stability of the system. The main tools for maintaining the momentary power and energy balance within the power system are *frequency controlled normal reserves (FNR)*, *frequency controlled disturbance reserves (FDR)* and *manual secondary frequency reserves (Fast active disturbance reserves)*. (ENTSO-E 2007, chap. Appendix 2)

2.2 Frequency quality

In order to maintain the grid frequency at 50.00 +/-0.100 Hz that has been set as the normal operational frequency band by the Nordic TSOs (ENTSO-E 2007, kap. Appendix 3), there needs to be a balance between the produced and consumed power. To keep the frequency within operational guidelines, the TSOs' have frequency controlled reserves at their disposals, these will be explained in the next section. When a power disturbance occurs within the system that the frequency controlled reserves cannot compensate for hastily enough, a frequency deviation outside the normal operational band may occur. This is defined as when the frequency deviates outside the normal operation band of 50.00 +/- 0.100 Hz. During the last ten years the accumulated deviations have increased drastically which can be seen in Figure 1.

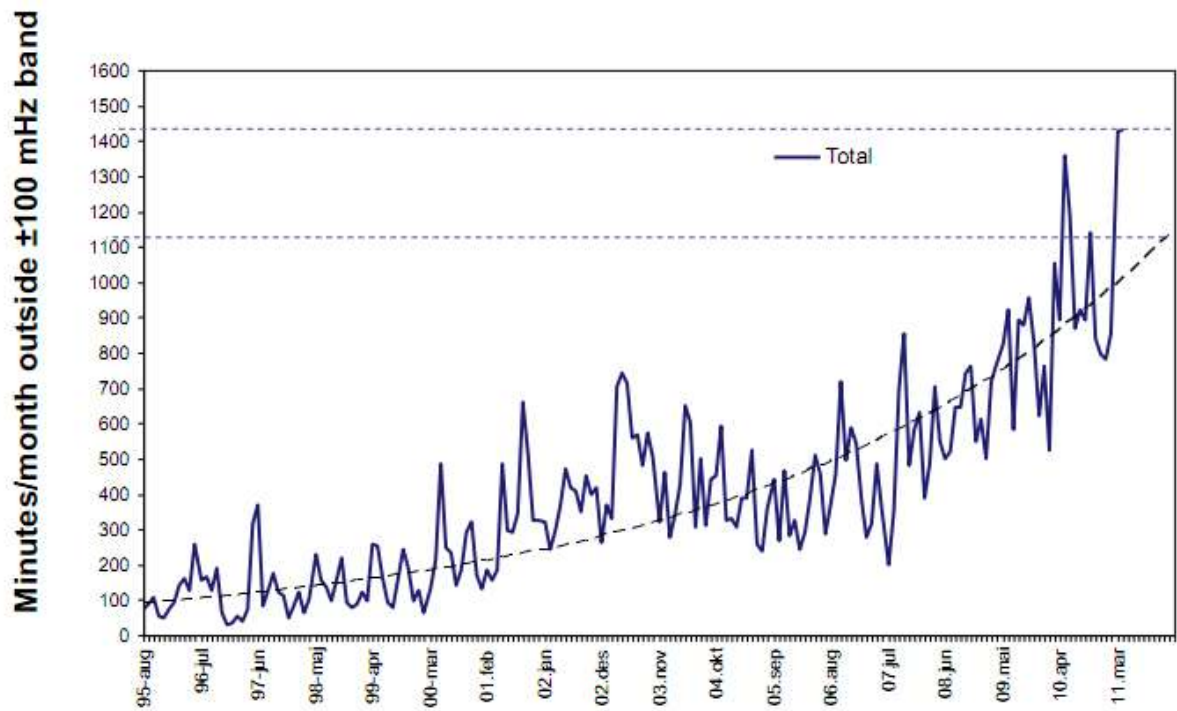


Figure 1: Frequency deviation in minutes/month in the NORDIC synchronous system from august 1995 to march 2011 (ENTSO-E 2011a, fig.3)

There is also a correlation between the inter-hour shifts and frequency deviations which are believed to be correlated to the Nordpool market where energy is traded over the entire hour, see Figure 2.

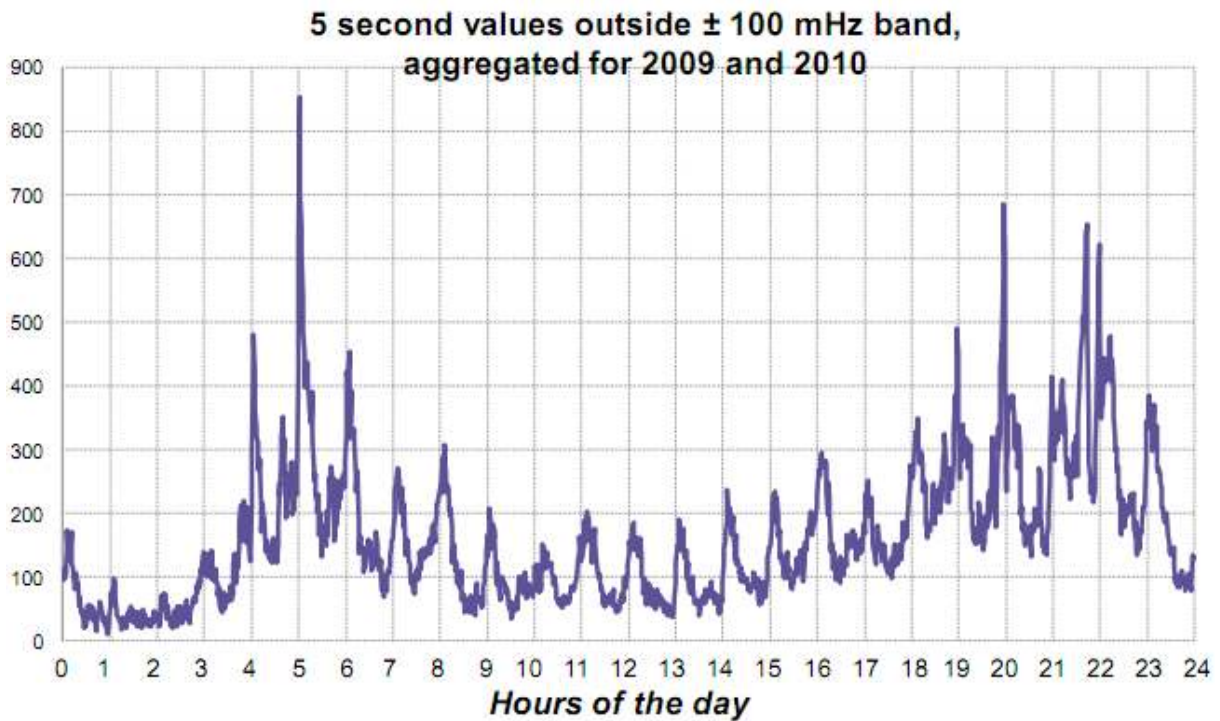


Figure 2: Aggregated 5 second frequency deviations over the period 2009-2010 displayed as a function of the time of the day. (ENTSO-E 2011a, fig.4)

2.3 Frequency regulation reserves

Within the NORDIC system there are today three main tools used for maintaining grid frequency; primary control reserves (FNR and FDR) and secondary manual control reserves. In the future, automatic *load frequency control* system will replace the manual control reserves as secondary reserves and the manual control reserves will then become tertiary reserves. These reserves are designed to complement each other by restoring each other in successive order of descent as can be seen in Figure 3.

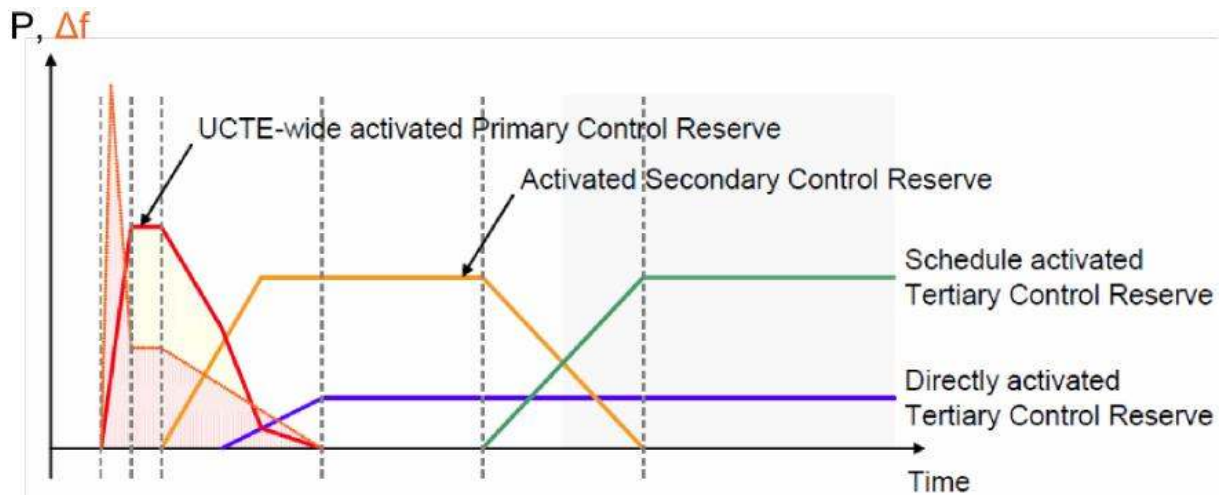


Figure 3: Order of restoration shown with a frequency deviation (Δf) and regulated power (P) from each respective reserve. (UCTE 2009, fig.3)¹

Within the *European Network for Transmission System Operators for Electricity* (ENTSO-E), a new definition has been created to replace the abbreviation for primary regulation reserves (FNR and FDR) with *frequency containment reserves (FCR)* and the same goes for the secondary and tertiary reserves which are called *frequency restoration reserves (FRR)*. These ENTSO-E definitions will from now on be used in this thesis.

Within the NORDIC system, FCR is mainly provided by hydropower plants since these reserves need short time constants to operate efficiently. In short, FCR can be described as reserves maintaining the power balance within the system while the FRR maintains the rotational energy balance and absolute time deviation that occurs from accumulated frequency deviations.

2.3.1 Frequency Containment Reserves (primary reserves) – FNR and FDR

The FCR in the NORDIC system consists of *frequency controlled normal operation reserves (FNR)* and *frequency controlled disturbance reserves (FDR)* and are both bought in [MW] by the Nordic TSO on a daily and hourly basis. They are both automatic reserves implemented on turbine governors individually², with FNR being active within the normal operational band of 50.00 +/- 0.100 Hz and FDR within 49.9-49.5 Hz. It shall be stated though that it is up to each individual power company to decide if they wish to deliver these frequency reserves to the NORDIC market. Turbine governor requirements for FNR are that the proportional gain should be at least 2 % and the equivalent time

¹ UCTE - *Union for Coordination of the Transmission of Electricity* and is now part of ENTSO-E – *European Network for Transmission System Operators for Electricity*

² Generators with a capacity greater than 25 MW are required to have turbine-governors that can provide FNR. Exceptions are made for wind turbines and nuclear power plants. (Bäck 2011)

constant shall not be greater than 60 s. For FDR, the turbine governor requirement is that for a momentary frequency deviation to 49.500 Hz then 50 % should be regulated within 5 s and fully regulated within 30 s. The Nordic TSOs also have requirements to always reserve 600 MW FNR and enough FDR reserves to compensate a dimensioning fault according with the N-1 criteria³. (ENTSO-E 2007, chap. Appendix 2)

2.3.2 Frequency Restoration Reserves

For this thesis only load frequency control and manual FRR is of interest and therefore only these two will be described.

Automatic FRR (secondary reserves) - Load Frequency Control, LFC

Classic LFC control systems are designed to restore both the grid frequency deviation and the intertie-line connections between different systems. To give a better understanding for the system two new variables need to be defined; *control area* and *area control error*.

1. Control area (CA): "A power system, a part of a system, or a combination of systems to which a common generation control scheme is applied." (IEEE Standards Committee 1991 def. 103)
2. Area control error (ACE): "The frequency deviation of an isolated power system consisting of a single control area is the area control error. The area control error of a control area on an interconnected system is the net interchange minus the biased scheduled net interchange." (IEEE Standards Committee 1991 def. 124)

By using an ACE signal the TSOs are able to both restore the frequency deviations and the power interchange between different control areas.

The exact implementation of the LFC control system in the Nordic system has not yet been decided, but the plans point towards that the LFC signal will be distributed from the Nordic TSOs SCADA systems to a central SCADA system of the power station owner. It will then be up to the power station owners to distribute the signals within their system in accordance with the system requirements. (Bäck 2011)

Manual FRR (tertiary reserves) - Fast active disturbance reserve

The manual tertiary reserve is today used to restore the FCR and also to restore the system time deviation from the absolute time.⁴ The requirements for participating in the manual reserves is that bids can be placed in blocks of 10 MWs and be fully activated within 15 minutes. On the tertiary market, bids are sent to the local TSO who then coordinate all bids within the entire system in order to always be able to use the cheapest bid. When a need then arises bids are placed manually from the TSO to the respective bid owner. (ENTSO-E 2007, chap. Appendix 2)

2.4 Hydropower

There are two major components in a hydropower system:

³ "Dimensioning faults are faults which entail the loss of individual major components (production units, lines, transformers, bus bars, consumption etc.) and entail the greatest impact upon the power system from all fault events that have been taken into account." (ENTSO-E 2007, s.60)

⁴ When a frequency deviation occurs, electrical components, such as a clock, experience a different time lapse because their time is relative to the grid frequency. The accumulated grid frequency deviation is therefore in direct correlation to the absolute time deviation.

- A reservoir for storing water and thus potential energy.
- A hydropower station with turbines, generators etc. that convert the stored energy in the reservoir to electrical energy.

These two systems can in turn be geographically located at the same place or not, see Figure 4. The major difference is that for stations where the reservoir and station house are not at the same geographical location, then these are connected by either tunnels or canals.

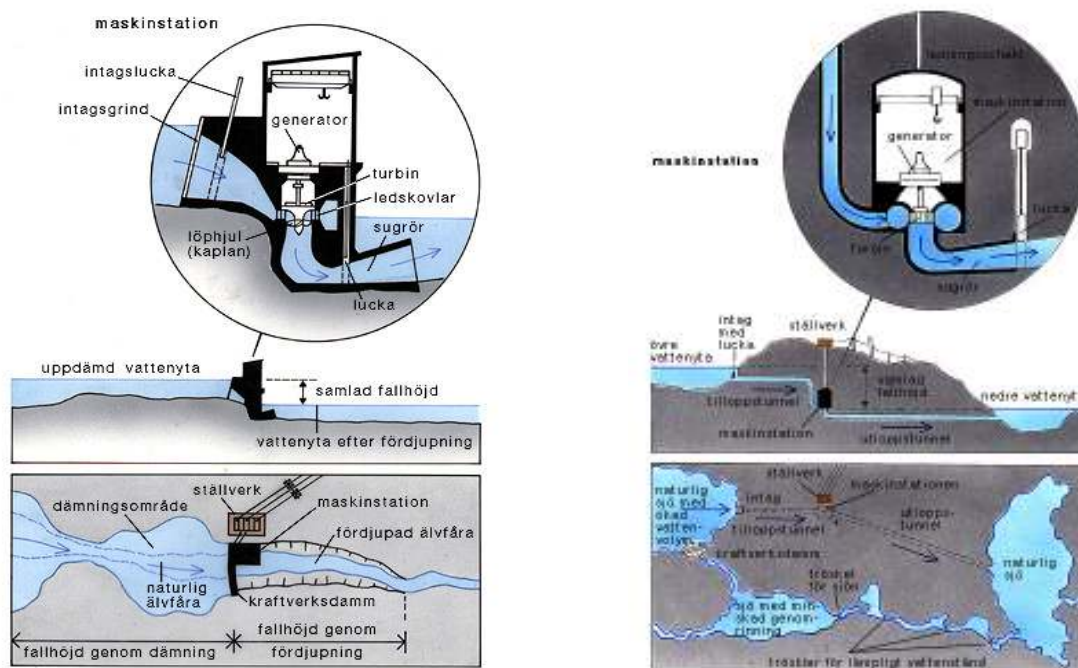


Figure 4: Two different hydropower stations, one station where reservoir and station house are at the same location and one station where a natural lake is used as a reservoir and the station is built within the bedrock between the reservoir and the outlet. (Ne.se 2011)

With the reservoir, a height difference can be created between the upper and lower water surfaces, thus creating a potential energy difference which can be extracted as electric power. At the same time the reservoir acts as a storage unit from which water and thus energy can be withdrawn at a later date. In Sweden this stored energy capacity is roughly 33 TWh (Svensk Energi 2011). With a design feature that stores energy for future use and the fact that a hydropower station can change its power output from 0-100% within minutes, make it ideal for use in frequency control reserves.

As mentioned there are two major station types. It is also possible to categorize stations as being part of a river system (Swedish stations) or being able to operate more independently by directly connecting the reservoir with the ocean (Norwegian stations). For stations being a part of a river system, cooperation between upstream and downstream stations is needed, independently of whether these are owned by the same company or not.

For rivers in which there is more than one power company operating, there is a Swedish law stating that a *river regulating company* has the overall responsibility for planning and maintaining water resources within the said river. This is to both ensure cooperation of the physical resource and at the

same time create a competitive market between the different companies. The river regulating companies are then in turn owned by the different power companies that operate within the river. These river regulating companies make plans for water usage ranging from day to season planning. (Vattenregleringsföretagen.se 2011)

3 Theory

This section will describe the necessary theory and the set of equations needed to produce a working model.

3.1 Hydropower

As described in an earlier section hydropower produces its electrical energy by converting potential energy to electrical energy through the use of a turbine and generator as follows.

$$\text{eq. 1} \quad E_{\text{potential}} = mgH$$

$$\text{eq. 2} \quad P_{\text{theoretical}} = \frac{dE_{\text{potential}}}{dt} = \dot{m}gH = \rho gQH$$

E = energy [J]

P = power [W]

m = water mass [kg]

Q = water discharge [m^3/s]

H = head between upper and lower reservoir water surfaces [m]

g = gravitational constant [m/s^2]

In eq. 2 there are two sets of parameters; those set by nature, the density of water and the gravitational constant, and then those set as a design parameter for the hydropower station, the maximum water discharge and the created height difference. The station design for the maximum water discharge is usually made from either the yearly mean flow or a higher value if the station is to be able to deliver high loads of concentrated power output. eq. 2 also shows the theoretical power that can be produced at a hydropower station omitting losses. By introducing losses we instead get eq. 3.

$$\text{eq. 3} \quad P_{\text{electric}} = \eta_{\text{total}}\rho gQH$$

η_{total} = total efficiency for the station [1]

3.1.1 Degree of efficiency

The efficiency factor in eq. 3 is not constant but varies with the total discharge, the net head at the current station and also upper surface level at the station downstream's. When dealing with several turbine-generator units for one station it is economically vital that the unit combination with the highest degree of efficiency is running and producing at the desired station power output. For these purposes power companies often create *Station OPTimization* tables (SOPT) that contain the optimal discharge distribution between the different units, see Figure 5.

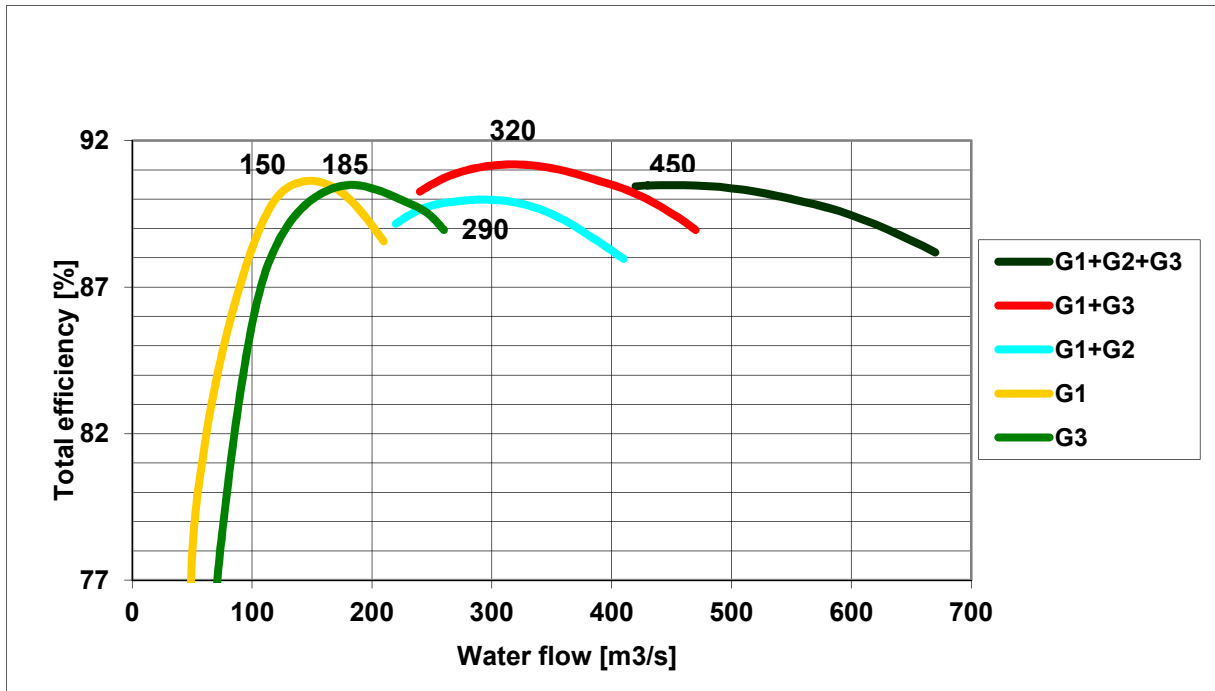


Figure 5: Generation unit combination for a hydropower station with three turbines-generator units.

3.1.2 Turbine Governor

In Figure 6 a simplified turbine governor is shown as it is implemented by Vattenfall in their hydropower plants (Spiegelberg 2011). It consists of two major parts: PI-controller and the droop characteristics. The governor can be set up with a variety of different parameters depending on the current operational situation; start up, normal, disturbed etc. For this study we will only focus on operation within the normal operational frequency interval +/- 100 mHz. For ease of understanding the parameters will be given in per unit values. (Spiegelberg 2011, p.1,2)

The turbine governor has two inputs; the grid frequency deviation [Hz] from the nominal value of 50 Hz and also a power setpoint value [MW]. The *power setpoint signal* will also be used later in the thesis, for example when describing how the LFC signal is distributed, it will then be referred to as the *operational setpoint* and is chosen by the power company.

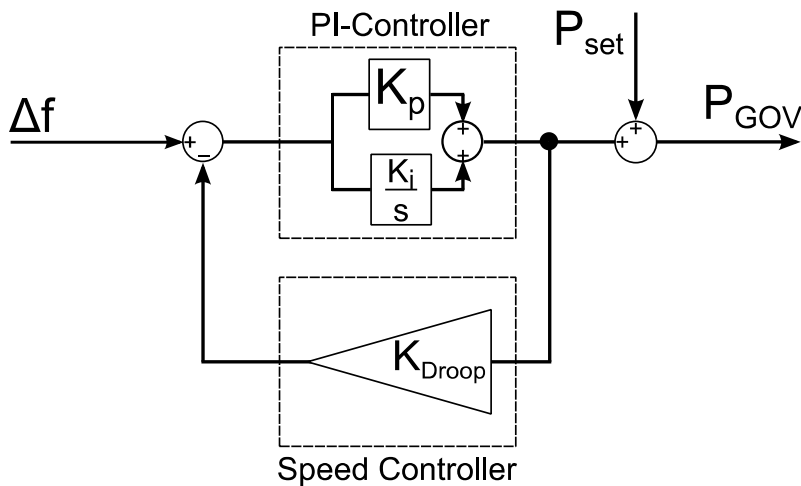


Figure 6: Simplified turbine governor outlay from Vattenfall with input; frequency deviation (Δf) and power setpoint (P_{set}), output; mechanical power (P_{gov}) and internal parameters; proportional gain K_p , integral time constant $1/K_i$ and speed droop setting K_{droop} . (Kaisinger 2011)

Typical values for the turbine governor are:

- $K_p = 1$; turbine governor proportional gain [1]
- $T_i = 6, 2.4$ (ep0, ep1); turbine governor integral time constant [s] ($=1/K_i$)
- $K_{droop} = 0.1, 0.04$ (ep0, ep1) ; speed droop setting [1]

K_p and T_i are PI-governor parameters, K_{droop} is the speed droop-characteristics for the machine and ep0, ep1 are different regulation setpoints set by the operator to define how many MW's of regulation power each unit shall deliver. The speed droop value sets the total amount of regulation that the machine will contribute with at a frequency deviation as is defined as follows. (Högström 2006 eq. 5)

$$\text{eq. 4} \quad K_{droop} = \frac{\Delta f / f_{nominal}}{\Delta P / P_{base}}$$

R = strength of regulation [MW/Hz]

K_{droop} = speed droop setpoint [1]

Δf = frequency deviation from the nominal frequency [Hz]

$f_{nominal}$ = nominal grid frequency [Hz]

ΔP = regulated power at a certain frequency deviation [MW]

P_{base} = base power output for the turbine-generator unit [MW]

In Figure 6, the hydraulic servo and guide vanes have been ignored because these have much smaller time constants than the turbine governor and are not needed to complete the project aim. The turbine governor of Figure 6 can therefore be described by:

$$\text{eq. 5} \quad P_{gov}(s) = dP_{gov}(s) + P_{set}(s) = \left(K_p + \frac{1}{sT_i} \right) (\Delta f(s) - K_{droop} dP_{gov}(s)) + P_{set}(s)$$

eq. 5 can then be simplified further which will then later on be used when modelling the turbine governor.

$$\text{eq. 6} \quad P_{gov}(s) = \frac{1}{K_{droop}} \frac{1 + K_p T_i s}{1 + \frac{1 + K_{droop} K_p}{K_{droop}} T_i s} \Delta f(s) + P_{Set}(s)$$

By only looking at the impact from the frequency deviation we can rearrange eq. 6 to eq. 7 and then extract the equivalent time constant, eq. 8

$$\text{eq. 7} \quad \Delta P_{gov}(s) = \frac{1}{K_{droop}} \frac{1 + K_p T_i s}{1 + \frac{1 + K_{droop} K_p}{K_{droop}} T_i s} \Delta f(s)$$

$$\text{eq. 8} \quad T_{PI} = \frac{(1 + K_{droop} K_P) T_i}{K_{droop}} \approx \frac{T_i}{K_{droop}}$$

T_{PI} = turbine governor equivalent time constant [s]

Using the values specified earlier this results in a system time constant of $T = 60$ s which is required for FCR operation within the normal operation band.

3.1.3 Power to Water usage

In real life the turbine governors do not govern the power output but the guide vane setpoint's that in turn set the water discharge. The water discharge/guide vane opening can then be related to the power output of the turbine through a transfer function often referred to as the Penstock-Turbine transfer function, see (De Jaeger m.fl. 1994). These transfer functions operate with much faster time constants than the other modules within this study and have therefore been left out. Instead, SOPT-tables have been used to connect the electric power and water circuits within the model.

3.1.4 River

A river is a very dynamic and non-linear system that can be difficult to model accurately. Two methods of modelling this though are the St Venant's equations, a hydraulic method with partial differential equations, and the Muskingum method, a simplified hydrological method which will be used when modelling a river reach. (Koussis 2009, chap.1,2)

The Muskingum method is a significantly simplified hydrological river routing method that is based on equations linking conservation of volume with the inflow and outflow of the river. The method specifically links the inflow, outflow and storage within the river to a set of two constants; one describing the time it takes for a wave to propagate through a river reach and the other a dimensionless weighting factor linking the storage to the inflow and outflow of the reach. This result in the following equations: (Bedient m.fl. 2008, s.219)

$$\text{eq. 9} \quad \frac{dV_{river}}{dt} = Q_{river}^{in} - Q_{river}^{out}$$

$$\text{eq. 10} \quad V_{river} = T_{river}(\Theta Q_{river}^{in} - (1 - \Theta)Q_{river}^{out})$$

V_{river} = river storage [m^3]

Q_{river} = water flow [m^3/s]

T_{river} = river propagation time [s]

Θ = Muskingum weighting factor [1]

By combining eq. 9 and

eq. 10 a discrete numerical method is presented that can be used for calculating the propagation of water through a river reach.

$$\text{eq. 11} \quad Q_{river}^{out}(t) = aQ_{river}^{in}(t) + bQ_{river}^{in}(t - \Delta t) + cQ_{river}^{out}(t - \Delta t)$$

Δt = discrete step time [t]

$$a = \frac{-\Theta T_{river} + 0.5\Delta t}{(1 - \Theta)T_{river} + 0.5\Delta t}$$

$$b = \frac{\theta T_{river} + 0.5\Delta t}{(1-\theta)T_{river} + 0.5\Delta t}$$

$$c = \frac{(1-\theta)T_{river} - 0.5\Delta t}{(1-\theta)T_{river} + 0.5\Delta t}$$

For numerical stability, two limits need to be imposed that in turn give a relation between the river's travel time and the simulation's step time. (Achleitner & Rauch 2007, p.63)

$$\text{eq. 12} \quad \begin{aligned} a, b, c &> 0 \\ T_{river} &> \Delta t \end{aligned}$$

$$\text{eq. 13} \quad \frac{1}{2\theta} \leq \frac{T_{river}}{\Delta t} \leq \frac{1}{2(1-\theta)}$$

The dimensionless weighting factor θ describes a relation between the storage of the river to the inflow and outflow of the system and is in the interval of 0-0.5. According to (Bedient m.fl. 2008, s.219) a typical value for θ in a natural stream is 0.2, whereas a value 0.5 in a smooth uniform canal results in a pure translation of the wave. For more information on determining the value of θ , see (Bedient m.fl. 2008, s.222). For our purposes, a value of $\theta = 0.2$ has been deemed sufficient, since θ affects the form of the wave more than the wave speed itself. (Bedient m.fl. 2008, p.222)

eq. 10 also gives rise to two types of storages within the river; wedge storage and prism storage described by eq. 14 and eq. 15, see Figure 7. This is important to keep in mind during transitional phases of the river when the outflow does not equal the inflow. Within the Muskingum method the prism storage follows the bedslope's inclination, seen in Figure 7 where the bottom of the river is non-horizontal. With the inclination a potential difference is created over longer distances, which acts as the fundamental driver for mass transportation. The wedge storage on the other hand acts as a volume storage for a wave that is propagated through the river reach and is thereby only present during transient stages.

$$\text{eq. 14} \quad V_{river}^{wedge} = T_{river} \theta (Q_{river}^{in} - Q_{river}^{out})$$

$$\text{eq. 15} \quad V_{river}^{prism} = T_{river} Q_{river}^{out}$$

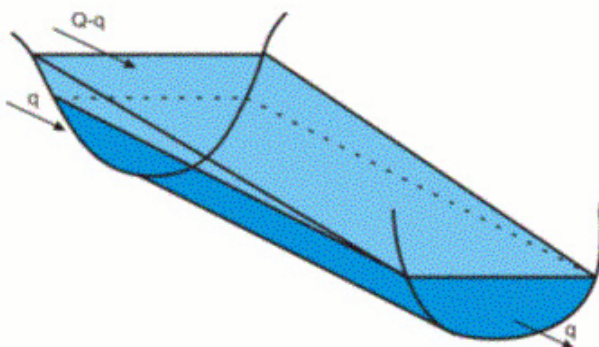


Figure 7: Graphical representation of a river reach with wedge (transparent) and prism (solid) storage (VICAIRE 2011)

Within some rivers there are also natural restrictions such as rapids and bridges. These act on the river by changing the topology through which the water needs to flow. These restrictions can be modelled as a surface spillway for which the surface level on the upstream side needs to be raised relative to the down stream's side before reaching a new equilibrium for a certain flow. For a change in flow, there will always be a transient period for these water levels. These effects have been *omitted* to create a simpler model.

3.1.5 Reservoir

A reservoir has two major functions; storage of water and creating the necessary difference in height between the upper and lower surface levels. The stored water within the reservoir can then be calculated with eq. 16.

$$\text{eq. 16} \quad V_{\text{reservoir}} = \int A_{\text{reservoir}}(h) dh$$

$V_{\text{reservoir}}$ = stored water volume within the reservoir [m³]

$A_{\text{reservoir}}$ = reservoir surface area [m²]

h = reservoir surface level [m]

From eq. 16 the surface level can be linked to the difference in incoming and outgoing flow from the reservoir, eq. 17, which will be used for modelling the reservoir.

$$\text{eq. 17} \quad h(t) = h_0 + \frac{1}{A_{\text{reservoir}}} \int (Q_{\text{reservoir}}^{\text{in}} - Q_{\text{reservoir}}^{\text{out}}) dt$$

h_0 = reservoir surface initial setpoint above the lower reservoir limit [m]

3.2 Frequency control systems

The grid frequency and balance between produced and consumed power can be linked via the *swing-equation*. By omitting voltage and rotor angle dynamics, as stated in 1.3 Limitation in scope, the equation can be simplified to the following (Bevrani 2009, p.17).

$$\text{eq. 18} \quad \Delta P_{\text{generated}}(t) - \Delta P_{\text{consumed}}(t) = 2J \frac{d\Delta f(t)}{dt} + D\Delta f(t)$$

P = electric power [MW]

J = system inertia constant [MWs/Hz]

f = grid frequency [Hz]

D = load dampening coefficient [MW/Hz]

With Laplace's transformation this can be transformed to

$$\text{eq. 19} \quad \Delta f(s) = \frac{\Delta P_{\text{generated}}(s) - \Delta P_{\text{consumed}}(s)}{D + 2Js}$$

To keep the grid frequency at a constant level the active power delivered by generators needs to equal the power consumed by the system loads including losses seen in eq. 19.

3.2.1 Frequency Containment Reserves – primary frequency control

The static regulated power by the FCR reserves is given by eq. 20 and is graphically described by Figure 8. The path that these frequency controlled reserves take to this static value though is defined individually by the turbine governor parameters and the penstock-turbine transfer function.

$$\text{eq. 20} \quad \Delta P_{FCR} = -\frac{\Delta f}{K_{\text{droop}}} \quad \Delta P_{\text{mech}} = -R\Delta f$$

$1/K_{\text{droop}} = R = \text{strength of regulation [MW/Hz]}$

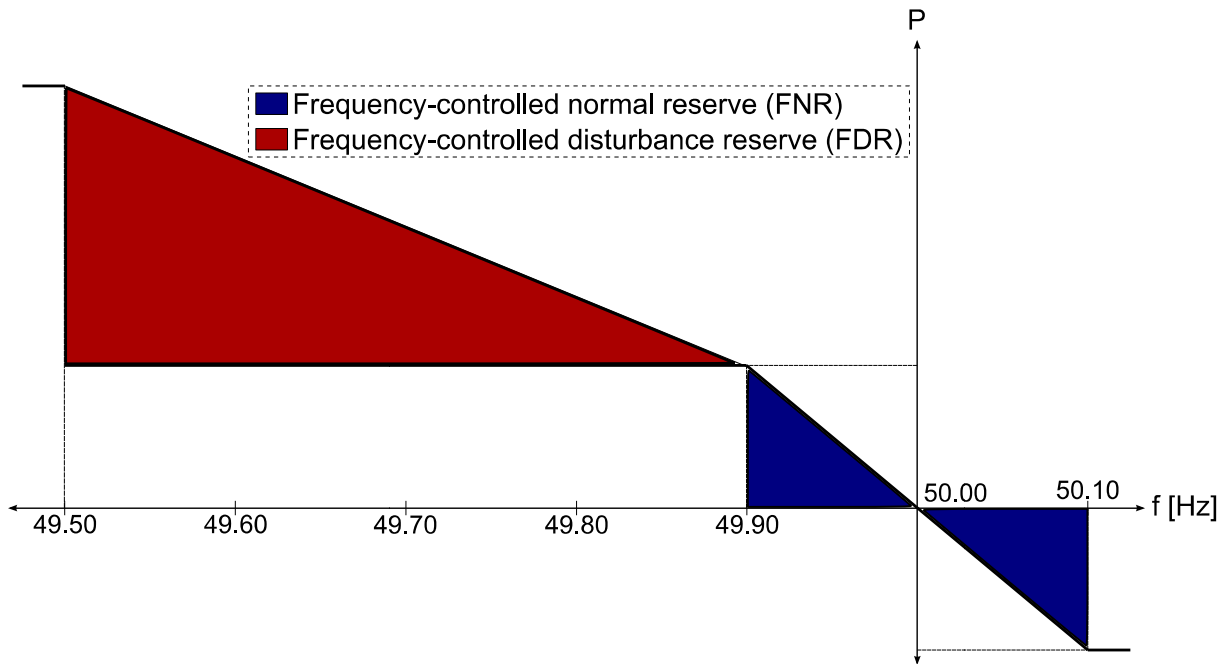


Figure 8: Graphical description of the static regulated power by FNR and FDR regulation at a certain frequency deviation. FDR regulation is also made during over balanced systems but this is not a requirement in the Nordic Grid Code (Kaisinger 2011)

eq. 20 also states that there is only a proportional relationship to the frequency deviation and no integral relationship, thereby the FCR regulation can only hinder the frequency from deviating further and not recover it to its nominal value.

3.2.2 Automatic Frequency Restoration Reserves - LFC

To understand the concept of *load frequency control*, the two variables defined in 2.3.2 Frequency Restoration Reserves are used; a *control-area (CA)* and an *area control error (ACE)*. The ACE is defined as follows, see Figure 9 for graphical description. (Bevrani 2009, p.23)

$$\text{eq. 21} \quad ACE(t) = \Delta P(t)_{\text{interchange}} + \beta \Delta f(t)$$

$$\text{eq. 22} \quad \beta = \frac{1}{K_{\text{systemDroop}}} + D_{\text{loadDampening}}$$

ACE = area control error [MW]

$\Delta P_{\text{interchange}}$ = tie-line interchange deviation between two CA's [MW]

Δf = grid frequency deviation [Hz]

$K_{\text{systemDroop}}$ = speed droop characteristics for the entire system [Hz/MW]

D = system load dampening coefficient [MW/Hz]

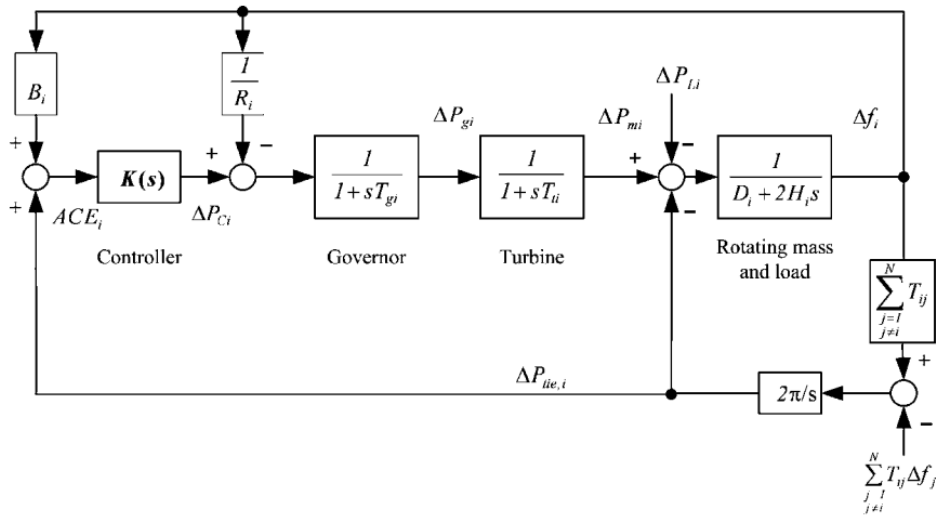


Figure 9: Power system with a single generating unit and an overlying LFC governor. The factor R in this figure is not the strength of regulation but its inverse ($=K_{\text{droop}}$) (Bevrani 2009, fig.2.10)

The ACE control signal is allocated to a controlling unit, in this case a controller $K(s)$, which in turn creates an external input signal for the turbine governor, see Figure 9. An LFC controller is often also used to control multiple power generating facilities which in turn requires it to create a participation factor for each individual power plant, see eq. 23, eq. 23 and Figure 10. In the modern power system these participation factors need to be highly dynamic. (Bevrani 2009, chap.2.4)

$$\text{eq. 23} \quad \Delta P_{LFC \text{ setpoint}} = \gamma_n \Delta P_{LFC \text{ demand}}$$

$$\text{eq. 24} \quad \sum_{n=1}^N \gamma_n = 1$$

$\Delta P_{LFC \text{ demand}}$ = total LFC demand as calculated by the controller $K(s)$ [MW]

γ = participation factor [1]

n = station number [1]

N = total number of stations [1]

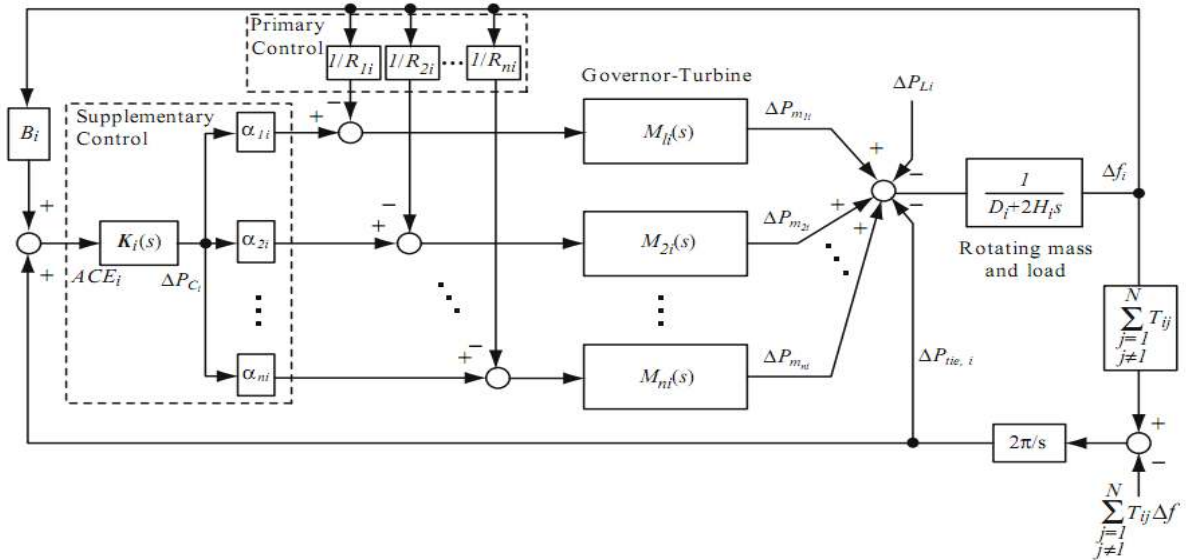


Figure 10: Power system with multiple generating units and an overlying LFC governor. The factor R in this figure is not the strength of regulation but its inverse ($=K_{droop}$) (Bevrani 2009, fig.2.13)

4 Method and Model development

The main approach has been to create a modular system based on simple modules that can be upgraded in due time when and where a problem or opportunity arises. The created modules are:

- Hydro power plant (river, reservoir, turbine governor, turbine-to-flow function)
- LFC-distribution optimizer

These two module types are then grouped together to create a LFC governed river system with multiple hydropower stations, for an example see Figure 11. The created river system is then implemented in a larger model, retrieved from *ENTSO-E* that was developed in the project *Analysis & Review of Requirements for Automatic Reserves in the Nordic Synchronous System* (ENTSO-E 2011a).

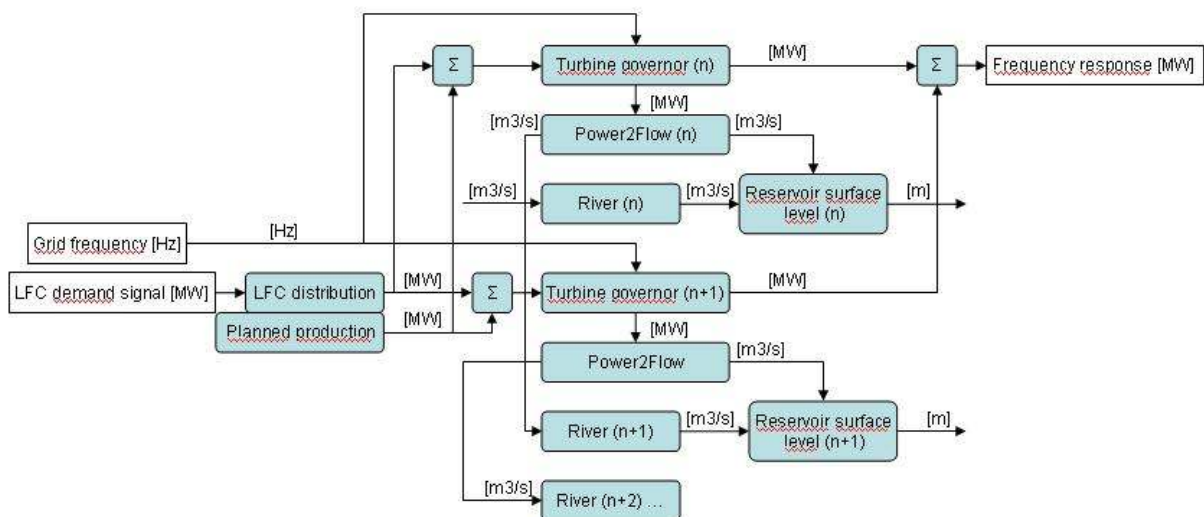


Figure 11: Schematic flow chart for a created river system (blue), including LFC distribution, and input/output (white) for the river system module that connects to ENTSO-E's LFC module.

4.1 ENTSO-E model

The ENTSO-E model, Figure 12, includes modules for the current FCR and future FRR/LFC capacity of the Nordic system, a set of input (production and load) which are dependent on the simulation at hand, and a module for the system inertia. More details and a model description can be found in (ENTSO-E 2011b).

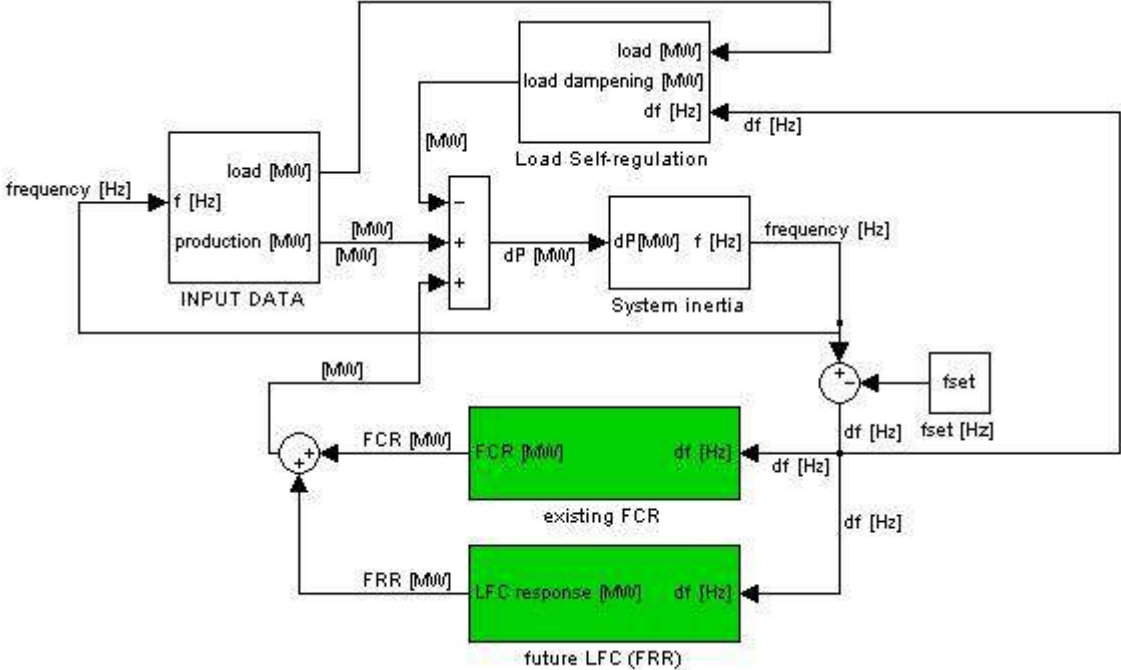


Figure 12: ENTSO-E model for the Nordic synchronous system with automatic frequency controlled reserves and future load frequency control system. (Extra modules not used in this thesis have been stripped from the original model) (ENTSO-E 2011b)

The created river system is then implemented as a generation block within LFC module of the ENTSO-E model, see Figure 13. Input for the river system module is the grid frequency and the created LFC control signal. The grid frequency is used to create an FCR response within the river reach and the LFC signal is used to change the operational setpoint for each hydropower station. It was also chosen to truncate the incoming LFC signal to the river reach at +/- 10 MW since this is the size of the bid blocks for the manual FRR market today. With the LFC signal truncated, the original *generation* module from the ENTSO-E model was kept to deal with the remaining +/- 390 MW, of the total maximum 400 MW, LFC demand, that is *not* handled by the river system. This was done by creating a module that always directs the first +/-10 MW of the LFC control signal to the river system and the rest to the ENTSO-E generation module and it can thereby be said that the river system always places the cheapest LFC bid.

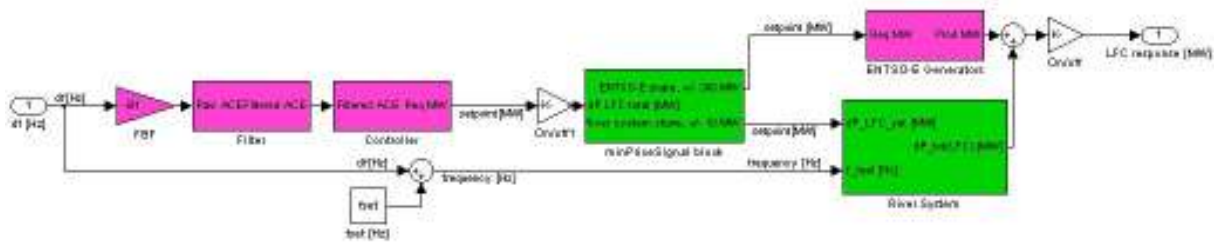


Figure 13: ENTSO-E LFC module. Input/Output is grid frequency deviation [Hz] and LFC response [MW]. Purple blocks are the original LFC module blocks starting with *frequency bias factor*, *LP-filter*, *PI-controller*, *generator*. Our implementations are the green blocks with the *minimum price block* and *river system*.

To give a graphical understanding of how the LFC PI-governor reacts to a frequency deviation ENTSO-E has made step response tests of which one is shown in Figure 14.

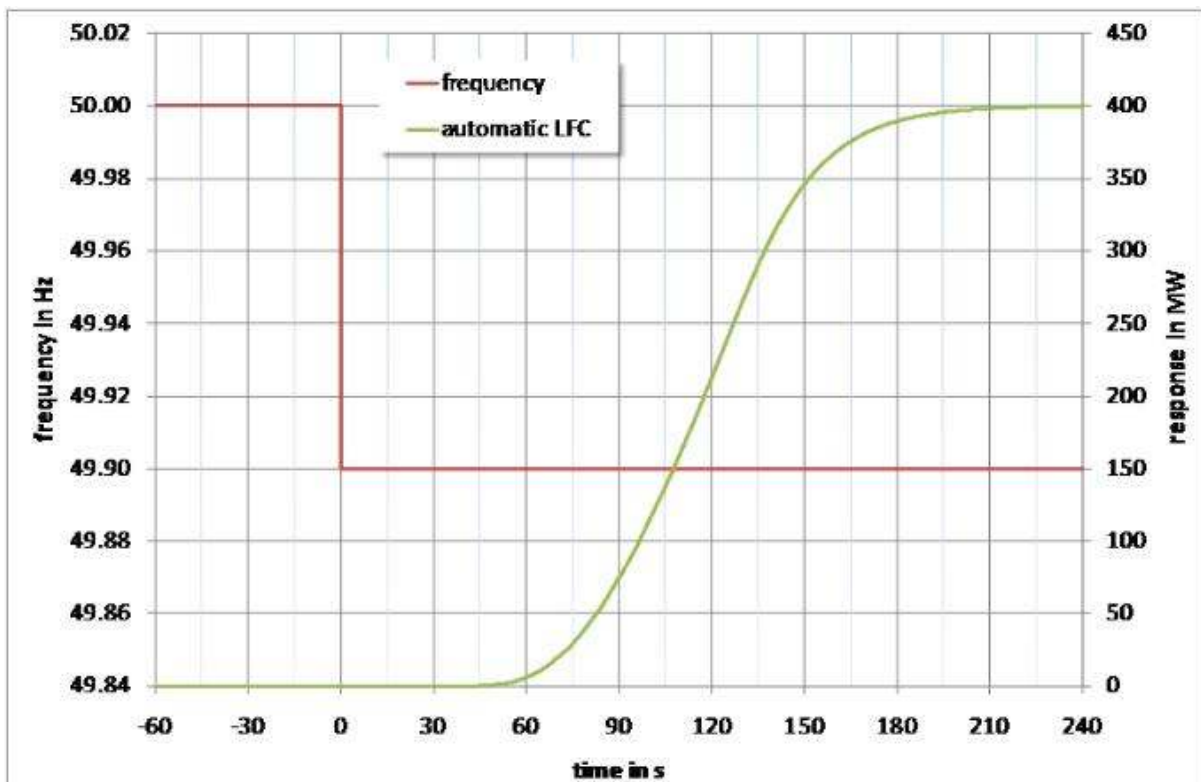


Figure 14: Step response test of the ENTSO-E LFC governor with an input step of -100mHz. (ENTSO-E 2011b, fig.80)

4.1 Hydro Power station

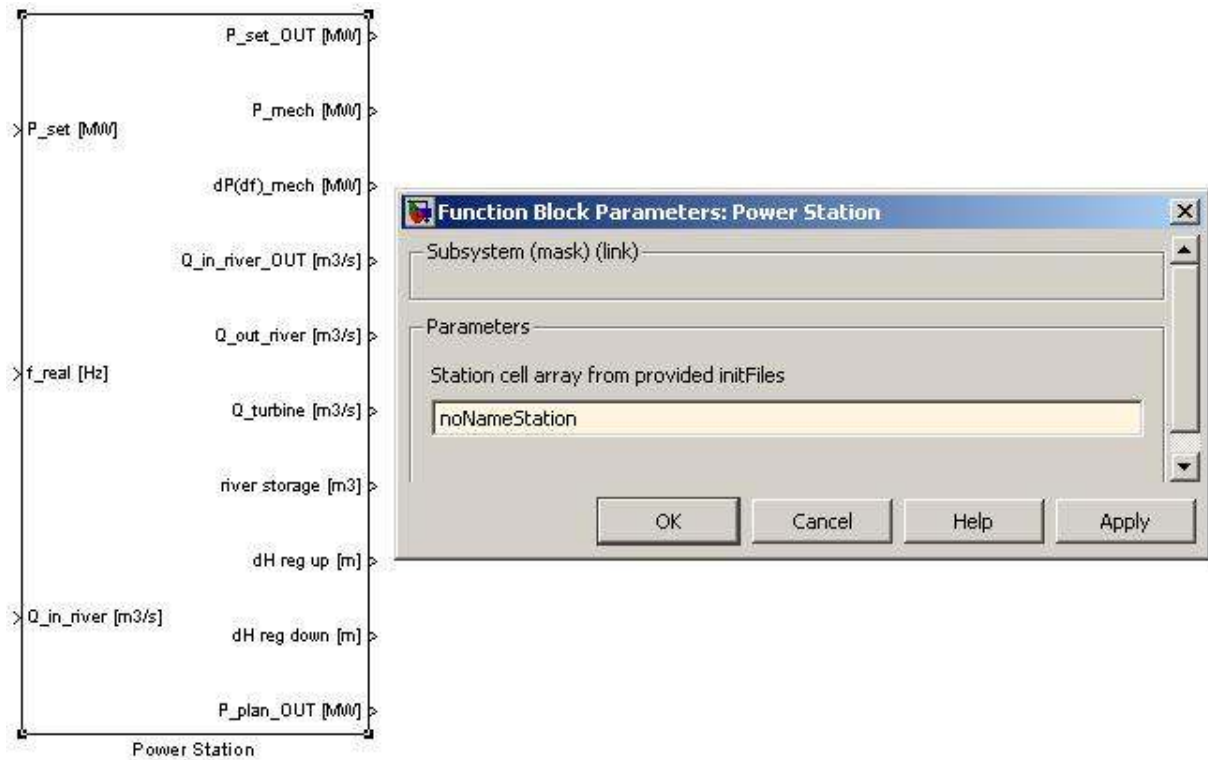


Figure 15: Hydropower station module with input/output (I/O) and general user interface (GUI) for internal parameters

Within the next four sections, the sub modules that make up the hydropower station module, see Figure 15, will be described. They will then in turn be grouped together as a power module (*turbine governor* and *power to flow* working in series) working in parallel with a water module (*river reach* and *reservoir* working in parallel) with the turbine flow connecting the two modules. The hydropower station module is then used to create a river system consisting of multiple hydropower stations connected in series. For more information on input/output and internal variables see Appendix A – Model Modules.

4.1.1 River

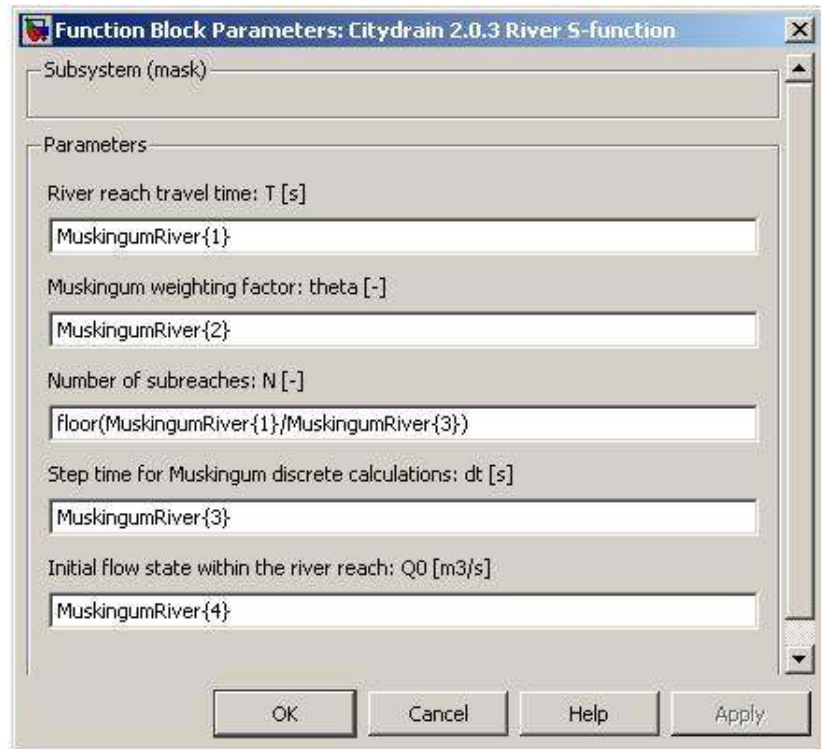
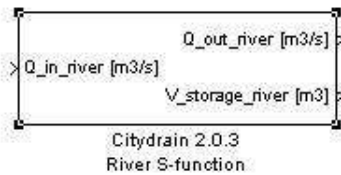


Figure 16: River module with I/O and GUI for internal parameters

The river module, Figure 16, was implemented with the Muskingum river routing method by using another Simulink model developed for a program called *CityDrain 2.0.3*. This program is an open source ware and was developed at the *University of Innsbruck* for modelling urban drainage systems. The program contains several different modules that can be used for river routing, of which the module “*Muskingum oM-Q*” was deemed to have the best properties for this thesis purposes and was therefore implemented in the river module. See (Achleitner & Rauch 2007) for more information of the *CityDrain* modules.

The module simulates the flow of water from input to output by dividing an entire river reach in to smaller sub reaches and it’s thereby possible to achieve a higher resolution in time while maintaining the numerical stability criterias stated in eq. 13. To be able to use the “*Muskingum oM-Q*” module, another module called *CD Parameters*, from *CityDrain* also needs to be included. This module needs to be put in the top most module-block for the whole simulations.⁵

As mentioned in the theory section the river also acts as a storage unit ahead of the reservoir and contains both a prism volume and a wedge volume. These volumes will be addressed later in the section concerning governing of the LFC-control, see section 4.2 LFC – distribution module.

Module validation

The river module has been tested for its physical properties by performing two tests; one step response to see how much it can resemble a real river reach and one impulse response to see how a wave propagates through the system.

⁵ The CD-paramaters module contains information on how the module shall communicate with the Simulink interface.

Figure 17 describes a step response from a step in inflow at the Midskog power station and how the outflow is affected at the downstream station Näverede. According to the staff at DC Bispgården a step at Midskog takes 11 minutes before reaching Näverede and after 15 minutes Näverede will have fully regulated its turbines in order to keep a constant surface level (Damgren 2011). As seen in Figure 17 the step response of the river reach reaches Näverede after roughly 11 minutes and has leveled out by 15 minutes. The river module should thereby be a good enough approximation of the river reach.

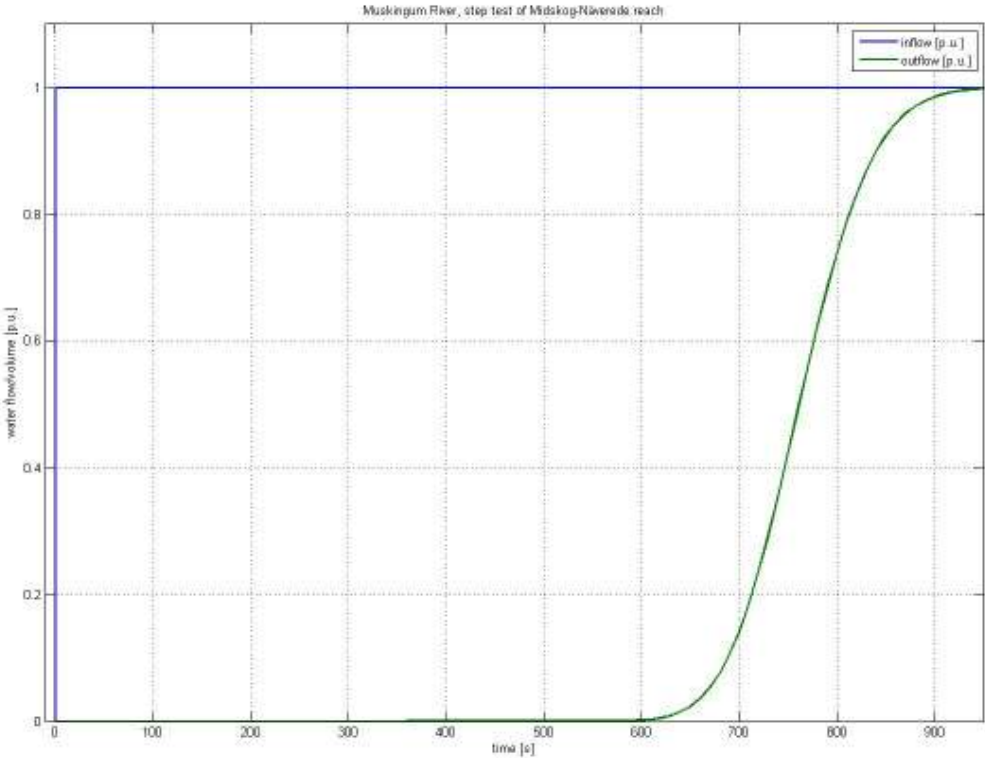


Figure 17: Step test of 1 p.u. inflow at Midskog (blue) with resulting outflow (green) at Näverede. The river reach has a travel time of 11 minutes (660 s).

Figure 18 shows how a wave will become dispersed at the outflow after propagating through the river reach with the Muskingum method. As seen the wave is dispersed fairly equally in space whereas in reality the wave should have a steeper wavefront compared to its backside (Dahlbäck 2011). This dispersion shouldn't pose a problem for this thesis's purposes though since the model mainly is in need of the low pass filtering and transport delay properties of the river in order to accomplish its the objectives.

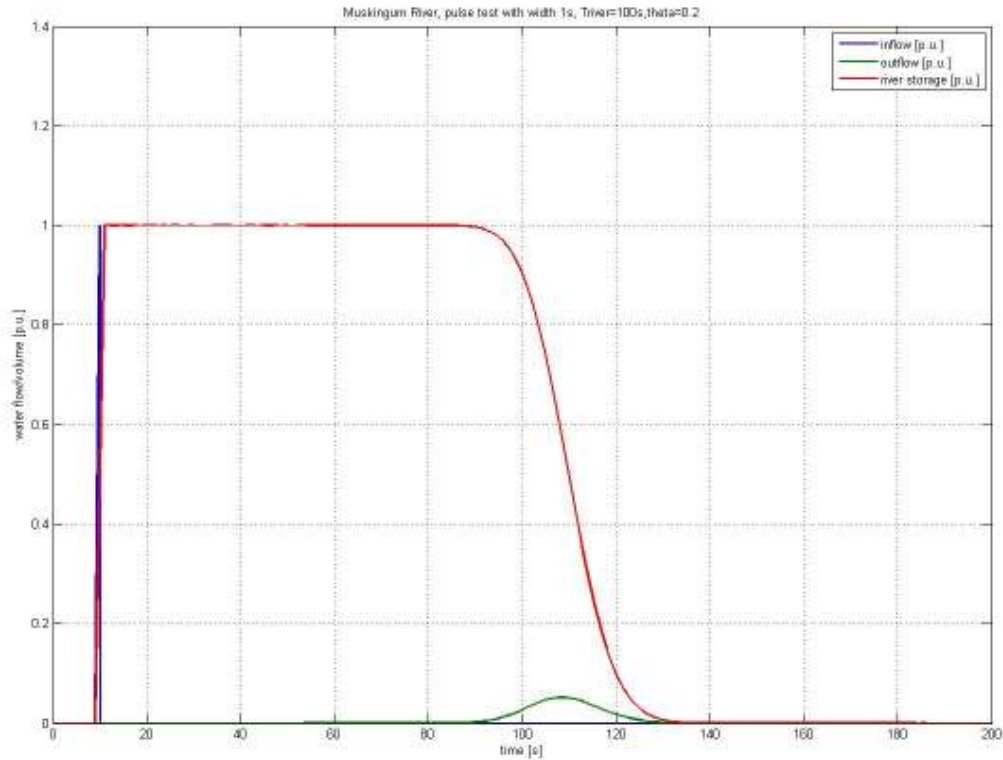


Figure 18: Pulse test of the Muskingum method for river routing. The incoming pulse (blue) has a total volume of 1 p.u., this is then “stored” in the river (red) before the outflow (green) drains the river with 1 p.u. volume.

4.1.2 Reservoir

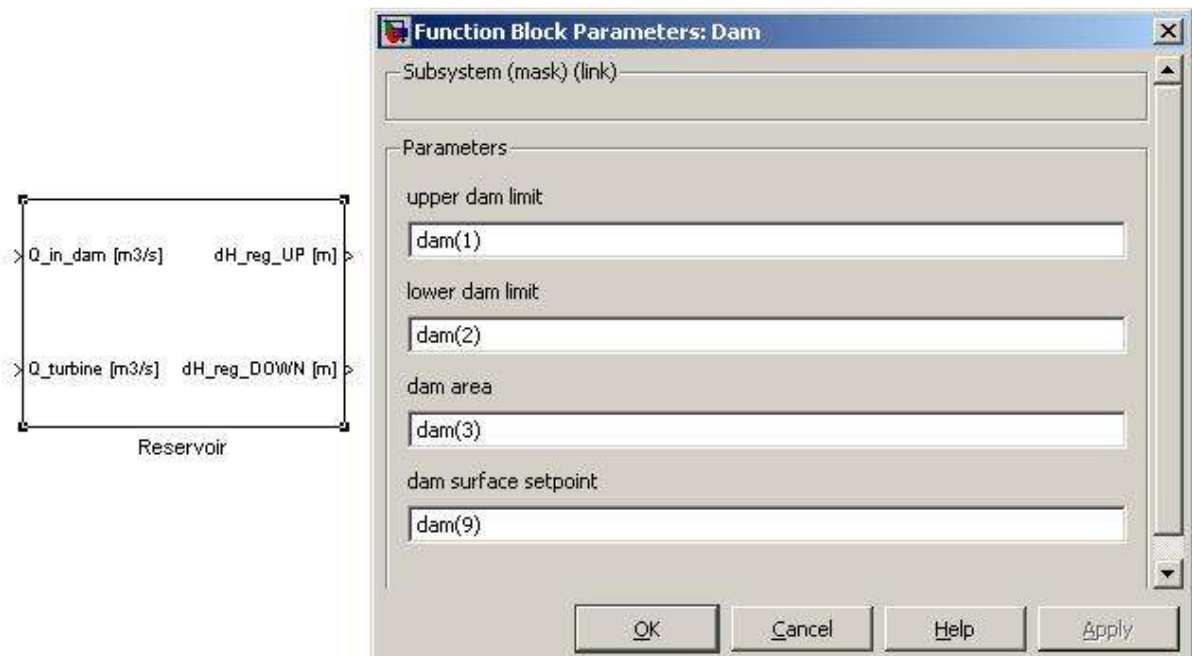


Figure 19: Reservoir module with I/O and GUI for internal parameters

The *reservoir* module, Figure 19, is modelled as follows.

$$\text{eq. 25} \quad h(t) = h_0 + \frac{1}{A_{\text{reservoir}}} \int (Q_{\text{reservoir}}^{\text{in}} - Q_{\text{reservoir}}^{\text{out}}) dt$$

$$\text{eq. 26} \quad A_{\text{reservoir}} = \frac{V_{\text{reservoir}}}{DGr - SGr}$$

$$\text{eq. 27} \quad \Delta h_{\text{reg up}} = DGr - h(t)$$

$$\text{eq. 28} \quad \Delta h_{\text{reg down}} = h(t)$$

Δh_{reg} = regulation capacity to either upper or lower reservoir limitation [m]

$A_{\text{reservoir}}$ = surface area [m²]

DGr = upper reservoir limit (sv. *Dämninggräns*) [m]

SGr = lower reservoir limit (sv. *Sänkingsgräns*) [m]

With this method of calculating the reservoir surface level, the turbine is able to use the entire water volume within the reservoir momentarily compared, to naturally where the turbine discharge needs to lower the water surface at the dam structure before water within the reservoir can start to flow toward the turbine.

Module validation

The reservoir module has been validated by performing a double impulse response test. This is done by first sending a pulse to the inflow of the reservoir and then a moment later a pulse to the outflow of the reservoir. The surface should thereby first rise and then fall accordingly which can be seen in Figure 20.

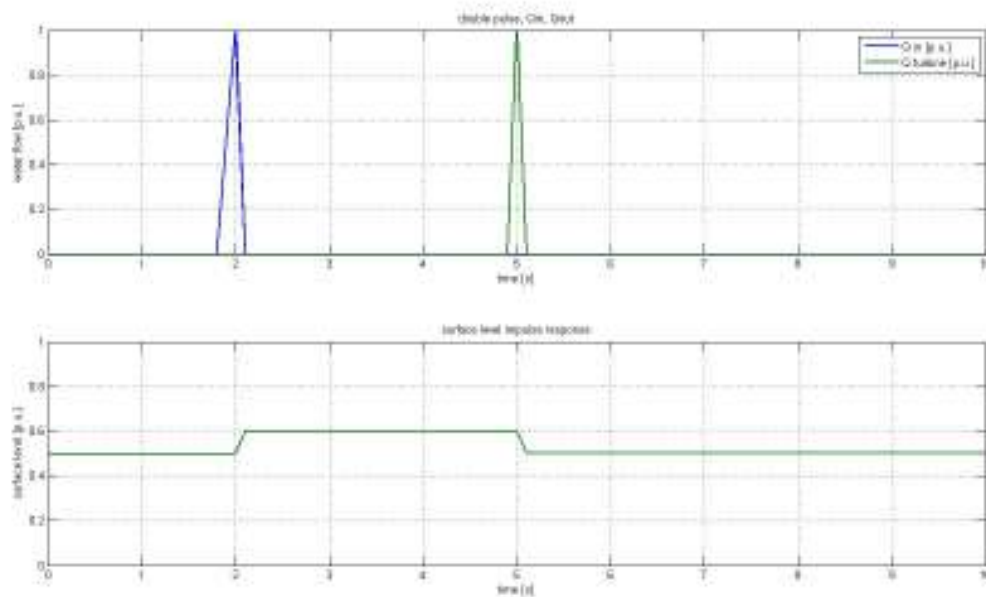


Figure 20: Reservoir double pulse test. In the upper figure, the inflow (blue) receives a pulse first and then the outflow (green) receives a pulse of the same magnitude, resulting surface level deviation seen in the lower figure.

4.1.3 Turbine governor

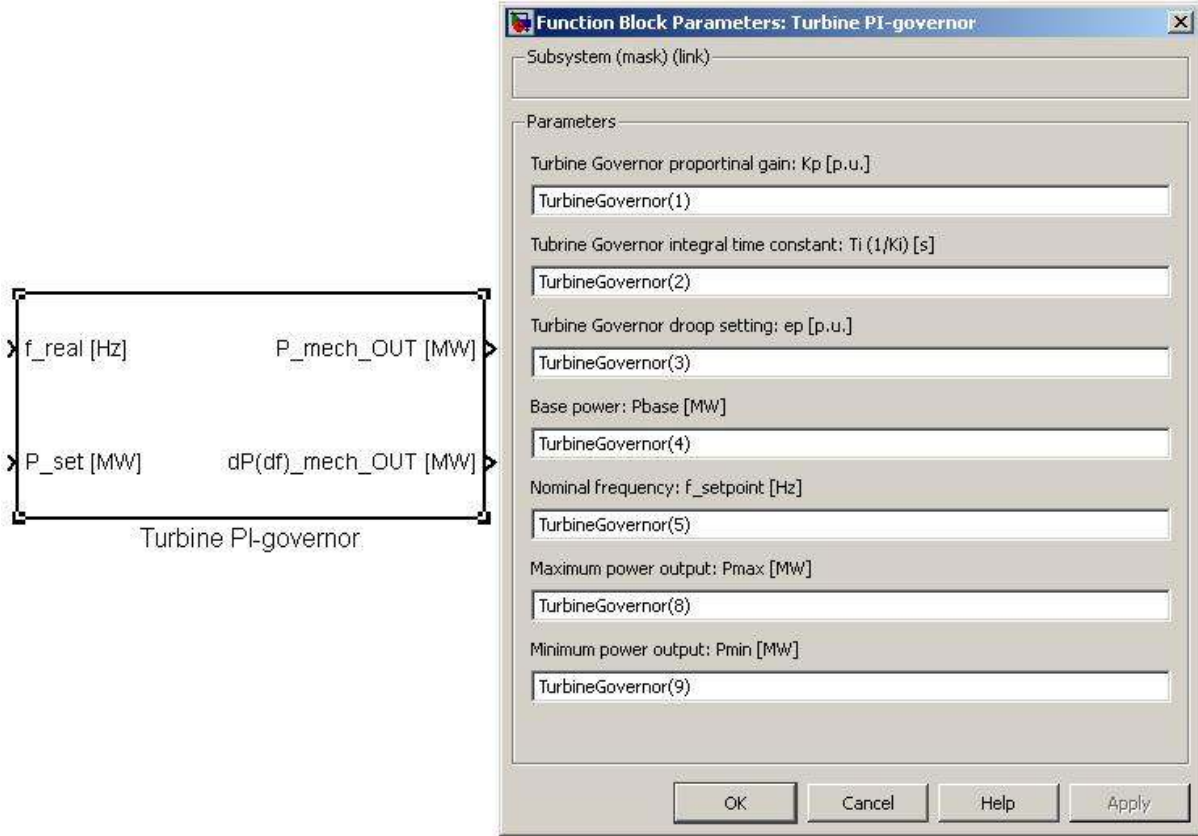


Figure 21: Turbine Governor: Module with I/O and GUI for internal parameters

The *turbine governor* module, Figure 21, has been implemented with the transfer function in eq. 6. With the turbine governor parameters, from section 3.1.2 Turbine Governor, being generalized in p.u. settings, the input and output signals have been scaled accordingly. A saturation block has also been implemented on the P_{mech} output signal in order to ensure that the signal is within physical limits defined by P_{max} and P_{min} for each station.

Module validation

The module has been validated by performing a step test response with a frequency deviation of 0.002 p.u. ($\Delta f = 0.1$ Hz). According to the final value theorem the step test should converge to the following value $\Delta P_{\text{mech}} = 0.02$.

$$\text{eq. 29} \quad \Delta f(s) = \frac{0.002}{s}, K_{\text{droop}} = 0.1$$

$$\text{eq. 30} \quad \Delta P(t \rightarrow \infty) = \lim_{s \rightarrow 0} s \left(\frac{1}{K_{\text{droop}}} \frac{1 + K_p T_i s}{1 + \frac{1 + K_{\text{droop}} K_p T_i s}{K_{\text{droop}}}} \right) \Delta f(s) = \frac{0.002}{0.1} = 0.02 \text{ [p. u.]}$$

In Figure 22 the step test response is shown for the 0.002 p.u. frequency deviation and it is shown to respond according to the theory. The numerical point closest to the time constant has also been marked in the graph.

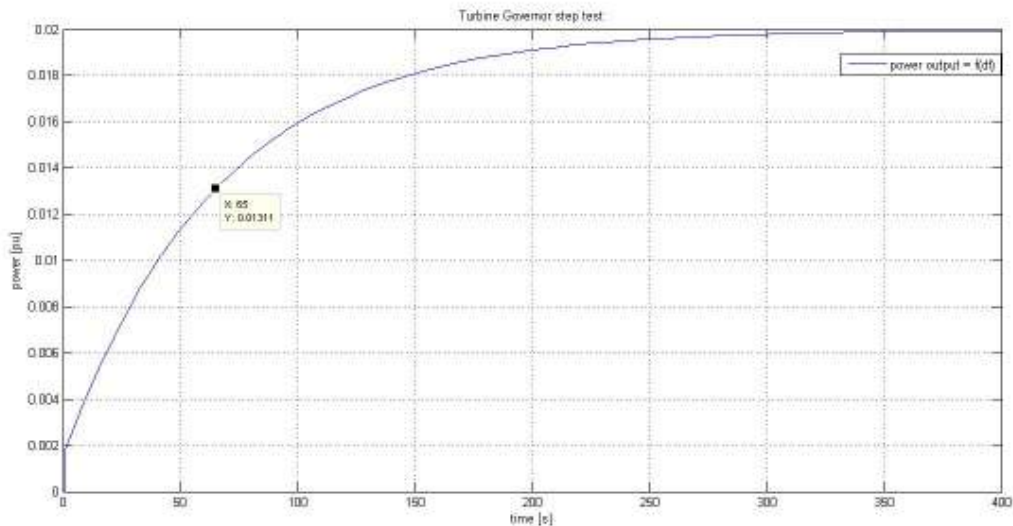


Figure 22: 0.002 p.u. (=0.1 Hz) step test of the turbine governor module with resulting 0.02 p.u. power regulation. The numerical point closest to the time constant $T=60$ s has been marked.

4.1.4 Turbine flow function

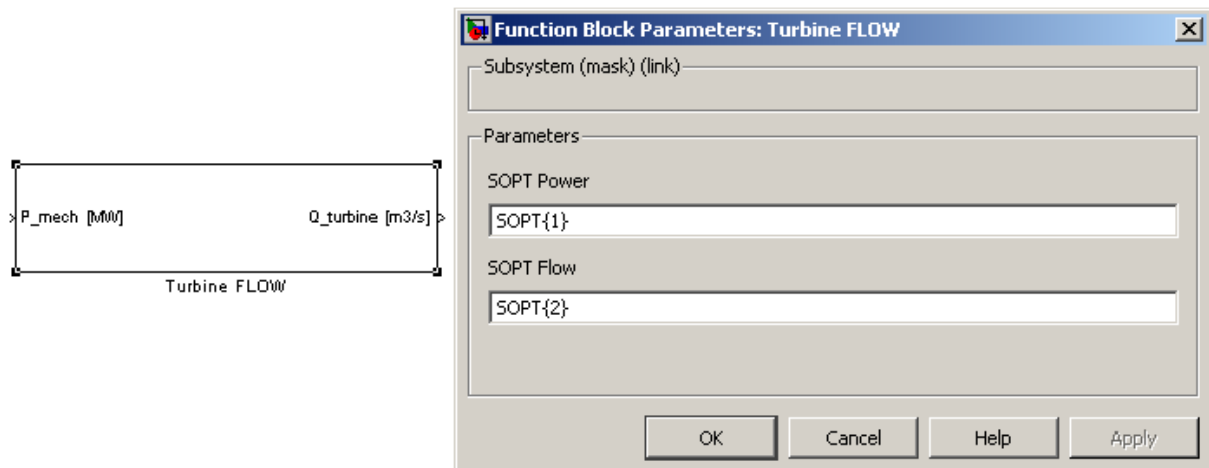


Figure 23: Turbine flow module with I/O and GUI for internal parameters

In the *turbine flow module*, Figure 23, a Matlab Simulink “Look-Up table” module is used with power as the input value and water discharge as the output value. The module approximates a one-dimensional function and interpolates the input value to the specified table values, the SOPT-tables, to create the output value.

Module validation

The power to flow module has been validated by performing a ramped test, Figure 24, to see that the power matches with the expected discharge from given SOPT-tables, Figure 25. The ramping range spans from the absolute minimum to maximum discharge for a station and thereby also over several unit combinations.

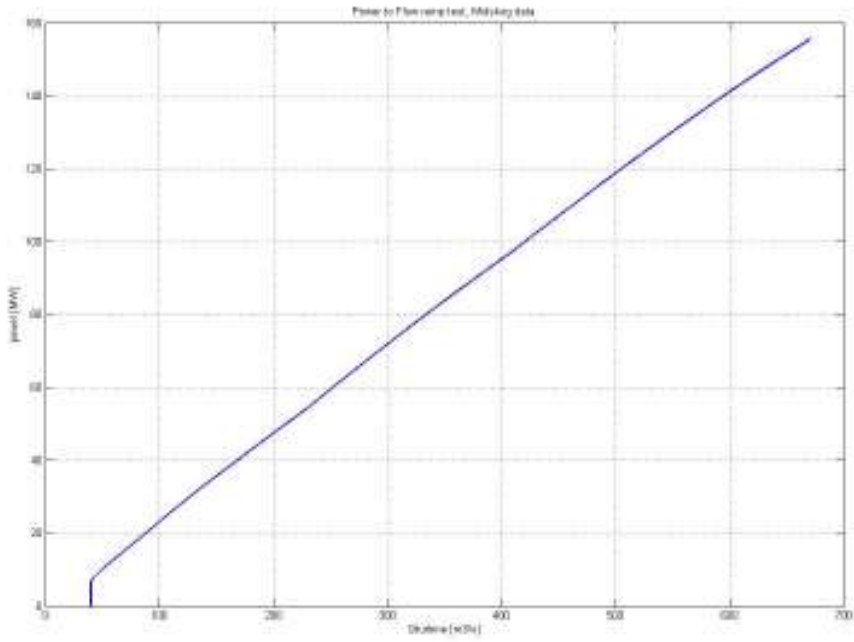


Figure 24: Ramping test of the Midskog power to flow module. The discharge range spans from the absolute minimum to absolute maximum for the Midskog hydropower station and thereby also over several generation unit combinations.

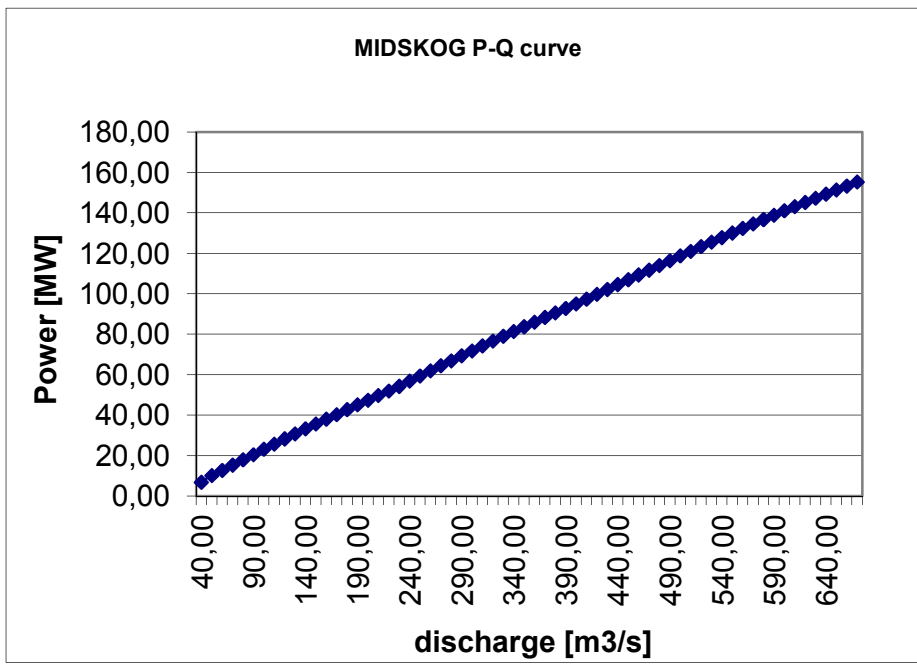


Figure 25: A power vs. discharge curve for the Midskog hydropower station taken from SOPT-tables provided by Vattenfall.

As you can see Figure 24 follows the curve of Figure 25 close enough for our purposes.

4.2 LFC – distribution module

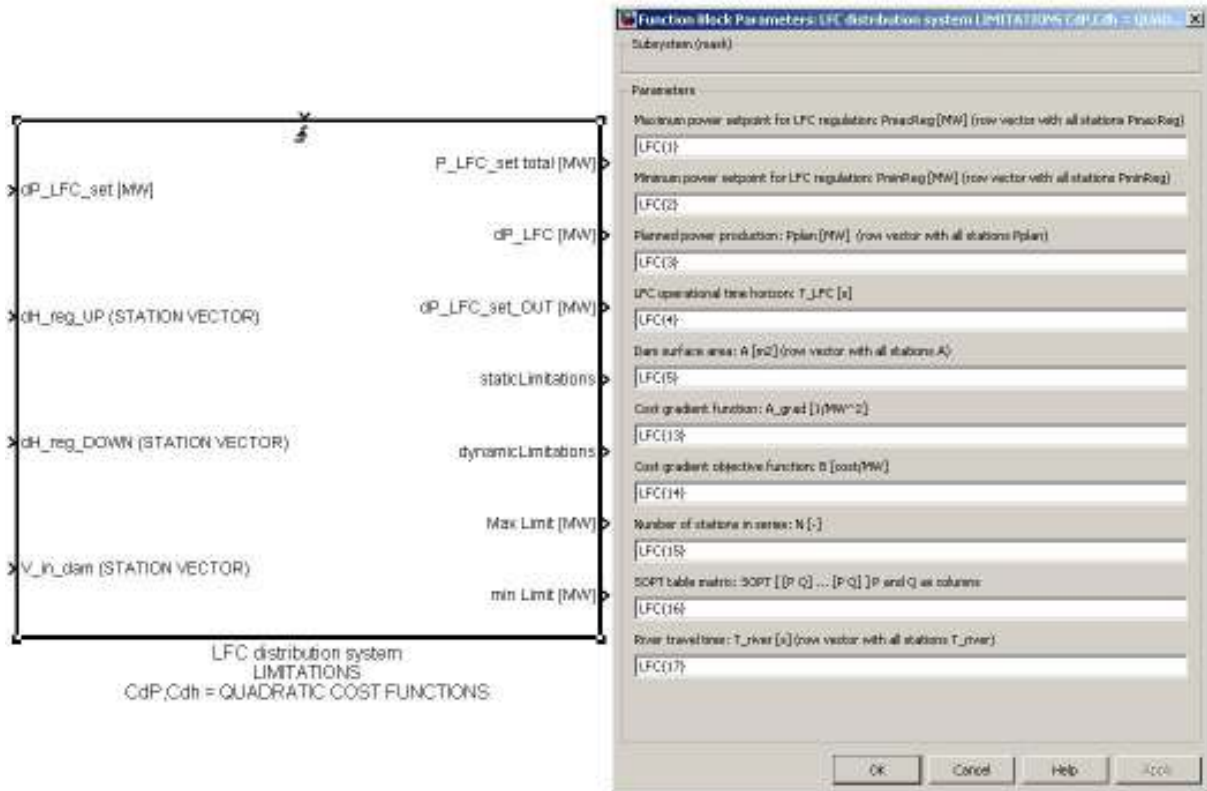


Figure 26: LFC distribution module with I/O and GUI for internal parameters

The purpose of the *LFC distribution module* is to distribute the incoming LFC demand signal, from the TSO's SCADA systems, by minimizing a target function restricted by certain limitations, see eq. 31 to eq. 33.

$$\text{eq. 31} \quad \Delta \bar{P}_{LFC \text{ setpoint}} = \min(C_{\text{tot}}) = \min(C_{\Delta P} + C_{\Delta H})$$

$$\text{eq. 32} \quad \bar{P}_{\text{setpoint}} = \bar{P}_{\text{plan}} + \Delta \bar{P}_{LFC \text{ setpoint}}$$

$$\text{eq. 33} \quad \max(P_{\text{min Static}}^n, P_{\text{min Dynamic}}^n) \leq P_{\text{setpoint}}^n \leq \min(P_{\text{min Static}}^n, P_{\text{min Dynamic}}^n)$$

C_{tot} = total target function

$C_{\Delta P}$ = power deviation target function

$C_{\Delta H}$ = power deviation target function

P_{plan} = planned power production [MW]

$\Delta P_{LFC \text{ setpoint}}$ = distributed LFC setpoint [MW]

P_{setpoint} = setpoint signal used for the turbine governors [MW]

P_{Static} = static limitation [MW]

P_{dynamic} = dynamic limitation [MW]

4.2.1 Limitations

The implemented limitations for the LFC-distribution are:

- Water limits: Upper/Lower reservoir limits, min/max discharge

- Power limits: Min/max power output for current generation unit.

From the limitations above one static and one dynamic power interval is created. The static interval is the maximum and minimum power production that each generation unit can deliver power within in combination with overall min/max discharge regulations for the station and reservation for FCR capacity. This interval is then defined as

$$\text{eq. 34} \quad P_{\min} + \Delta P_{\text{FCR}} \leq P_{\text{setpoint}} \leq P_{\max} - \Delta P_{\text{FCR}}$$

$$\text{eq. 35} \quad P_{\min \text{ Static}} = P_{\min} + \Delta P_{\text{FCR}}$$

$$\text{eq. 36} \quad P_{\max \text{ Static}} = P_{\max} - \Delta P_{\text{FCR}}$$

$P_{\max/\min}$ = max/min capability of current generation setup [MW]

ΔP_{FCR} = reserved FCR capacity [MW]

To be able to use this entire interval the river needs to be accelerated or decelerated in order to keep the water levels within their limits. For this reason a dynamic limit was developed for the power interval.

Say that a station is working at a power level of P_{setpoint} . Then there is a maximum and minimum power level that the station is able to change its power setpoint to and hold for a time T_{LFC} so that the water levels do not exceed the reservoir limitations. When the limitations are exceeded the reservoir is either *full* or *empty*. The dynamic interval is calculated as follows:

$$\text{eq. 37} \quad V_{\text{reservoir}}^n(t + T_{\text{LFC}}) = V_{\text{reservoir}}^n + (< Q_{\text{in reservoir}}^n(t) > - Q_{\text{out reservoir}}^n(t))$$

$$V_{\text{reservoir}}^n(t + T_{\text{LFC}}) = \text{empty, full} = 0, A_{\text{reservoir}}^n \Delta H_{\text{reservoir}}^n$$

$$\text{eq. 38} \quad < Q_{\text{in reservoir}}^n(t) > = \frac{V_{\text{river}}^n(t)}{T_{\text{river}}^n}$$

$$\text{eq. 39} \quad Q_{\text{out reservoir}}^n = \text{flow}(P_{\text{setpoint}}^n) \leftrightarrow P_{\text{setpoint}}^n = \text{flow}^{-1}(Q_{\text{out reservoir}}^n)^6$$

$V_{\text{river}}(t)$ = stored water volume within the river [m³]

T_{river} = river propagation time [s]

$\Delta H_{\text{reservoir}}$ = regulation capacity within the reservoir [m]

$A_{\text{reservoir}}$ = reservoir surface area [m²]

eq. 38 is used to predict what the mean flow in the river by relating the stored volume in the river to the wave propagation time. It's then used to give a greater accuracy for the river outflow to the reservoir may be. The minimum value for the power setpoints can then calculated by

$$\begin{aligned} \text{eq. 40} \quad V_{\text{reservoir}}^n(t + T_{\text{LFC}}) &= A_{\text{reservoir}}^n \Delta H_{\text{reservoir}}^n \\ &= A_{\text{reservoir}}^n \Delta h_{\text{reg down}}^n(t) + (< Q_{\text{in reservoir}}^n(t) > - Q_{\text{out reservoir MIN}}^n(t)) T_{\text{LFC}} \end{aligned}$$

$$\text{eq. 41} \quad Q_{\text{out reservoir MIN}}^n(t) = < Q_{\text{in reservoir}}^n(t) > - \frac{A_{\text{reservoir}}^n}{T_{\text{LFC}}} (\Delta H_{\text{reservoir}}^n - \Delta h_{\text{reg down}}^n(t))$$

⁶ The function *flow()* referred to is a Simulink Look-up table with P vs. Q data (SOPT-tables, see 4.1.4 Turbine flow function)

$$= \langle \mathbf{Q}_{\text{in reservoir}}^n(\mathbf{t}) \rangle - \frac{\mathbf{A}_{\text{reservoir}}^n}{\mathbf{T}_{\text{LFC}}} \Delta \mathbf{h}_{\text{reg up}}^n(\mathbf{t})$$

Substituting eq. 41 into eq. 39 gives the maximum allowed power setpoint.

$$\text{eq. 42} \quad \mathbf{P}_{\text{min Dynamic}}^n(\mathbf{t}) = \text{flow}^{-1} \left(\langle \mathbf{Q}_{\text{in reservoir}}^n(\mathbf{t}) \rangle - \frac{\mathbf{A}_{\text{reservoir}}^n}{\mathbf{T}_{\text{LFC}}} \Delta \mathbf{h}_{\text{reg up}}^n(\mathbf{t}) \right)$$

The same procedure is then used to calculate the maximum allowed power setpoint.

$$\text{eq. 43} \quad \mathbf{V}_{\text{reservoir}}^n(\mathbf{t} + \mathbf{T}_{\text{LFC}}) = \mathbf{0} \\ = \mathbf{A}_{\text{reservoir}}^n \Delta \mathbf{h}_{\text{reg down}}^n(\mathbf{t}) + (\langle \mathbf{Q}_{\text{in reservoir}}^n(\mathbf{t}) \rangle - \mathbf{Q}_{\text{out reservoir MAX}}^n(\mathbf{t})) \mathbf{T}_{\text{LFC}}$$

$$\text{eq. 44} \quad \mathbf{P}_{\text{max Dynamic}}^n(\mathbf{t}) = \text{flow}^{-1} \left(\langle \mathbf{Q}_{\text{in reservoir}}^n(\mathbf{t}) \rangle - \frac{\mathbf{A}_{\text{reservoir}}^n}{\mathbf{T}_{\text{LFC}}} \Delta \mathbf{h}_{\text{reg down}}^n(\mathbf{t}) \right)$$

To enforce the limitations, two Booleans are created, *staticLimitations* and *dynamicLimitation*. These are set to [-1;0;1] if the incoming LFC demand signal is less than, within or greater than the sum of all allowed static and dynamic limits respectively.

$$\text{eq. 45} \quad \begin{aligned} \Delta \mathbf{P}_{\text{LFC demand}} \leq \sum_{n=1}^N (\mathbf{P}_{\text{min Static}}^n - \mathbf{P}_{\text{plan}}^n) & \quad \text{staticLimitations} = -1 \\ \sum_{n=1}^N (\mathbf{P}_{\text{min Static}}^n - \mathbf{P}_{\text{plan}}^n) \leq \Delta \mathbf{P}_{\text{LFC demand}} \leq \sum_{n=1}^N (\mathbf{P}_{\text{max Static}}^n - \mathbf{P}_{\text{plan}}^n) & \quad \text{staticLimitations} = 0 \\ \sum_{n=1}^N (\mathbf{P}_{\text{max Static}}^n - \mathbf{P}_{\text{plan}}^n) \leq \Delta \mathbf{P}_{\text{LFC demand}} & \quad \text{staticLimitations} = 1 \end{aligned}$$

$$\text{eq. 46} \quad \begin{aligned} \Delta \mathbf{P}_{\text{LFC demand}} \leq \sum_{n=1}^N (\mathbf{P}_{\text{min Dynamic}}^n - \mathbf{P}_{\text{plan}}^n) & \quad \text{dynamicLimitations} = -1 \\ \sum_{n=1}^N (\mathbf{P}_{\text{min Dynamic}}^n - \mathbf{P}_{\text{plan}}^n) \leq \Delta \mathbf{P}_{\text{LFC demand}} \leq \sum_{n=1}^N (\mathbf{P}_{\text{max Dynamic}}^n - \mathbf{P}_{\text{plan}}^n) & \quad \text{dynamicLimitations} = 0 \\ \sum_{n=1}^N (\mathbf{P}_{\text{max Dynamic}}^n - \mathbf{P}_{\text{plan}}^n) \leq \Delta \mathbf{P}_{\text{LFC demand}} & \quad \text{dynamicLimitations} = 1 \end{aligned}$$

If the static- or dynamic limitation booleans are initiated, then the incoming LFC signal is truncated as to fit within the desired interval in eq. 47.

$$\text{eq. 47} \quad \sum_{n=1}^N (\max(\mathbf{P}_{\text{min Static}}^n, \mathbf{P}_{\text{min Dynamic}}^n) - \mathbf{P}_{\text{plan}}^n) \leq \Delta \mathbf{P}_{\text{LFC setpoint}} \leq \sum_{n=1}^N (\min(\mathbf{P}_{\text{max Static}}^n, \mathbf{P}_{\text{max Dynamic}}^n) - \mathbf{P}_{\text{plan}}^n)$$

4.2.2 Target functions

The target functions are designed with the minimization of deviation as the objective. These deviations are

- Power setpoint deviation from original plan
- Surface level deviation

From this, the target functions are defined, eq. 48, with eq. 49 used as a constraint which in turn sets the last station as a “slack-unit” to make sure that the LFC demands are met, eq. 50.

$$\text{eq. 48} \quad \mathbf{C}_{\text{tot}} = \mathbf{C}_{\Delta \mathbf{P}} + \mathbf{C}_{\Delta \mathbf{H}}$$

$$\text{eq. 49} \quad \sum_{n=1}^N \Delta \mathbf{P}_{\text{LFC setpoint}}^n = \Delta \mathbf{P}_{\text{LFC demand}}$$

$$\text{eq. 50} \quad \Delta \mathbf{P}_{\text{LFC setpoint}}^N = \Delta \mathbf{P}_{\text{LFC demand}} - \sum_{n=1}^{N-1} \Delta \mathbf{P}_{\text{LFC setpoint}}^n$$

Within the next two sections the two target functions will be described briefly, for more detailed explanations see Appendix A.6 LFC – distribution module.

4.2.2.1 Power deviation target function

The power deviation target function, eq. 51, is designed to minimize LFC frequency regulation at each station by penalizing a power deviation from the planned production:

$$\text{eq. 51} \quad C_{\Delta P} = \sum_{n=1}^N k_n \frac{(\Delta P_{\Delta P, \text{LFC setpoint}})^2}{P_{\text{base}}^n}$$

k_n = weight factor [1]

eq. 51 can also be expressed as a quadratic matrix equation

$$\text{eq. 52} \quad C_{\Delta P} = \mathbf{X}_{\Delta P}^T \mathbf{K}_{\Delta P} \mathbf{X}_{\Delta P}$$

With the target function being quadratic it is possible to analytically calculate its minimum point.

$$\text{Eq. 53} \quad \nabla C_{\Delta P} = \begin{bmatrix} dC_{\Delta P} / d\Delta P_{\text{LFC setpoint}}^1 \\ \vdots \\ dC_{\Delta P} / d\Delta P_{\text{LFC setpoint}}^{N-1} \end{bmatrix}^{N-1 \times 1} = \mathbf{0}$$

Substituting eq. 52 into Eq. 53 gives

$$\text{eq. 54} \quad \nabla C_{\Delta P} = \mathbf{X}_{\Delta P}^{\text{grad}} \Delta P_{\text{LFC setpoint}} - \mathbf{B}_{\Delta P} = \mathbf{0}$$

eq. 54 can be solved by

$$\text{eq. 55} \quad \Delta P_{\text{LFC setpoint}}^{\text{minCost}} = (\mathbf{X}_{\Delta P}^{\text{grad}})^{-1} \mathbf{B}_{\Delta P}$$

4.2.2.2 Surface level deviation

The surface level deviation target function, eq. 56, is designed to minimize the collection, or withdrawal, of water volumes more from one part of the river than the other, by penalizing deviations in flow between two stations connected in series.

$$\text{eq. 56} \quad C_{\Delta H} = \sum_{n=1}^N k_n \left(\frac{\Delta h_{\text{LFC}}^n}{\Delta H^n} \right)^2 = k_n \left(\frac{T_{\text{LFC}}}{A_{\text{reservoir}}^n \Delta H^n} \right)^2 (\Delta Q_{\text{turbine}}^{n-1} - \Delta Q_{\text{turbine}}^n)^2$$

ΔH = total regulation capacity within the reservoir [m]

Δh_{LFC} = reservoir surface level change from LFC governing [m]

k_n = weight factor [1]

$A_{\text{reservoir}}$ = reservoir surface area [m²]

Q_{turbine} = water discharge [m³/s]

The model does not have direct access to these discharges but these can be derived from eq. 3.

$$\text{eq. 57} \quad Q_{\text{turbine}} = \frac{P}{\eta \rho H} = \alpha P$$

By linearization around a working point and setting this to zero, an expression for the discharge deviation as a result of power regulation can be created.

$$\text{eq. 58} \quad \Delta Q_{\text{turbine}} = \alpha P_0 - Q_0 + \alpha \Delta P$$

$$\text{eq. 59} \quad \Delta Q_{\text{turbine}} = \alpha \Delta P$$

Using eq. 59 and expressing the cost function, eq. 56, as a matrix equation gives the following expression

$$\text{eq. 60} \quad C_{\Delta P} = \mathbf{X}_{\Delta H}^T \mathbf{K}_{\Delta H} \mathbf{X}_{\Delta H}$$

The minimum point can again be found analytically.

$$\text{eq. 61} \quad \nabla C_{\Delta H} = \begin{bmatrix} dC_{\Delta H} / d\Delta P_{LFC \text{ setpoint}}^1 \\ \vdots \\ dC_{\Delta H} / d\Delta P_{LFC \text{ setpoint}}^{N-1} \end{bmatrix}^{N-1 \times 1} = \mathbf{0}$$

The cost gradient can then be expressed by substituting eq. 60 in to eq. 61.

$$\text{eq. 62} \quad \nabla C_{\Delta H} = \mathbf{X}_{\Delta H}^{\text{grad}} \Delta P_{LFC \text{ setpoint}} - \mathbf{B}_{\Delta H} = \mathbf{0}$$

eq. 62 can then be solved by

$$\text{eq. 63} \quad \Delta P_{LFC \text{ setpoint}}^{\text{minCost}} = (\mathbf{X}_{\Delta H}^{\text{grad}})^{-1} \mathbf{B}_{\Delta H}$$

4.2.2.3 Total target minimization

The objective is now to find the operational setpoint that minimizes the total target function of power and surface level deviations, given the said limits.

The total target function and target function gradient within the system are defined by

$$\text{eq. 64} \quad C_{\text{tot}} = C_{\Delta P} + C_{\Delta H}$$

$$\text{eq. 65} \quad \nabla C_{\text{tot}} = \nabla C_{\Delta P} + \nabla C_{\Delta H} = \mathbf{0}$$

Minimization of eq. 64 is then made by combining eq. 55, eq. 56 and eq. 62, eq. 63 with eq. 65.

$$\text{eq. 66} \quad \Delta P_{LFC \text{ setpoint}}^{\text{minCost}} = (\mathbf{X}_{\Delta H}^{\text{grad}} + \mathbf{X}_{\Delta P}^{\text{grad}})^{-1} (\mathbf{B}_{\Delta H} + \mathbf{B}_{\Delta P})$$

To calculate the last stations power setpoint eq. 50 is used.

The operational setpoint then has to be checked against the limits given by eq. 47. If any of the operational points lies outside the boundaries then the target matrices are rearranged according to the following structure.

$$\text{eq. 67} \quad \begin{cases} P_{\min}^n = \max(\Delta P_{\min \text{ Static}}^n, \Delta P_{\min \text{ Dynamic}}^n) \\ P_{\max}^n = \min(\Delta P_{\max \text{ Static}}^n, \Delta P_{\max \text{ Dynamic}}^n) \end{cases}$$

$$\text{eq. 68} \quad \begin{cases} \Delta P_{LFC \text{ setpoint}}^n < \max(\Delta P_{\min \text{ Static}}^n, \Delta P_{\min \text{ Dynamic}}^n), \Delta P_{LFC \text{ setpoint}}^n = P_{\min}^n \\ \Delta P_{LFC \text{ setpoint}}^n > \min(\Delta P_{\max \text{ Static}}^n, \Delta P_{\max \text{ Dynamic}}^n), \Delta P_{LFC \text{ setpoint}}^n = P_{\max}^n \end{cases}$$

$$\text{eq. 69 } \mathbf{X}_{\text{tot}}^{\text{grad}} = \begin{bmatrix} \mathbf{X}_{\text{tot}(1,1)}^{\text{grad}} & \dots & \dots & \mathbf{X}_{\text{tot}(1,n)}^{\text{grad}} & \dots & \dots & \mathbf{X}_{\text{tot}(1,N-1)}^{\text{grad}} \\ \vdots & \ddots & \vdots & \vdots & \vdots & \vdots & \vdots \\ \mathbf{X}_{\text{tot}(n-1,1)}^{\text{grad}} & \dots & \mathbf{X}_{\text{tot}(n-1,n-1)}^{\text{grad}} & \mathbf{X}_{\text{tot}(n-1,n)}^{\text{grad}} & \mathbf{X}_{\text{tot}(n-1,n+1)}^{\text{grad}} & \dots & \mathbf{X}_{\text{tot}(n-1,N-1)}^{\text{grad}} \\ \mathbf{0} & \dots & \mathbf{0} & \mathbf{X}_{\text{tot}(n,n)}^{\text{grad}} = \mathbf{1} & \mathbf{0} & \dots & \mathbf{0} \\ \mathbf{X}_{\text{tot}(n+1,1)}^{\text{grad}} & \dots & \mathbf{X}_{\text{tot}(n+1,n-1)}^{\text{grad}} & \mathbf{X}_{\text{tot}(n+1,n)}^{\text{grad}} & \mathbf{X}_{\text{tot}(n+1,n+1)}^{\text{grad}} & \dots & \mathbf{X}_{\text{tot}(n+1,N-1)}^{\text{grad}} \\ \vdots & \vdots & \vdots & \vdots & \vdots & \ddots & \vdots \\ \mathbf{X}_{\text{tot}(N-1,N-1)}^{\text{grad}} & \dots & \dots & \mathbf{X}_{\text{tot}(N,n)}^{\text{grad}} & \dots & \dots & \mathbf{X}_{\text{tot}(N-1,N-1)}^{\text{grad}} \end{bmatrix}$$

$$\mathbf{B}_{\text{tot}} = \begin{bmatrix} \mathbf{B}_{\text{tot}(1)} \\ \vdots \\ \mathbf{B}_{\text{tot}(n-1)} \\ \mathbf{0} \\ \mathbf{B}_{\text{tot}(n+1)} \\ \vdots \\ \mathbf{B}_{\text{tot}(N-1)} \end{bmatrix} - \mathbf{X}_{\text{tot}(n,n)}^{\text{grad}} = \Delta P_{LFC}^n \text{ setpoint} \begin{bmatrix} \mathbf{X}_{\text{tot}(1,n)}^{\text{grad}} \\ \vdots \\ \mathbf{X}_{\text{tot}(n-1,n)}^{\text{grad}} \\ \mathbf{X}_{\text{tot}(n+1,n)}^{\text{grad}} \\ \vdots \\ \mathbf{X}_{\text{tot}(N,n)}^{\text{grad}} \end{bmatrix}$$

$$\text{eq. 70 } \mathbf{X}_{\text{tot}}^{\text{grad}} = \mathbf{X}_{\Delta H}^{\text{grad}} + \mathbf{X}_{\Delta P}^{\text{grad}}$$

$$\text{eq. 71 } \mathbf{B}_{\text{tot}} = \mathbf{B}_{\Delta H} + \mathbf{B}_{\Delta P}$$

By rearranging the target matrices accordingly, it's possible to eliminate row and column n , that contains the now constant power setpoint and thereby a gradient=0, and at the same recalculate the new power setpoints, without rearranging the power setpoint vector.

Module validation

The LFC distribution module was tested in three ways with a ramped LFC signal; no limitations, static limitations and dynamic limitations.

The first test was with a LFC signal ranging from -30 MW to +30 MW. As one can see both cost functions behave very similar in distributing their signals, see Figure 27.

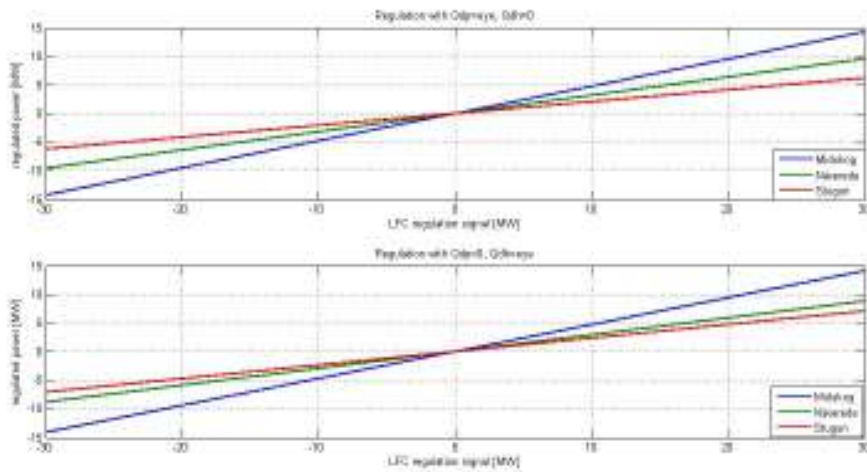


Figure 27: LFC distribution test for the individual cost functions. The weights for the cost function are both set to the identity matrix.

The system was then test with the static and dynamic limitations. For this some parameters need to be defined as seen below.

- Surface setpoint levels: Midskog = 0.5 m, Näverede = 0.05 m and Stugun = 0.05 m.
- Static inflow $Q_0=500 \text{ m}^3/\text{s}$.
- LFC ramp: -50 to +60 MW.

As one can see in Figure 28 the system distributes the LFC signal, but with a non-linear behavior. This non-linearity occurs when a limitation is reached and thereby forcing new distribution setpoints. With the last station acting as a slack-unit, it has been difficult to keep this station within its limits, which shall be seen later in 5.3 Results and discussed in 6.1.3 Governing of the LFC-distribution.

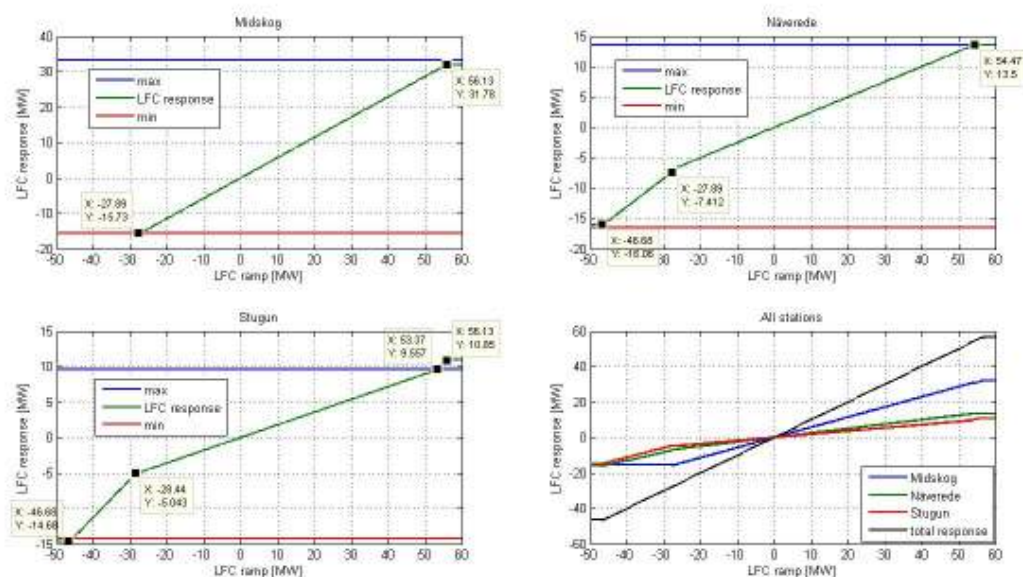


Figure 28: LFC distribution of the river reach Midskog to Stugun with static limitations. Shown are the individual LFC responses box in inside each stations limitation and also a summary of all LFC responses. The points marked are where a station releases or is restricted by its limitation.

It's difficult to test the dynamic limitations, since these are time-dependent, in a static test for the LFC ramp. To test the dynamic limits, the incoming volume in the upstream river has had to be modelled which is made by using the distributed LFC responses from the static simulation as initial values and then calculating the dynamic limitations. The LFC distribution can then be tested with its dynamic limitations and the results can be seen in Figure 29. If one looks closely at the graph it's possible to see that the overshoot and undershoot at *Stugun* matches the undershoot of both *Midskog's* and *Näverede's* limitations respectively. But as seen the entire LFC response is still limited which is related the truncation of the LFC signal as described by eq. 47. As stated earlier, these results will be discussed more in 6.1.3 Governing of the LFC-distribution.

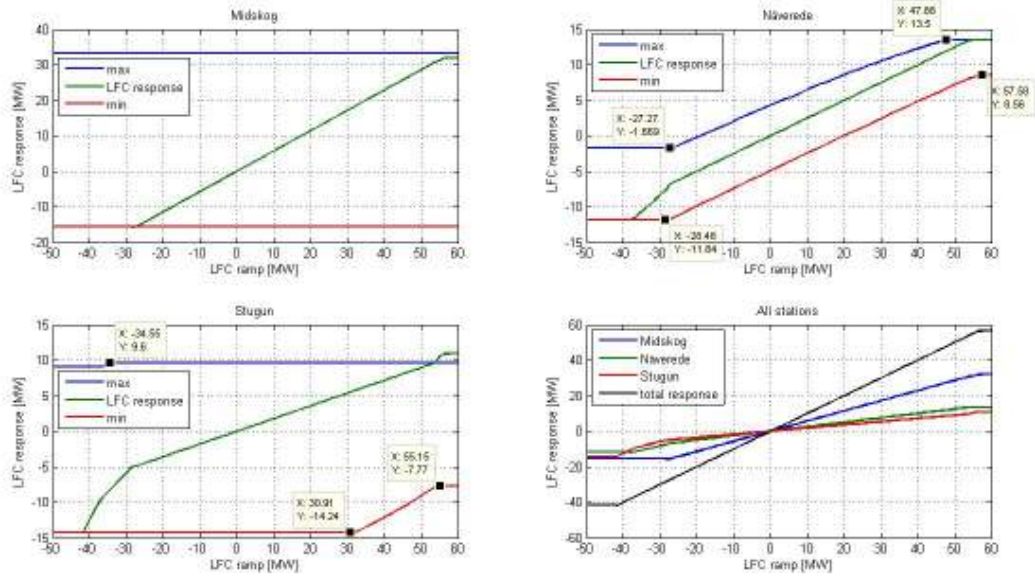


Figure 29: LFC distribution of the river reach Midskog to Stugun with dynamic limitations. Shown are the individual LFC responses box in inside each stations limitation and also a summary of all LFC responses. The points marked are where the limitations change.

4.3 Economical gains and losses from LFC sales⁷

To get a rough estimate of what the automatic LFC market could generate it was chosen to make a calculation of the LFC sales for one simulation, the December 6th simulation, see 5.2 Simulation setup more information on different simulations. This was done by importing the regulation bid prices from the day at hand from Svenska Kraftnät and multiplying this with the sold regulation,

eq. 72. These also need to be compared to some type of losses afflicted by the system,

eq. 73. For this it was decided to only calculate the losses resulting from the lowered reservoir surfaces needed in order to create the extra regulation capacity.

$$\text{eq. 72} \quad SEK_{income} = \sum_t \Delta P_{LFC}^{tot}(t) (RK_{price}(t) / 3600) \Delta T(t)^8$$

$$\text{eq. 73} \quad SEK_{loss} = \left(\frac{\sum_i \Delta h_{station,i}^{loweredSurface}}{\sum_i H_{station,i}^{netHead}} \right) \sum_t P_{plan}(t) (NordPoolSpot_{price}(t) / 3600) \Delta T(t)$$

ΔP_{lfc} = LFC regulation at time t [MW]

RK_{price} = FCR regulation price [SEK/MWh]

$NordPoolSpot_{price}$ = the Nordpool Spot price at time t [SEK/MWh]

Δh = regulated surface setpoint [m]

H = net head for each station [m]

ΔT = time step for simulation at time t [s]

⁷ It should be stated that the TSOs have not yet decided on how this market should work. Therefore this is only on way it theoretically could operate.

⁸ The price has been scaled to SEK/MWs.

5 Simulations

This chapter will describe the initiation for the simulations and also briefly describe the river reaches from a general term of view. After this a summary of the results will be shown, the rest of the results can be found in Appendix C – Simulation results.

5.1 River reaches

5.1.1 Jämtkraft

From Jämtkraft a reach of Indalsälven downstream from Östersund in Jämtland was simulated. The reach consists of three hydropower stations; Hissmofors, Kattstrupefors and Granbofors with the following general characteristics seen in Table 1.

Table 1: General description for the Jämtkraft river reach

	Hissmofors	Kattstrupefors	Granbofors
Pmax [MW]	68	62	24
minimum discharge [m³/s]	50	50	50
maximum discharge [m³/s]	440	440	440
maximum head [m]	20	18	6
reservoir volume	14515 [DU] ⁹	830 [HU] ¹⁰	142 [HU]
reservoir regulations capacity [m]	2,75	0,75	0,25
river travel time [min]	-	2	2

5.1.2 Vattenfall

From Vattenfall a reach of Indalsälven down streams from Östersund in Jämtland was also simulated. The reach consists of three hydropower stations; Midskog, Näverede and Stugun with the following general characteristics seen in Table 2.

Table 2: General description for the Vattenfall river reach

	Midskog	Näverede	Stugun
Pmax [MW]	155	67	48
minimum discharge [m³/s]	100	100	100
maximum discharge [m³/s]	650	670	675
maximum head [m]	27	13	7.3
reservoir volume [HU]	4800	50	280
reservoir regulations capacity [m]	0,6	0,1	0,1
river travel time [min]	-	11	45

⁹ 1 [DU] = 1 daily unit = the volume from a flow of 1 m³/s for a whole day = 24 [h] * 3600 [s/h] * 1 [m³/s]

¹⁰ 1 [HU] = 1 hourly unit = the volume from a flow of 1 m³/s for a whole hour = 3600 [s] * 1 [m³/s]

5.1.3 Fortum

From Fortum a reach of Ljusnan was simulated from the hydropower station at Sveg to Öjeforsen with four stations in between them with the following general characteristics seen in Table 3.

Table 3: General description for the Fortum river reach

	Sveg	Byaforsen	Krokströmmen
Pmax [MW]	34,5	18,5	116,6
minimum discharge [m³/s]	0	0	0
maximum discharge [m³/s]	210	210	200
maximum head [m]	19	10	60
reservoir volume	2743 [DU]	180 [HU]	850 [HU]
reservoir regulations capacity [m]	11	0,4	0,5
river travel time [min]	-	10	75
	Långströmmen	Storåströmmen	Öjeforsen
Pmax [MW]	56,6	27,5	31,4
minimum discharge [m³/s]	0	0	60
maximum discharge [m³/s]	205	190	190
maximum head [m]	31,5	16,5	17,5
reservoir volume	210 [HU]	520 [HU]	250 [HU]
Reservoir regulations capacity [m]	0,35	0,4	0,5
river travel time [min]	15	20	15

5.2 Simulation setup

The simulations have been setup using a pre-defined simulation in the model from (ENTSO-E 2011a) called *imbalanceSim*. In this simulation a load imbalance from three different 24 hour frequency series, May 3rd, Aug 2nd and Dec 6th of 2010, are created with a time resolution of one second, see **Fel! Hittar inte referensälla..** The overlying LFC governor, in the ENTSO-E model, is a normal PI-governor using a second-order low pass filtered frequency signal as input and discrete update rate and block size as output (ENTSO-E 2011b, kap.4.5 2.8.2). The LFC PI-governor has been setup with the following parameters:

$$K_p = 0.3 [1]$$

$$T_i = 200 [s]$$

$$T_{\text{update rate}} = 10 [s]$$

$$\text{Min block size} = 10 [\text{MW}]$$

$$T_{\text{filter}} = 100 [s]$$

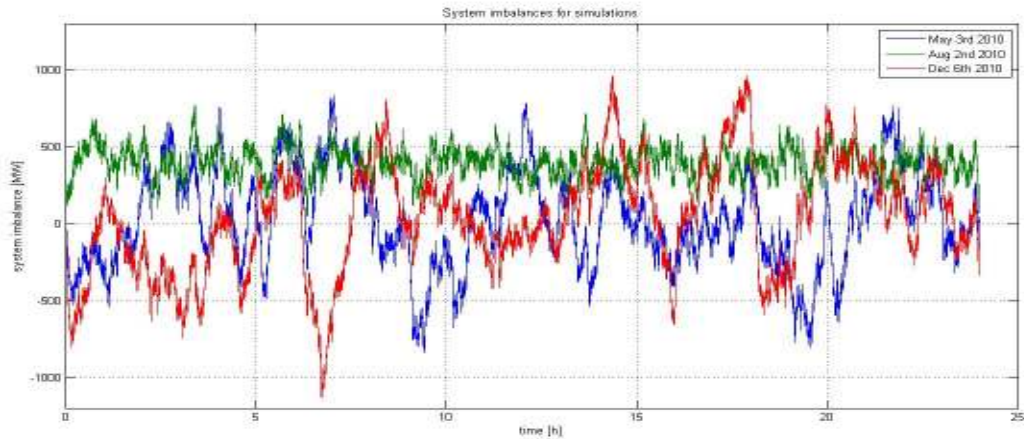


Figure 30: System imbalances used for simulations in the ENTSO-E Simulink model. The August imbalance depicts an only over balanced power system whereas the May and December imbalances depict an oscillating power balance in the power system.

The scope for this thesis project includes an analysis of how a river reach with small regulation capacities, so called *run-of-river* stations, can contribute with regulating capabilities in a system with low load, medium load and a high load. These load conditions are to be represented with the simulations at hand of Aug 2nd, May 3rd and Dec 6th respectively

In order to create a more realistic simulation, the plans for each simulated day have been collected for the three different reaches. Unfortunately this is also where one of the major drawbacks with this model comes in to play; the model can only use one discharge plan per hydropower station and simulation.¹¹ Because of this, a static discharge has had to be chosen that “resembles” the discharge plan during the day. These discharge plans were created by trying to set a discharge that would resemble the larger part of the day.

The original plan was to include both FNR and FDR regulation reserves in the simulations. When the first simulations was setup it was found that the LFC and FDR regulation used too much of each other’s reserved capacity and the FDR regulation was therefore neglected. *The reserved regulation capacity for most simulations therefore only includes FNR regulation capacity.*

For more information concerning the individual set up of each simulation and power stations see Appendix B – Initiation files/values.

5.3 Results

This section will only show the results from the Vattenfall river reach, for Fortum and Jämtkraft see Appendix C – Simulation results. This reach was chosen because it was deemed as the most extreme case scenario with small reservoir volumes and reservoir regulation capacities, which has been said to be the largest obstacles for using this type of automatic regulation. (Byström 2011)

For each simulation four distinct graphs have been created:

¹¹ During the early stages of planning the model it was unknown if access to the ENTSO-E model would be granted. It was therefore decided that a static flow plan was to be used for simplicity. There are however methods for implementing a dynamic signal by importing vectors from the Matlab workspace to Simulink but it’s been chosen to not implement this.

1. Mechanical power output [MW] for each station and current grid frequency [Hz]. A moving average is also implemented on the frequency and is only used to create a better understanding of what the frequency is and is not used as an input for *any* simulations. Figure 33 for an example.
2. Active regulation of each power station, both FCR (green) and LFC (blue) regulation [MW]. This graph also contains the maximum (red)/minimum (turquoise) LFC regulation capacity per station [MW]. See Figure 35 for an example.
3. Resulting flows in the river with incoming flow to the river, incoming flow to the reservoir and discharge through the turbine draining the reservoir, all values are given in [m³/s]. See Figure 37 for an example.
4. Resulting water levels [m] in each reservoir, including maximum and minimum water level according to operational guidelines. This graph also includes a derivation of the reservoir volumes which is calculated as $dV/dt = Q_{in} - Q_{out}$ [m³/s]. See Figure 39 for an example.

Each simulation has been simulated with the automatic LFC turned *on* and *off*, to show the major differences in operation. This was chosen since the built model is not an exact replica of the physical system and because it does not have an active surface level governor implemented¹².

To give you an idea of the entire system behaviour the ENTSO-E model has been simulated in its original form for the three different load imbalance scenarios, with the LFC turned on and off, see Figure 31. This has been done to show you the entire LFC demand and how the frequency is changed with the LFC control system implemented. One can see that for the May and December simulations the system is both over and underbalanced with an oscillating LFC demand as a result. With LFC reserves implemented the grid frequency is more centred on the nominal of 50 Hz, which is seen with the frequency histograms on the right hand side in Figure 31 for all three scenarios.

¹² A surface level governor is used to keep the dam surface at a certain reference setpoint within the reservoir. It was chosen not to use these to let the surfaces “float” more freely within the reservoir regulation interval. The model has instead implemented power setpoint limitations to trap the surfaces within the reservoir limitations and can thereby only limit the surfaces at the extreme end points and not govern the surface to a specific point.

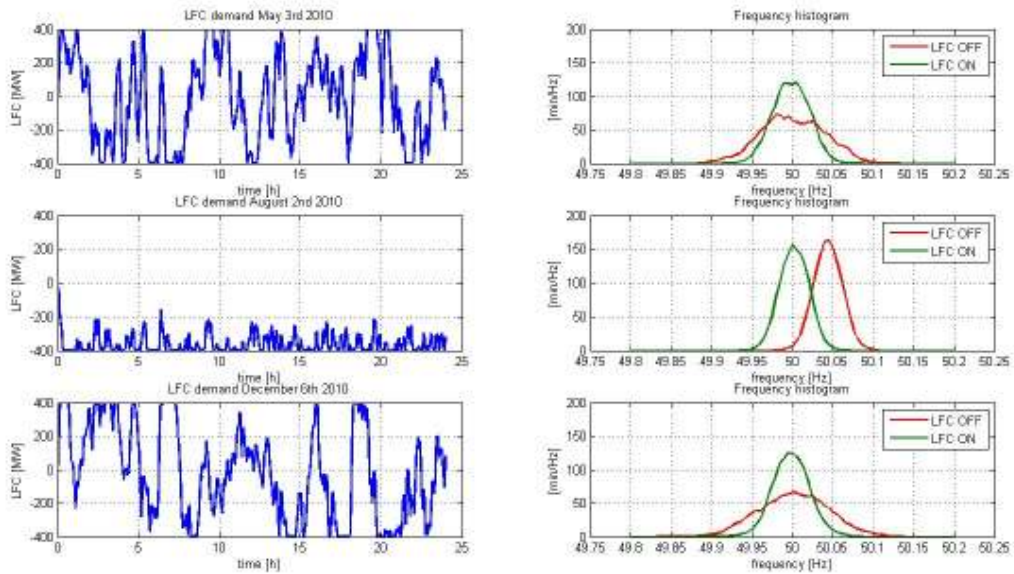


Figure 31: Imbalance simulations made with the original ENTSO-E model. Shown are the total LFC demands [MW] and the frequency histograms for each simulation.

5.3.1 Vattenfall

For this reach four graphs will be displayed for one of the simulations, Dec 6th 2010. For May 3rd and Aug 2nd, only the power/frequency and the water level developments will be shown. The remaining graphs can be found in Appendix C – Simulation results. A brief comment will also be given to each graph in order to explain the developments.

December 6th 2010

Figure 32 and Figure 33 displays the mechanical power output from Midskog, Näverede and Stugun as a result of a stationary planned discharge of $Q_0=500 \text{ m}^3/\text{s}$ with only Midskog providing FCR regulation but with all three stations contributing with LFC regulation.

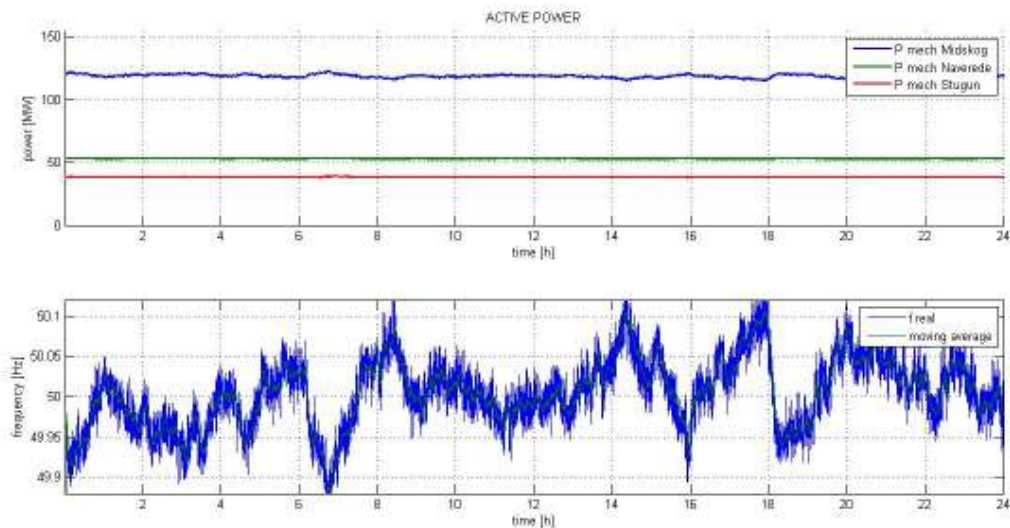


Figure 32: LFC = OFF, 2010-12-06 simulation. Mechanical power delivered by Midskog, Näverede and Stugun displayed with the resulting grid frequency.

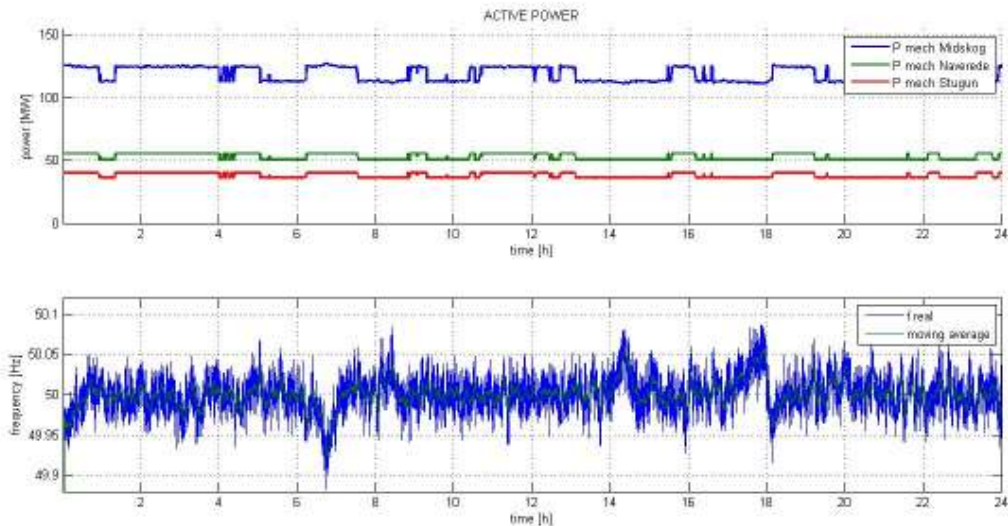


Figure 33: LFC = ON, 2010-12-06 simulation. Mechanical power delivered by Midskog, Näverede and Stugun displayed with the resulting grid frequency.

Figure 34 and Figure 35 displays how each station reacts to the resulting grid frequency with the LFC governor turned on or off. Take special notice that only Midskog that delivers FCR regulation. In Figure 34 one can also see the impact of the distributed LFC signals reaching a limit forcing another distribution. This redistribution is seen at Midskog and Stugun which govern up and down respectively due to a limitation at Näverede. This limitation at Näverede is a result from a surface level deviation in the Näverede reservoir which is seen in Figure 38. One also sees the two different limitations imposed on the system; static and dynamic. At Näverede the dynamic limitations are chosen since these have the tightest constraints whereas for Stugun the static limitation is used.

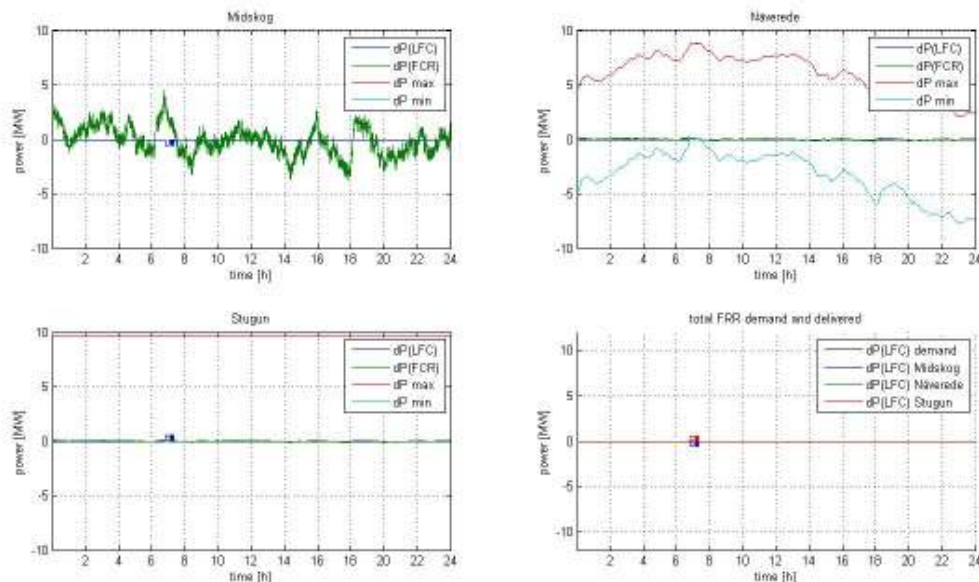


Figure 34: LFC = OFF, 2010-12-06 simulation. Active power regulation delivered by Midskog, Näverede and Stugun. The graph also includes a section showing all LFC regulation compared to the incoming LFC signal. The limitations imposed on the stations are also shown, but as for Midskogs, these may lie outside the total LFC regulation demand of +/- 10 MW and are therefore not in the graphs.

In Figure 35 one can see the direct impact that the LFC system has on FCR regulation at Midskog. By implementing the LFC system the grid frequency is kept closer to the nominal value and thereby the FCR does not have to regulate as much. One can however see that the LFC signal is larger in terms of both power and energy which is closely related for the economical market, see 6.2.1 Active Power regulation for more information.

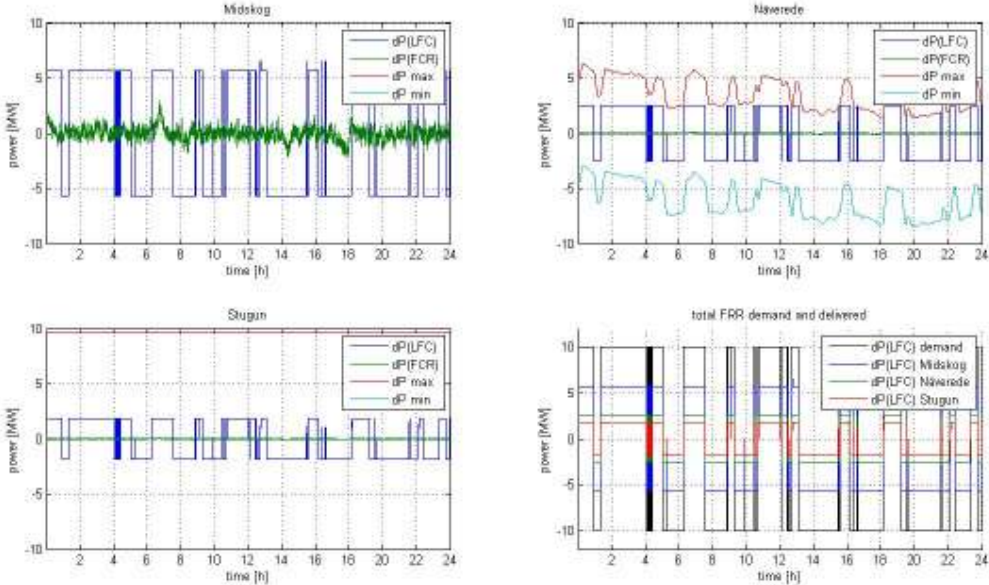


Figure 35: LFC = ON, 2010-12-06 simulation. Active power regulation delivered by Midskog, Näverede and Stugun. The graph also includes a section showing all LFC regulation compared to the incoming LFC signal. The graph for Midskog clearly shows the impact that the LFC system has on FCR regulation when compared to Figure 34.

The difference in regulation with LFC on or off also result in different water flow patterns which can be seen in Figure 36 and Figure 37. Take special notice to the phase delay between the water entering the river (Q river) and exiting the river in to the reservoir (Q reservoir) since this in one of the major drivers for a surface level deviations.

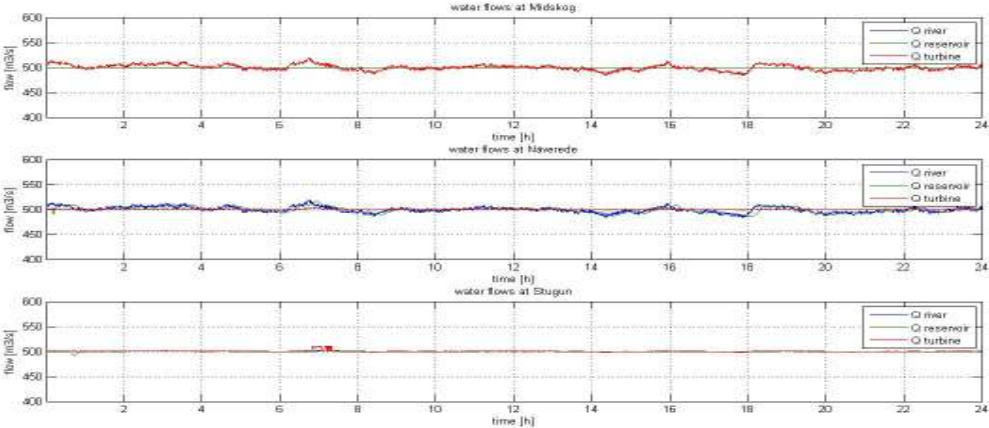


Figure 36: LFC = OFF, 2010-12-06 simulation. Resulting water flows entering the river (for Midskog, the flow entering and exiting the river is the same since this is kept as constant), entering the reservoir and discharge used by the turbine to provide mechanical power.

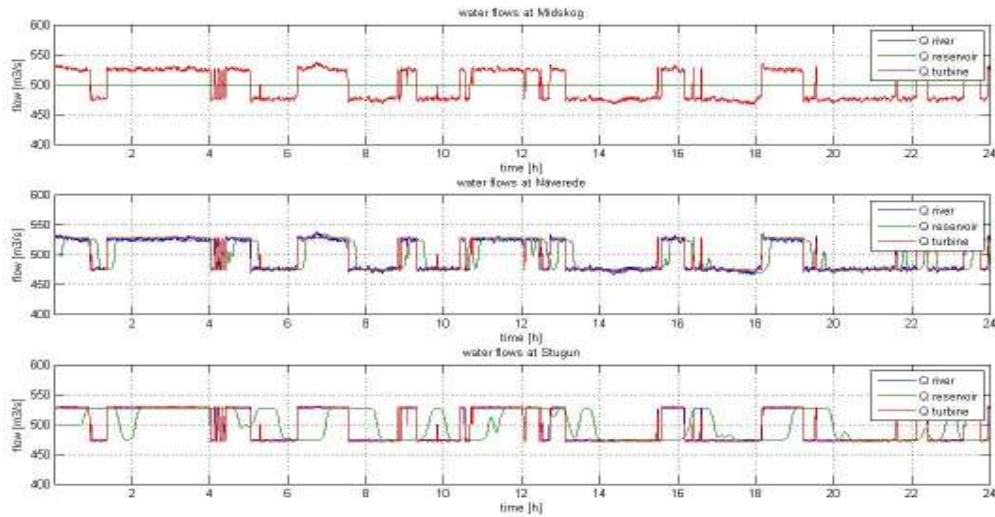


Figure 37: LFC = ON, 2010-12-06 simulation. Resulting water flows entering the river for Midskog, the flow entering and exiting the river is the same since this is kept as constant), entering the reservoir and discharge used by the turbine to provide mechanical power.

From water flows above, the reservoir surface level development can be extruded, see Figure 38 and Figure 39. The graphs also include a derivative of the volume change within the reservoir derived as inflow minus outflow. For Figure 38 it is important to remember that there is no surface level governor implemented within the system and the Näverede surface thereby deviates as a result of FCR regulation at Midskog. This could have been compensated some by letting Näverede also take part in FCR regulation but this is not done in practise.

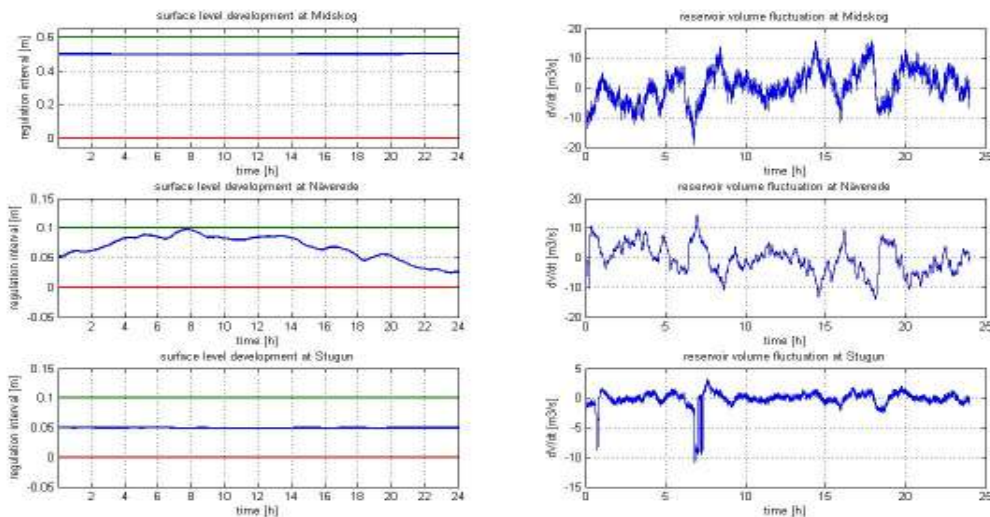


Figure 38: LFC = OFF, 2010-12-06 simulation. Resulting water levels in the reservoirs of Midskog, Näverede and Stugun. The derivative of the reservoir volume fluctuation is also shown.

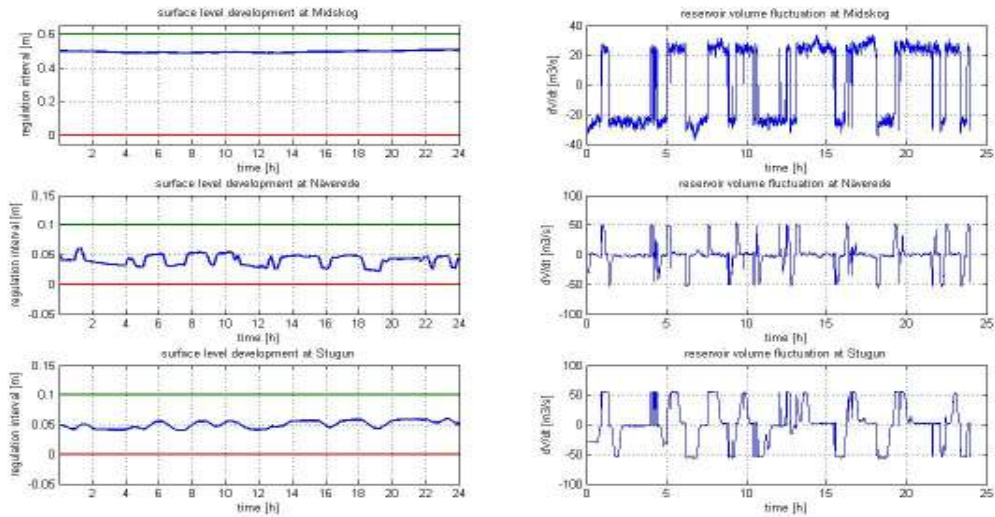


Figure 39: LFC = ON, 2010-12-06 simulation. Resulting water levels in the reservoirs of Midskog, Näverede and Stugun. The derivative of the reservoir volume fluctuation is also shown.

For this simulation, Dec 6th, an economical calculation was also made in accordance with eq. 72 and eq. 73.

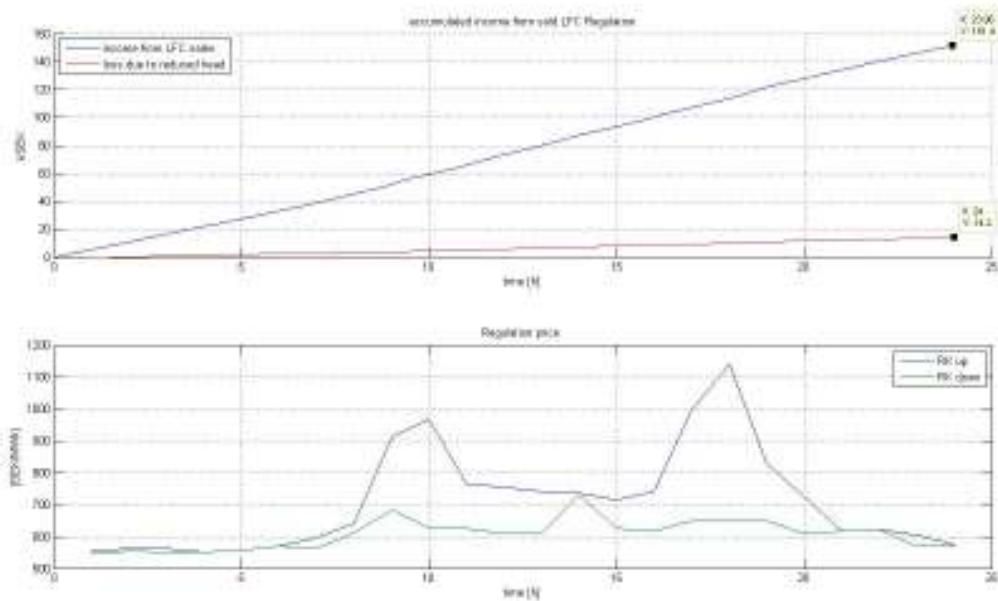


Figure 40: Accumulated income and losses from LFC sales and the MWh price (RK up, RK down) for regulation bids of 2010-12-06.

May 3rd 2010

As said before, only the power/frequency graph and the resulting reservoir surface level graphs will be shown in this section. For explanatory comments see section describing the simulation for December 6th 2010.

This simulation has a stationary planned discharge of $Q_0=310\text{m}^3/\text{s}$, Midskog providing FCR regulation and with all three stations providing LFC regulation.

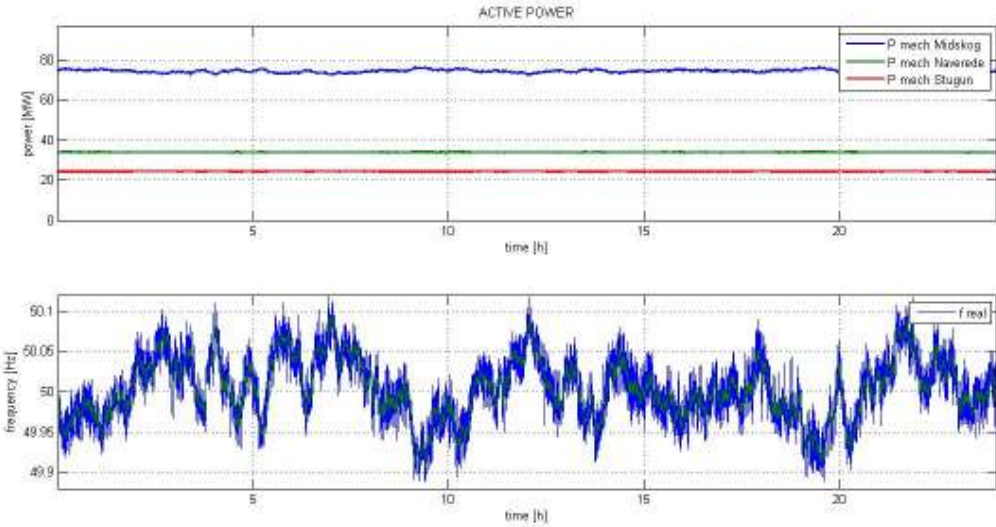


Figure 41: LFC = OFF, 2010-05-03 simulation, Mechanical power delivered by Midskog, Näverede and Stugun displayed with the resulting grid frequency.

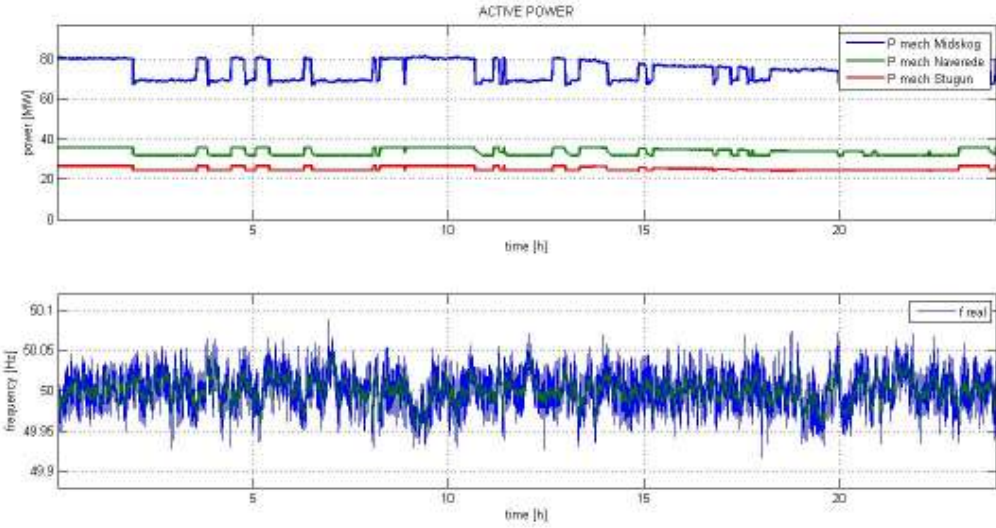


Figure 42: LFC = ON, 2010-05-03 simulation, Mechanical power delivered by Midskog, Näverede and Stugun displayed with the resulting grid frequency.

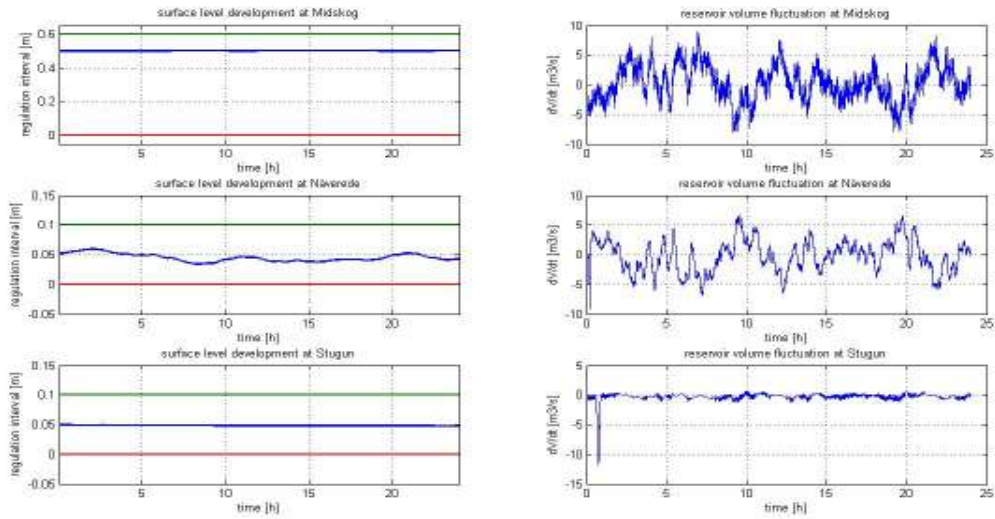


Figure 43: LFC = OFF, 2010-05-03 simulation, Resulting water levels in the reservoirs of Midskog, Näverede and Stugun. The derivative of the reservoir volume fluctuation is also shown.

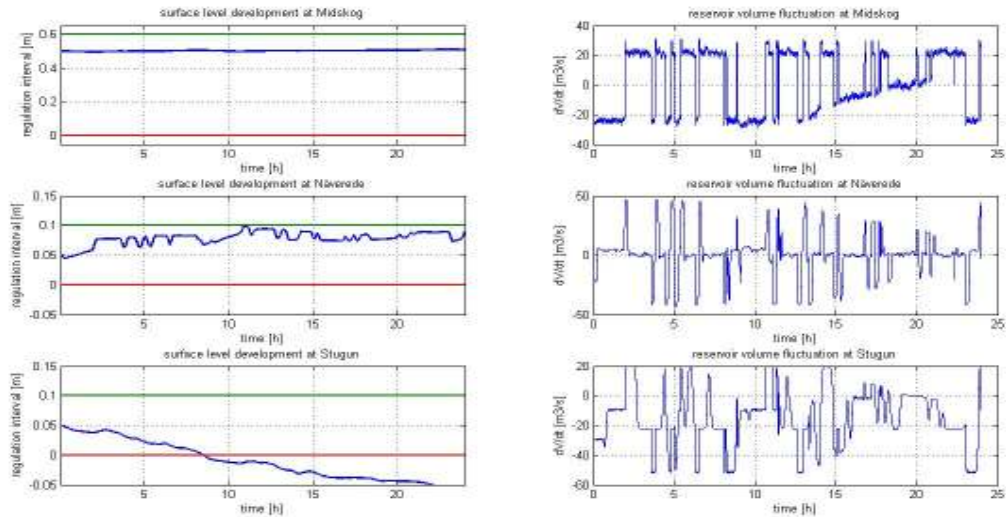


Figure 44: LFC = OFF, 2010-05-03 simulation, Resulting water levels in the reservoirs of Midskog, Näverede and Stugun. The derivative of the reservoir volume fluctuation is also shown.

As you can see here in Figure 44 the lower reservoir limit is breached for Stugun. This will be explained more in 6.1 Model implementation.

August 2nd 2010

The static planned discharge for this simulation is $Q_0=75 \text{ m}^3/\text{s}$.

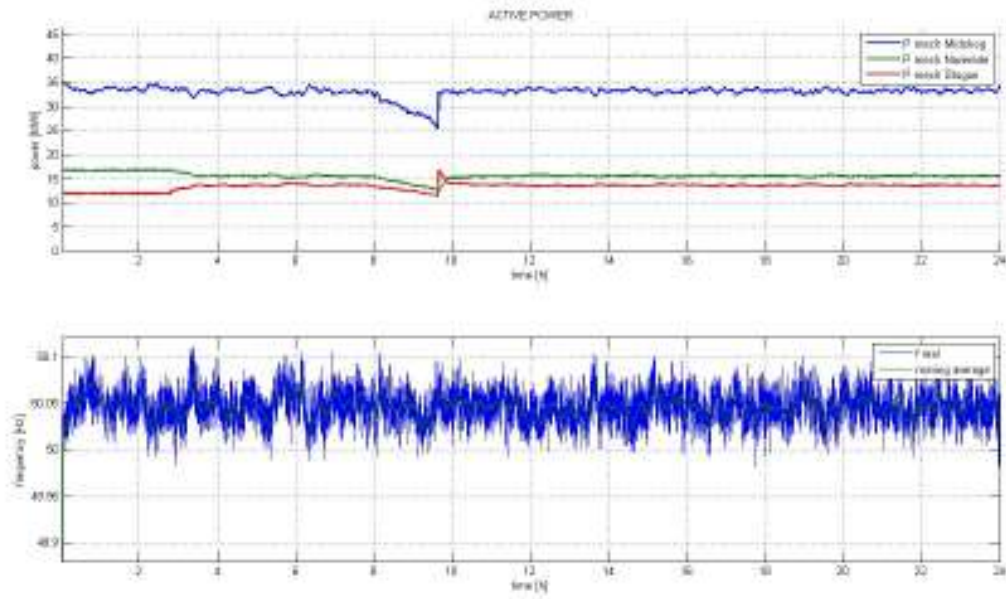


Figure 45: LFC = OFF, 2010-08-02 simulation, Mechanical power delivered by Midskog, Närke and Stugun displayed with the resulting grid frequency.

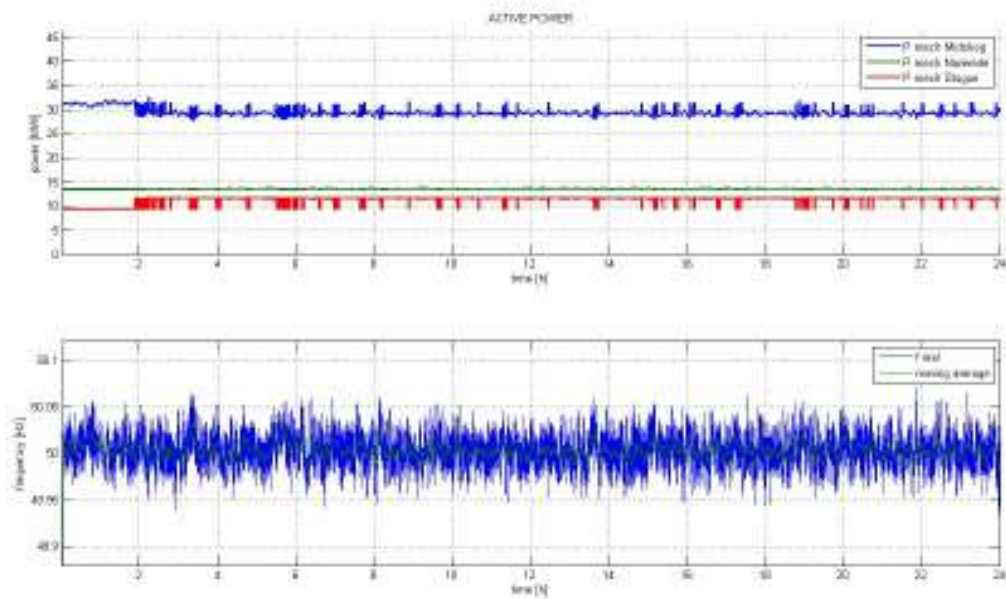


Figure 46: LFC = ON, 2010-08-02 simulation, Mechanical power delivered by Midskog, Närke and Stugun displayed with the resulting grid frequency.

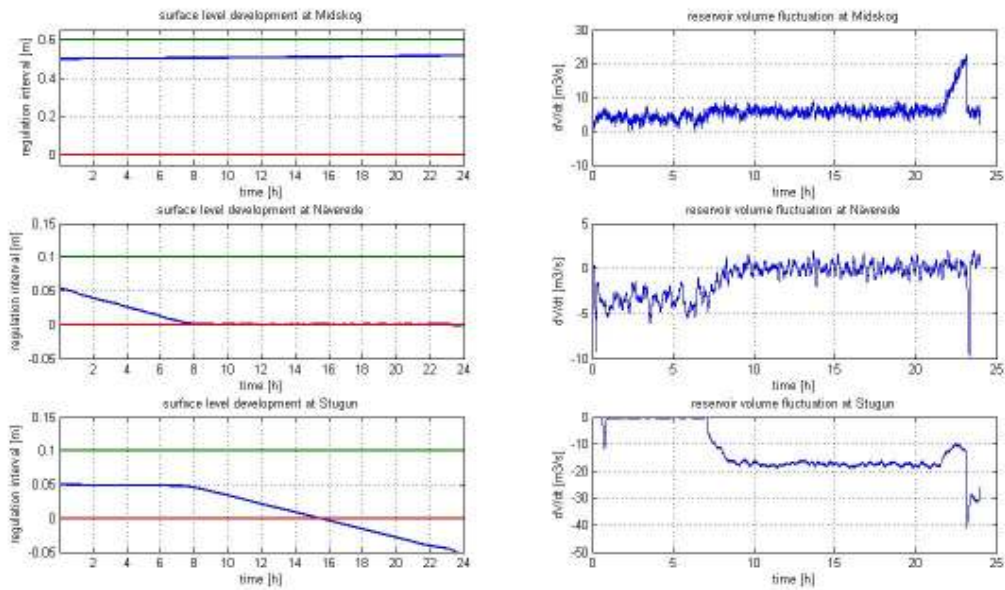


Figure 47: LFC = OFF, 2010-08-02 simulation, Resulting water levels in the reservoirs of Midskog, Näverede and Stugun. The derivative of the reservoir volume fluctuation is also shown.

The pulse seen in the reservoirs' volume derivative in Figure 47 is correlated to the upper limitation imposed on Näverede seen in Figure 102. It's unclear as to why this limitation acts as it does.

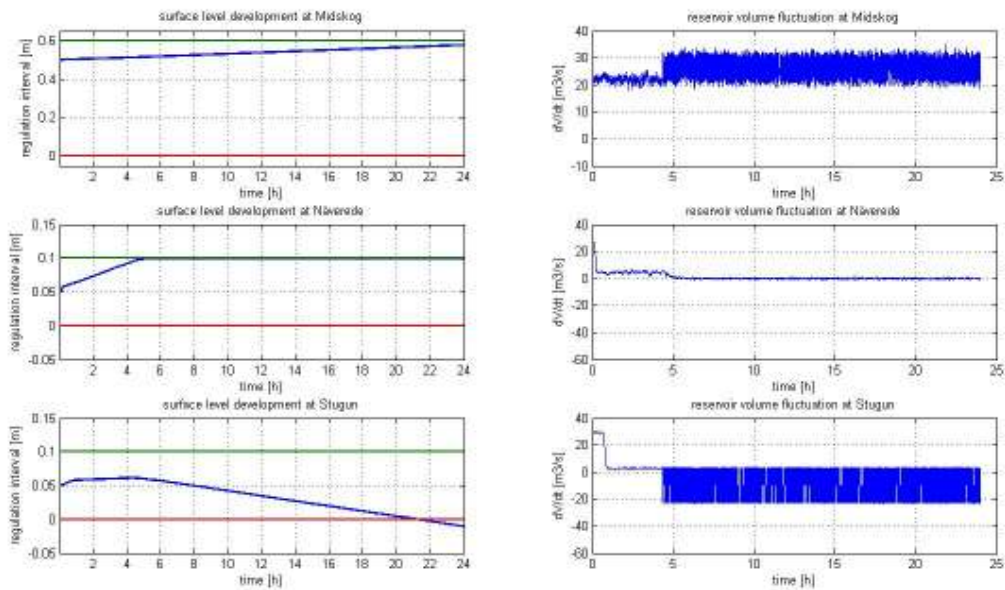


Figure 48: LFC = ON, 2010-08-02 simulation, Resulting water levels in the reservoirs of Midskog, Näverede and Stugun. The derivative of the reservoir volume fluctuation is also shown.

Again the reservoir limits are unfortunately breached which will be discussed in 6.1 Model implementation.

6 Discussion

This chapter will discuss the work made in the previous chapters from three major points of view; how the model was implemented, how to interpret the results and then summarize the discussion around the project aim.

6.1 Model implementation

6.1.1 Assumptions and restrictions

A brief reminder will now be given on the initial assumptions and restrictions that the model and system works within and why these were chosen.

- 1 *The system will only analyze hydropower stations connected in series and not in parallel.* This was chosen since run-of-river systems are mainly series connected systems. This also simplified the target functions by minimizing the cross-correlation between stations and thus creating a simpler target function matrix that could be generated within a *for-loop*. It is possible to create parallel river systems but then the target matrix has to be redefined.
- 2 *Only incoming water flow from a hydropower station upstream will be used as incoming flow for the next hydropower station. Thereby all other flows are treated as non-existent.* This was chosen to simplify all calculations. It is however possible to implement an extra inflow by adding this to eq. 60 or eq. 62, as is done for the first station with ΔQ . It would only be possible to do this as a static deviation for the entire simulation however, but by doing so it would be possible to simulate an incoming parallel river reach as is the case upstream from Midskog.
- 3 *Only a static discharge plan per hydropower station and simulation will be used.* This differs from reality where the discharge is changed during the course of the day to match the demand from the power market. It was set as a static value to increase the simplicity of the model and to reduce the number a variables that can affect the results.
- 4 *The reservoir is treated as a rectangular box, without wave properties, where only the stored water volume is of interest.* The only dynamical properties of interest concerning the water ways were the low pass filtering and transport delay system of the river as the phase delay was predicted to be of the largest concern. The reservoir was thereby chosen as a relatively static box. The next step in reservoir dynamics could be to implement wave properties that occur during regulation, as in (Jonsson 2009).
- 5 *All turbines and generators within a hydropower station are aggregated to one turbine-generator with the overall characteristics from each turbine-generator within the station.* This simplified the system as to be able to implement a hydropower station with only one *turbine-governor module*, instead of multiple modules. Another result is that the hydropower station module can be copied and implemented between different stations with only different input values defining each station.
- 6 *On aspects concerning the power grid and power flows, only active power flows will be analysed. Thereby other influences such as reactive power and bottle neck effects are omitted.* This seems to be the general outlay of most larger scale grid frequency studies (Bevrani 2009; Bevrani & Hiyama 2011; Murty 2011).

- 7 The hydropower stations in the river reach will only place LFC bids of a total of +/- 10 MW and will always plays the cheapest regulation bid. It was chosen to use bid blocks of +/-10 MW as this is the block size of the current manual FRR market. With an automatic bid system there should however be no problems in using a more continuous bidding ladder.

6.1.2 Library Modules

The modules were chosen to be as standardized as possible in order to be able to implement one set of blocks for each station with only the internal parameters defining the difference between them. To solve this in practise a *Matlab Simulink library* was created that contains the hydropower station module and all its sub-modules. Standardized blocks were also used in order to be able to upgrade the modular system without the need to upgrade every station using the specific block by only upgrading the referenced library block.

Future upgrades of the blocks can be:

- 1 Implementation of the *penstock-turbine* transfer function. This would allow the system to simulate the dynamics of the penstock and tail-race tunnels in order to see how this affects mass oscillation.
- 2 Using *system identification* to create a more specific module for the river and reservoir, see (Euren 2004) for an example.

6.1.3 Governing of the LFC-distribution

The LFC signal was distributed according and weighted to two criterias:

- 1 The power deviation target function is designed to minimize LFC frequency regulation at each station by penalizing a power deviation from the planned production
- 2 The surface level deviation target function is designed to minimize the collection, or withdrawal, of water volumes from one part of the river more than the other, by penalizing deviations in discharge between two stations connected in series. An effect from this function is that it minimizes the total amount of water needed to create the desired regulation by directing the demand to stations with large specific power¹³. It can also be seen as an early stage of *economical dispatch theory* (Zhu 2009, avs.4.2.3; Vrdoljak m.fl. 2010).

The implementation of the LFC distribution with a target function and limitations can be seen as a primal *model predictive controller* (MPC) in the sense that it distributes the signal according to where the system is at time t and where the system may be after a time horizon of $t+T_{LFC}$ by predicting what the maximum and minimum allowed power production at each unit will be, in order to not violate any reservoir limits. As a result of the simulations having a *static turbine-generator combination* per station and simulation and an LFC signal that is *only +/- 10 MW* and thereby in some sense a *boolean variable*, the distribution of *the LFC signal remains constant* for each regulation when operating within the limits imposed. This is related to that within the target functions of *power deviation* and *surface deviation*, the only time dependent variable is the incoming LFC signal. This

¹³ Specific power $Y = P/Q = \text{electric power} / \text{water flow} = [\text{MWs}/\text{m}^3]$.

also explains some of the stiffness within the system and why the distribution either needs to be extended with more feedback loops, such as a surface level governor, or a full implementation of a *model predictive control system (MPC)*.

As seen in the simulations for the Vattenfall reach on May 3rd and Aug 2nd the limitations imposed on the system do not exactly work as planned. This is accredited to the fact that when the signals are redistributed according to eq. 67, the target matrix only takes station 1 to N-1 in to account and thereby not the last station which instead acts as the “slack-unit”. The system is able to act on the “slack-unit’s” limitations, but only when these limitations are the *last* to be implemented. The “slack-unit” is then restricted by the total truncated LFC demand signal. For scenarios where the integral of the system imbalance is closer to zero it is possible to add extra weight on the “slack-unit’s” *power deviation target function*, this will keep the station’s regulation within a more narrow interval and thus within its limitations. There are several other work-a-round’s that could be implemented but it has been chosen not to because the distribution system is believed to be too stiff and thereby another type of distribution system may be better suited for this problem. The distribution system has therefore not been upgraded further.

There is also the problem of not finding a stable solution when one of the stations reaches a limit as seen in the Vattenfall simulation for Aug 2nd, see Appendix - C.2 Vattenfall - August 2nd 2010. This may be caused by a *trigger-function*, with a period time of 30 s, in the LFC-distribution module used to speed up the simulations. During the update time, the limitations may change and thereby resulting in a new setpoint at every update.

6.1.4 Simulation initiation

It was intended to create simulations that reflect the real power system during a specific day and therefore the *imbalanceSim* function was used in the ENTSO-E model. It needs to be stated that the load imbalance series created for this series is not the exact imbalance from the day at hand but an attempt to replicate it (ENTSO-E 2011b, sec.2.8.2).

To create an even more realistic simulation, the discharge plans for each day and station were retrieved from the respective companies in combination with the speed droop settings for the day. When creating the static discharge plan for a simulation, it was chosen to only try to resemble the discharge plan of the day and not to take the mean discharge for the day. This leads to a difference in sold energy and also a difference in transported water volume compared to the actual day at hand.

There was also a need to manually modify the plans further. This was made to ensure that the automatic LFC system would have a power interval to work with. An example of this was the simulation for Jämtkraft on December 6th where there was no room for the LFC at all in Hissmofors when using a discharge plan of $Q_0=380$ m³/s, it was therefore lowered to $Q_0=350$ m³/s instead in order to create this regulation capacity.

It was also found that the reserved regulation capacities for FCR (FNR+FDR) and LFC for some simulations could not be reserved at the same time without them interacting in each other’s reserved capacity. For the simulations where the LFC and FDR reserves interacted, it was chosen to disregard the FDR reserve and only deliver FNR and LFC regulation reserves. See Appendix for more information on individual setup of the reaches. LFC and FDR interaction is though an area where

much more optimization must be made, but to do this we need more information of the markets and also how the individual companies will act on the new markets.

6.1.5 Source of error – sensitivity analysis

As seen the model has a lot of parameters affecting the system and it's thus not feasible to create a sensitivity analysis for each parameter within the given time frame for this project. Each module has instead been tested with either step, impulse and/or ramp responses to give an idea of how it works and what affects it, see *Module Validations* within each section in 4 Method and Model development. As a brief sensitivity analysis it may be possible to create three categories of variables; physical constraints, modelling parameters and optimization weights which will now be discussed.

The given system has to work within the *physical parameters* given. These consist of multiple variables and can be grouped in to; transport delay within the river, reservoir regulation capacity, reservoir volume, turbine-generator unit combination and operational setpoint. It is also important to analyse where, geographically speaking, within this system the greatest limitation is with the system not being stronger than its weakest link.

An example of how the weakest link affects the system can be seen in the Fortum simulations (Appendix - C.3 Fortum, Figure 123). It can be seen that the operational setpoint at Storåströmmen is limited by the maximum static limitation. Because of this the other stations are required to increase their regulation in order to deliver the entire demand and thus the surfaces deviate more than necessary compared to if the planned operational setpoint would have been a few MWs less. In the same simulation it can also be seen that Byaforsen, which has the smallest reservoir volume and base power, is the station that regulates least (due to high costs) of all stations even though it has not reached any limit, see Figure 124. With Byaforsen giving only small volumes of regulation the surface at Krokströmmen deviates because this station can contribute with more downwards regulation which in turn affects the next station.

The *modelling parameters* are related with the model itself as opposed to the physical reality. These are the *Muskingum weighting factor*, the *step time* for the Muskingum module and the *trigger-time period* for the LFC distribution. The Muskingum weight factor can be viewed as a dampening factor ranging from $\Theta=0$, giving the outflow as a linear interpolation between inflow at time t and $t-dT$, to $\Theta=0.5$ that yields a mathematical pure translation of the wave in a uniform canal (Bedient et al. 2008, p.219). It must be stated though that the Muskingum method is a highly simplified model for river routing as stated in (Koussis 2009, chap.2) and should be treated as such. The step time for the Muskingum module shouldn't impose a high sensitivity as long as it is set to much smaller value than the river travel times. Within the simulations made, the step time has been on the scale of 30 s compared to the shortest travel time of 2 minutes for the Jämtkraft reach. The effect it could have if the step time and travel time start to impose on each other is that the river starts to behave in a more discrete manner compared to the physical continuous. The trigger-time (T) used for the LFC-module is used to speed up the simulations by only calculating the distributions at certain points in time. During these time periods the system may have changed to such a degree that the given power setpoint is either valid or invalid during the next time period. This is seen in the august simulations for Jämtkraft or when a surface level reaches its reservoir limit. It may thereby be a numerical instability which could probably be adjusted for by changing or completely removing the trigger-time T.

Finally there are the *distribution weights* that affect the regulation of the system. They affect the system in two different ways when weighted; the *power deviation* weight adds cost for regulation and thereby minimizes the regulation at said station, the *surface deviation* weight adds weight for any static surface change. The user is thereby able to govern the system by either weighting for a more constant power production or a more constant surface level at each individual station.

6.2 Results

6.2.1 Active Power regulation

There are two general and distinct observations that can be made for the active power regulation when analysing the system with the LFC regulation turned *on* or *off*; FCR-LFC interaction and market optimization.

The *first* observation is that with the LFC system turned *on* the FCR regulation is smaller compared to when the LFC is turned *off*. This is fairly self explanatory and relates to the fact that with an automatic LFC system the grid frequency is kept within a tighter frequency band and thereby the FCR does not have to operate at the same absolute levels on larger time scales.

On the other hand it can be seen that for stations delivering FCR, the LFC control signal has been larger in terms of absolute power and energy than the FCR. The regulated LFC power levels are related to how many stations that are coupled to the system and how the weights are set for the LFC distribution in the specific scenarios. The energy sold via LFC regulation on the other hand relates more to what the company wishes to sell and is thereby a question for the markets. For the simulations it was chosen to always place the cheapest bid and thereby large quantities of regulation energy has been sold. The simulations should thereby be seen as extreme scenarios in which the LFC is always operating.

The *second* distinct observation is that to act on the LFC market, new optimizations will be needed in which the power companies need to decide on which market power and energy shall be sold; the LFC regulation market or in the Nordpool Spot and ELBAS systems. As of today our simulations point toward that the combination of LFC and FDR regulation with the operating setpoints of today may act within each other's regulation interval which is *undesired*.

6.2.2 River flow

As expected, the river flows with the LFC system turned on have become much more regulated. The amplitude at which these flows oscillate has also become larger but this is correlated to the fact that a larger power regulation is sold at each station. These amplitudes may differ in the future depending on the block-size of regulation, in MWs, that the future LFC system will work with.

The amplitudes of the regulation shouldn't pose a problem since these are smaller than the difference between the hourly discharge plans. This can be seen by analysing the difference in discharge over the simulated days when looking at the planned discharge, see Figure 63, and the simulated discharge, see Figure 97Figure 105Figure 113.

The frequency with which these oscillations occur and the ramping speed of these regulations may pose a problem, it's unclear though as to how. Problems may include the effects on fish and other

water living organisms, change in local opinion, swells and so forth. It's the author's belief that these regulations will cause extra debate on how our hydro power systems are used.

6.2.3 Reservoir water surfaces

There will in reality be two major outcomes from an LFC system implementation on the reservoirs; static and dynamic (waves) surface deviations. In our model only the static deviations have been modelled.

With the LFC system turned off there are surface deviations within the modelled system that should not be there in reality with a *surface level governor* in place, but as stated earlier it was chosen not to implement this in order to let the surfaces "float" more freely and only constrain them at the upper and lower reservoir limits. The surface deviations are thereby a direct result of the difference in FCR regulation between the station at hand and its upstream station.

For the *imbalance simulations* made of May 3rd, Aug 2nd and Dec 6th the major difference is that the August simulation is an over balanced system while May and December simulations have oscillations with both over and under balance, see **Fel! Hittar inte referenskälla.** It's difficult to see the accumulated deviation in **Fel! Hittar inte referenskälla.** and therefore Figure 49 was created. The graph shows which of the two simulations, May or December, that has the largest momentary accumulated frequency deviation, and thus largest absolute time deviation. The absolute accumulated frequency deviation is used to see which system has the greatest accumulated imbalance.

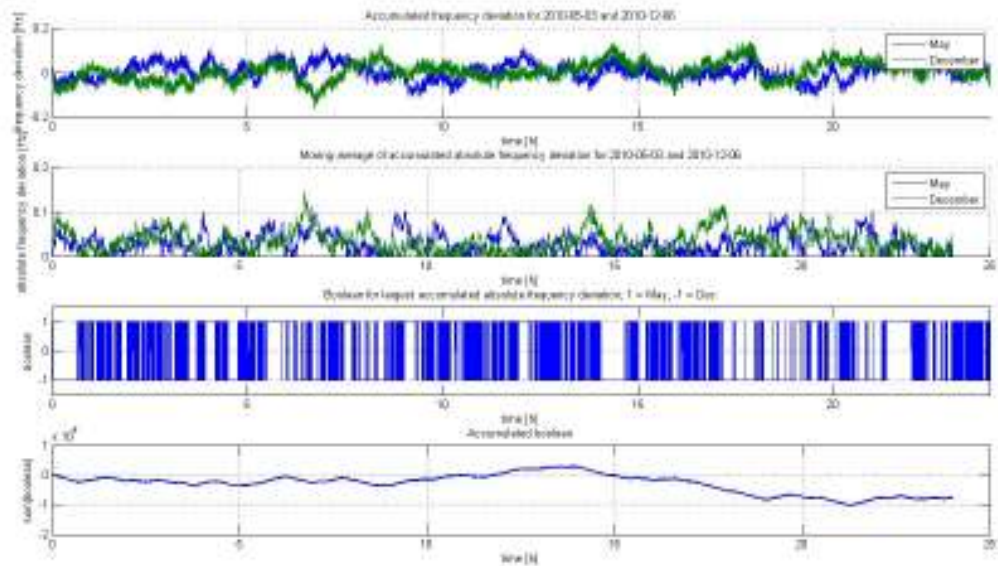


Figure 49: Analysis of the system balance for the May and December simulation without the LFC implemented. Shown are the accumulated frequency deviations and also a Boolean describing which of the two simulations that has the largest momentary accumulated deviation.

The August simulation imbalance depicts an over balanced system and therefore the LFC governor tries to withdraw rotational energy from the entire system which can be seen in Figure 45 and Figure

46 with the resulting water levels of Figure 47¹⁴ and Figure 48. As you can see the system is able to help with withdrawing rotational energy from the system but only for a short while, giving the TSOs an additional tool for system operation, but not a final tool for static over or under balanced systems. This can also be seen in the Jämtkraft simulation in Figure 81 and Figure 82 which was more successful in withdrawing rotational energy from the system (C.1 Jämtkraft - August 2nd 2010). For scenarios where the system is mainly over or under balanced the hydropower stations may need to be operated more individually and thus making it easier to accelerate or decelerate the entire river. This may create a better response and thus more effective reserves.

The May and December simulation imbalances are instead of the oscillating kind with the December simulation having a larger total system imbalance (Figure 49 – *accumulated boolean*). Thereby a quick conclusion would be that the May simulation should have been easier to compensate with the LFC system which was not the case. If you look at Figure 95 (Appendix - C.2 Vattenfall) you can see that the Näverede station is hindered from upwards regulation by its static limitation. As a result of this the reservoir surface deviates upwards with Midskog regulating more powerful than Näverede can handle, Figure 99. It may be possible to correct this by changing the internal weights for the LFC cost functions but this has not been tested. Another way would be to change the original discharge plan and thereby creating more regulation capacity but this is again a question for market optimization. For the December simulation on the other hand the surfaces remain surprisingly constant with only a ripple on the surface.

As stated first there would also be dynamic changes (waves) for the reservoir surfaces. These have not been modelled but it is the author's belief that these will be crucial to understand and predict to be able to implement this system on run-of-river stations with the small reservoir volumes and regulation capacities.

6.2.4 Available reserves and capacity

An issue raised in the beginning of this project was the question of how these different frequency controlled reserves, FCR and FRR, will interact. For an example it is crucial that the LFC regulation *does not* interfere with the *frequency controlled disturbance reserves* as this may lead to a major system disruption.

During the setup of the simulations it was found that with the implementation of an automatic LFC system the operational points of today would need to be changed in order to continue delivering both FNR and FDR reserves. It was therefore chosen to eliminate the FDR reserves from most simulations and only deliver FNR reserves instead. A further thought of this is to increase the diversity of regulating products so that different stations can work more specifically with one type of reserve. Worth mentioning is that these restrictions only concerns the static limitations for each station and not the dynamic limitations which also need to be addressed when placing bids.

To be able to better control the dynamic limitations and thereby capacities, new and higher level control strategies are believed to be one part of the solution by being able to more accurately predict the future state of the system. Within these limitations, there is also a question of how far in advance the reserves and capacities will need to be handed over to the TSOs bidding system, which further increases the need for accurate prediction of the system.

¹⁴ Remember that there is no surface level governor in the model

The capacities of each station and thereby the entire system is also extremely linked to the available regulation capacity of each reservoir, i.e. *how much capacity each producer is willing to offer for the LFC regulation*. For our simulations the entire judicial regulation capacity for the reservoir has been chosen and it should thereby be seen as extreme boundary conditions.

As seen in the simulations, *with the setup used*, there are scenarios where the system would have been able to deliver automatic LFC regulation but equally as many where the LFC system causes breaches of the imposed limitations. The system can thereby not be implemented as it is designed today but needs further upgrades and developments.

6.3 Project aim

The main focus of the project has been to answer the question of: *Can more reserves be created by using a more dynamic river governing?* To answer this question a model was created for which different hydropower systems can be built and then analysed.

The analysis show that by creating a central governing unit it may be possible to govern an entire river reach by coordinating the individual power stations at a much smaller time scale than today. This has been demonstrated by the *simulations of different river reaches in combination with different load conditions*. The simulations also give the reader a better understanding for different types of possibilities and problems within an LFC governed run-of-river system. As can be seen there are still many obstacles to overcome before implementation on rivers with small reservoir regulation capacities is possible.

At present it is not possible to say how much regulation capacity in terms of power or energy the different companies may be willing or able to provide. This is related to that this study has only taken in to account the dynamics of the river and not the wave properties in the reservoirs as discussed in 6.1.1 Assumptions and restrictions. Another factor preventing the prediction of available reserves is the fact that the new market is too under developed and thereby not making it possible to predict future strategies of the power companies.

Concerning the possibility for hydro power stations to *maintain their frequency controlled reserves during low load operation* more analysis is needed before any solid conclusions can be drawn. This is related to two larger factors:

1. The LFC market is under developed making it impossible to optimize water usage vs. Frequency reserve products.
2. The created model has difficulties in limiting the river system resulting in violations of the reservoir limitations.

For the low load simulations, it was chosen to only reserve FNR regulation because simulations with FDR in showed interference between the LFC and FDR. The simulations with only FNR show that there are scenarios where it is technically possible to sell both FNR and LFC regulation with a constraint on the LFC product being that only a small amount of regulation energy can be sold, i.e. the LFC regulation cannot operate for very long if all stations need to be regulated at the same time. This is shown in the August simulation for Jämtkraft and Vattenfall (see Appendix - C.1 Jämtkraft and C.2 Vattenfall) in which the surfaces deviate towards the reservoir limitations and then violate them. A further thought is that the manual tertiary reserves may therefore need to be kept in order to

relieve the LFC during these types of operations. It may be possible to operate both FNR, FDR and LFC at the same time given that the FDR requirements is only specified for regulation during which the system is under balanced (ENTSO-E 2007, chap. Appendix 2) which is usually not the case for low load conditions. Thereby the LFC downwards regulation shouldn't interfere with FDR upwards regulation.

The simulations made during low load operations have all breached the system limitations after a certain time. The chosen distribution algorithm is thereby not an optimal algorithm for this type of problem and needs to be upgraded before any more solid conclusions can be drawn.

The project aim also includes the question if there is a possibility to *impose any general requirements on hydropower stations*. At this point in time the answer to this will have to be that it is unclear because there are too many variables that affect the system behaviour that need to be analysed further in order to answer this question. These are variables ranging from market development, new optimization schemes, physical limitations, technical limitations etc.

7 Conclusions

The aim of this project was to study if more frequency controlled reserves could be implemented in river reaches, which today do not contribute with frequency controlled reserves, by implementing a more dynamic river governing. A more dynamic river governing was interpreted as a governing at a much smaller time steps compared to today. A method was therefore developed where a central governing unit uses the different states of each hydropower station to dispatch a demand signal from the Nordic TSOs.

While there are several issues left to overcome before an implementation of this type of dynamic river governing, the examples demonstrated show that the method developed does have a future potential for river governing. *A conclusion is therefore that more frequency controlled reserves can be implemented in Swedish run-of-river systems by coordinating these resources with a central governing unit.*

Another aim of the project was also to study the effects that the new automatic frequency controlled reserves would have on reserves already in place during low load operations. It was not possible to draw any solid conclusions without further analysis, but the results indicate that new market optimizations will be needed. New market optimizations will then also affect other automatic frequency controlled reserves since they all share the same physical resource; the water and the hydropower station.

The final question to be answered was if any general requirements could be made on hydropower stations of a certain size to be able to contribute to the new automatic LFC-system. Unfortunately no distinct conclusions can be drawn regarding this without further analysis of the system.

References

Books

Bedient, P.B., Huber, W.C. & Vieux, B.E., 2008. *Hydrology and floodplain analysis*, Prentice Hall.

Bevrani, H., 2009. *Robust Power System Frequency Control*, Springer.

Bevrani, H. & Hiyama, T., 2011. *Intelligent Automatic Generation Control*, CRC Press.

Murty, P., 2011. *Operation and control in power systems* 2nd ed., Hyderabad India ;Leiden: BS Publications ;CRC Press.

Zhu, J., 2009. *Optimization of Power System Operation*, John Wiley & Sons.

Peer reviewed articles

Euren, K., 2004. System Identification of Irrigation Channels with Overshot and Undershot gates. Available at: <http://urn.kb.se/resolve?urn=urn:nbn:se:uu:diva-88916> [Åtkomstdatum December 7, 2011].

De Jaeger, E. m.fl., 1994. Hydro turbine model for system dynamic studies. *IEEE Transactions on Power Systems*, 9(4), ss.1709-1715.

Jonsson, E., 2009. Simulering av vågförhållanden i vattenkraftmagasin. Available at: <http://urn.kb.se/resolve?urn=urn:nbn:se:uu:diva-113284> [Åtkomstdatum December 7, 2011].

Koussis, A.D., 2009. Assessment and review of the hydraulics of storage flood routing 70 years after the presentation of the Muskingum method. *Hydrological Sciences Journal*, 54, ss.43-61.

Vrdoljak, K., Perić, N. & Šepac, D., 2010. Optimal distribution of load-frequency control signal to hydro power plants. I *2010 IEEE International Symposium on Industrial Electronics (ISIE)*. 2010 IEEE International Symposium on Industrial Electronics (ISIE). IEEE, ss 286-291.

Documents

Achleitner, S. & Rauch, W., 2007. CityDrain 2.0.3 User Manual. Available at: <http://www.hydro-it.com/extern/IUT/citydrain/>.

ENTSO-E, 2011a. ANALYSIS & REVIEW OF REQUIREMENTS FOR AUTOMATIC RESERVES IN THE NORDIC SYNCHRONOUS SYSTEM.

ENTSO-E, 2011b. ANALYSIS & REVIEW OF REQUIREMENTS FOR AUTOMATIC RESERVES IN THE NORDIC SYNCHRONOUS SYSTEM - Simulink Model description.

ENTSO-E, 2007. Nordic Grid Code 2007 - Nordic collection of rules.

Högström, C.-M., 2006. Modellering av reglersystem, turbin och vattenvägar för implementering i el-nätssimulatoren ARISTO.

IEEE Standards Committee, 1991. IEEE Recommended Definitions of Terms for Automatic Generation Control on Electric Power Systems.

Ne.se, 2011. vattenkraftverk | Nationalencyklopedin. Available at: <http://www.ne.se/lang/vattenkraftverk#> [september 9, 2011].

Nordpool AS, 2011. Nordpool Markets. Available at: <http://www.nasdaqomxcommodities.com/trading/markets/> [ecember 7, 2011].

Spiegelberg, E., 2011. Nordiska primärregleringen som den realiseras i vattenkraftaggregatens turbinregulatorer.

Svensk Energi, 2011. Kraftläget i Sverige. Available at:
<http://www.svenskenergi.se/upload/Statistik/Kraftl%C3%A4get/mrapp.pdf> [Åtkomstdatum November 9, 2011].

UCTE, 2009. P1 – Policy 1: Load-Frequency Control and Performance [C]. Available at:
https://www.entsoe.eu/fileadmin/user_upload/_library/publications/ce/oh/Policy1_final.pdf.

Interviews

Byström, E., 2011. River governing, Fortum Generation AB.

Bäck, C., 2011. NORDEL Reserves, Svenska Kraftnät.

Dahlbäck, N., 2011. Hydraulic dynamics, Vattenfall AB.

Damgren, Å., 2011. the Midskog-Stugun river reach, Vattenfall AB.

Internet

École polytechnique fédérale de Lausanne. Available at:
http://echo2.epfl.ch/VICAIRE/mod_1b/chapt_5/summary.htm [September 14, 2011].

VICAIRE, 2011. VICAIRE - Module 1B - Chapter 5. *Virtual campus in hydrology and water resources*. Available at: http://echo2.epfl.ch/VICAIRE/mod_1b/chapt_5/summary.htm [January 06, 2012]

Vattenregleringsföretagen.se, 2011. Vattenregleringsföretagen - Verksamhet. Available at:
<http://www.vattenreglering.se/> [Åtkomstdatum December 7, 2011].

Graphical design

Kaisinger, R., 2011, Vattenfall AB.

Appendix

A – Model Modules

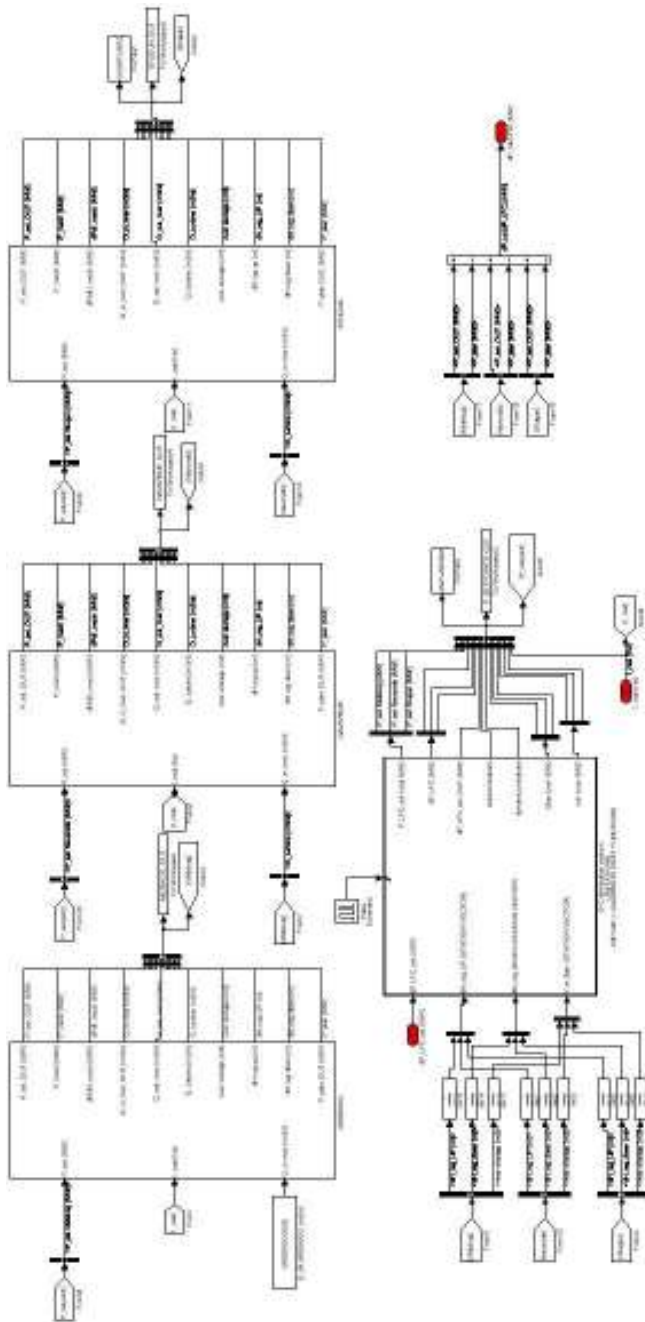


Figure 50: The Vattenfall river reach from Midskog to Stugun. The three identical blocks are the hydropower station modules that in turn make up Midskog, Näverede and Stugun. The input and output signals for the river reach a marked with red colour.

With the hydropower station module in this section, several river reaches were constructed of which Figure 50 is one example depicting Vattenfall’s river reach from Midskog to Stugun. For internal schematics of the hydropower stations , see Figure 51.

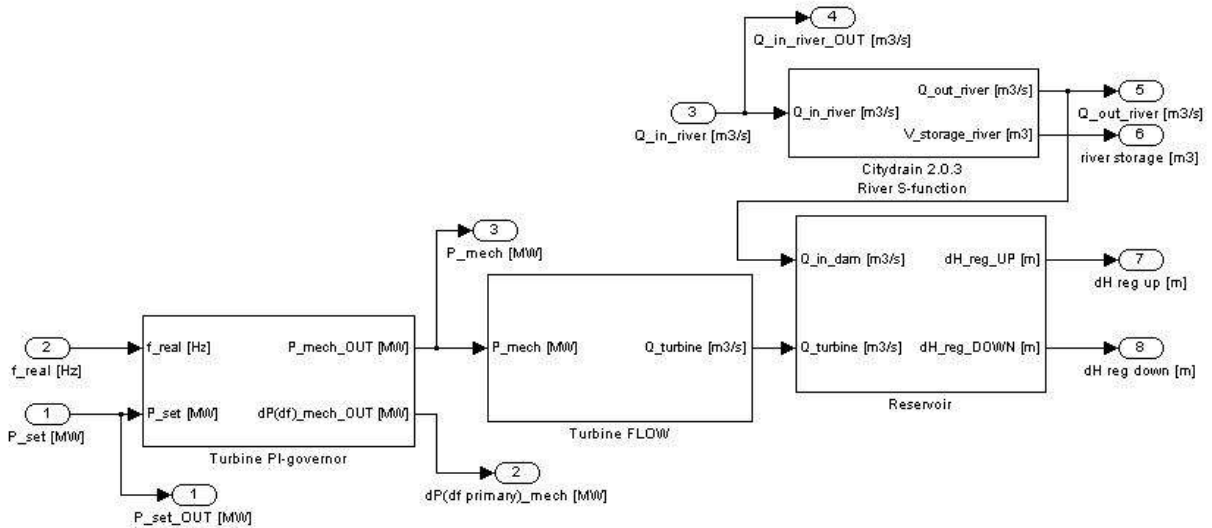


Figure 51: Internal schematics for the hydropower station module

A.1 Hydro Power station

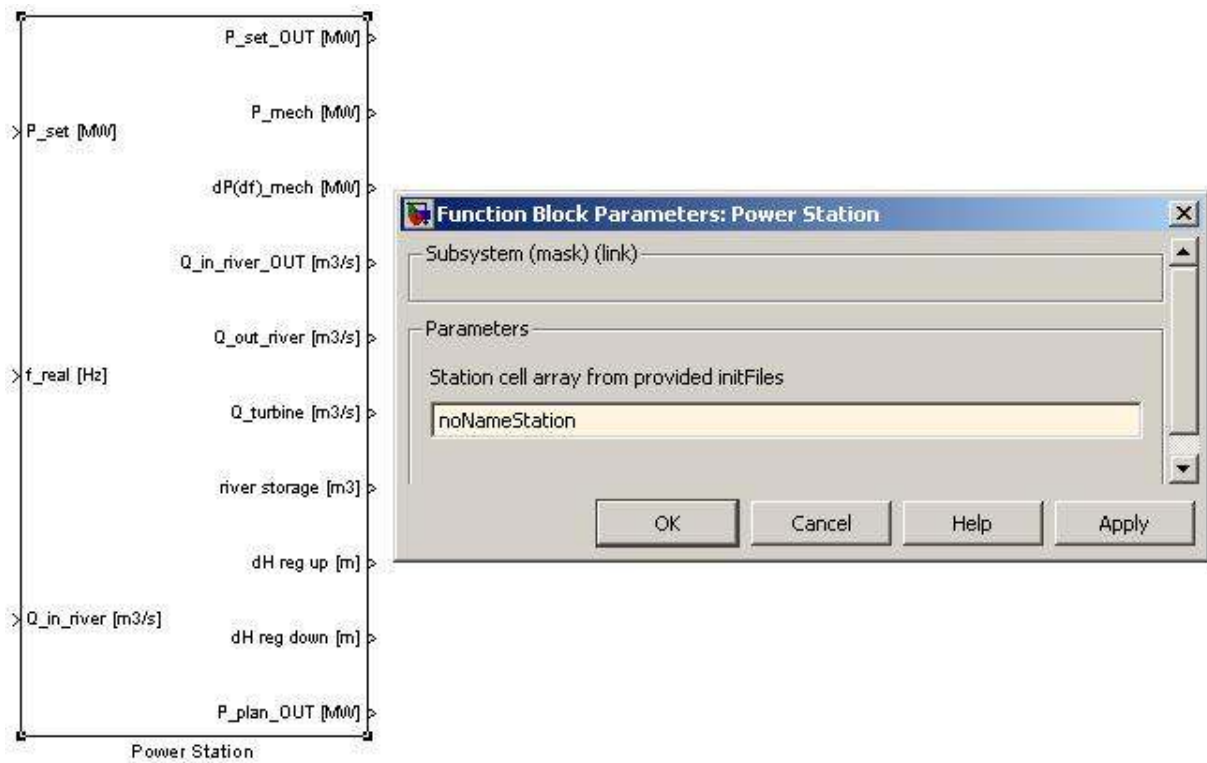


Figure 52: Hydro power station module, input/output and internal parameters

Input:

- P_{set} [MW] – setpoint value for the turbine governor module
- f_{real} [Hz] – grid frequency used for FCR regulation within the turbine governor module
- Q_{in_river} [m^3/s] – incoming water flow to the river module

Output:

- All outputs from the sub modules

Internal variables:

- Station cell array created with the provided initiation files for each hydro power station. The sub modules then draw their respective internal parameters from this cell array.

A.2 River

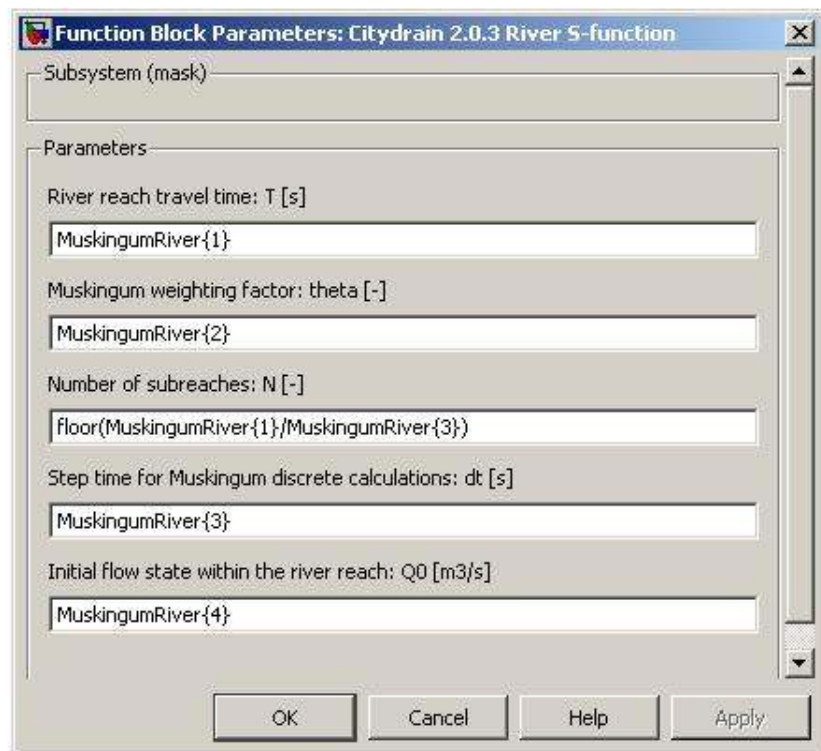
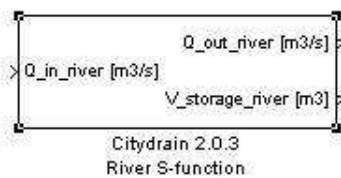


Figure 53: River module, input/output and internal parameters

Input:

- Q_{in} [m^3/s], this is the inflow to the river

Output:

- Q_{out} [m^3/s], this is the outflow of the river and thereby input to the reservoir module.
- $V_{storage_river}$ [m^3], total storage within the river

Internal variables:

- T_{river} [s] – approximate travel time constant for the river reach
- Θ [-] – dimensionless Muskingum method variable
- dt [s] – time step with which the module operates

- Q_0 [m^3/s] – initial state of river flow, vector form

A.3 Reservoir

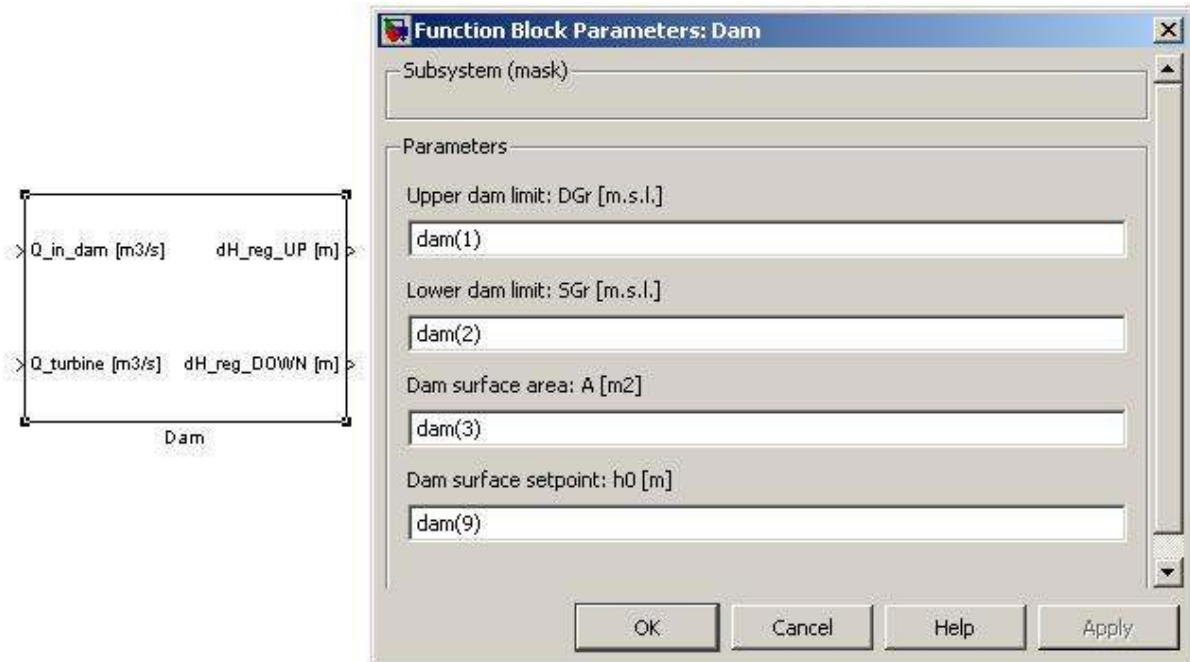


Figure 54: Reservoir module, I/O and internal parameters

Input:

- Q_{in} [m^3/s] – water flowing in from river
- $Q_{turbine}$ [m^3/s] – water flow extracted from the reservoir via the turbine

Output:

- dH_{up} [m] – regulation capacity to the upper reservoir limit
- dH_{down} [m] – regulation capacity to the lower reservoir limit

Internal variables:

- upper reservoir limit [m.s.l.]
- lower reservoir limit [m.s.l.]
- reservoir surface area [m^2]
- reservoir surface setpoint [m]

A.4 Turbine governor

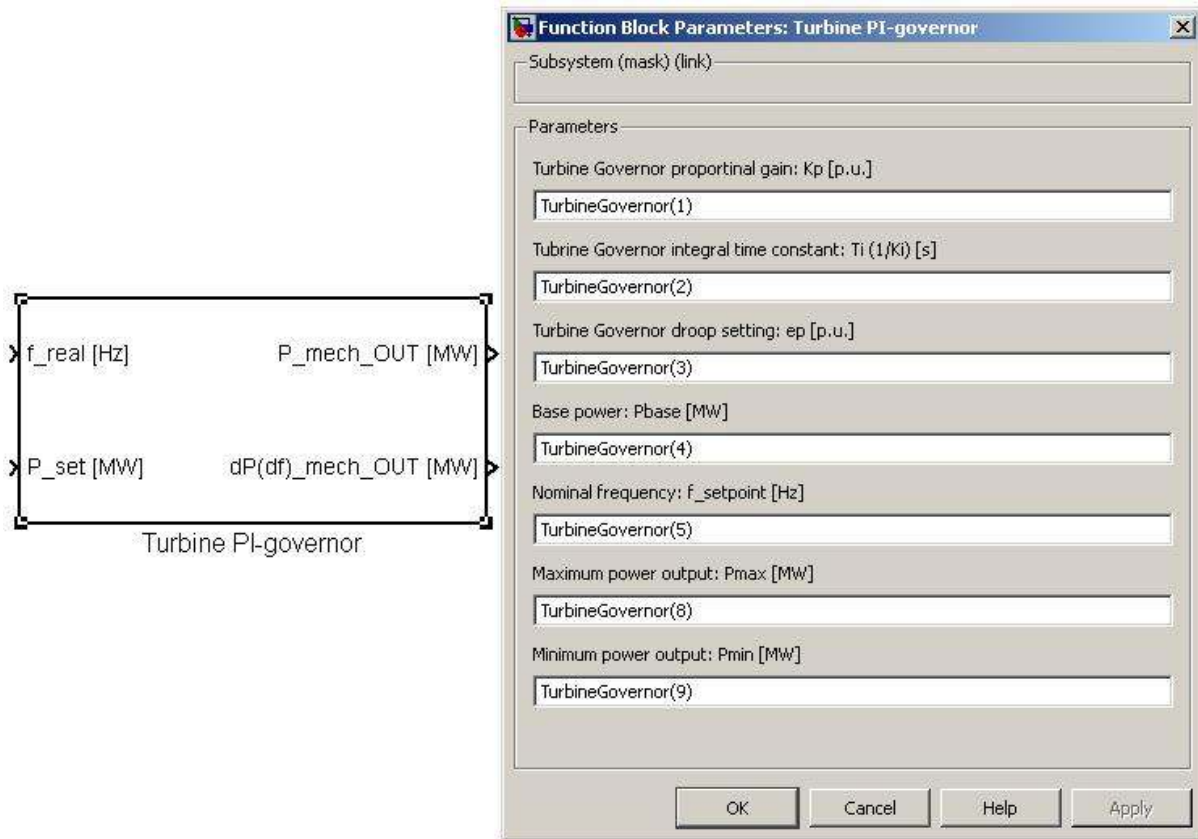


Figure 55: Turbine Governor: I/O and internal parameters

Input:

- f_real [Hz] – momentary frequency
- P_setpoint [MW] – power setpoint

Output:

- P_mech [MW] – total mechanical power production
- dP(df)_mech [MW] – momentary FCR regulation

Internal variables:

- Kp [-] - Turbine governor proportional gain
- Ti [s] - Turbine governor integration time constant
- ep [p.u.] - Turbine governor droop setting
- Pbase [MW] - Base power for the station
- f_setpoint [Hz] – grid frequency
- Pmax [MW] – maximum power output

- P_{min} [MW] – minimum power output

A.5 Turbine flow function

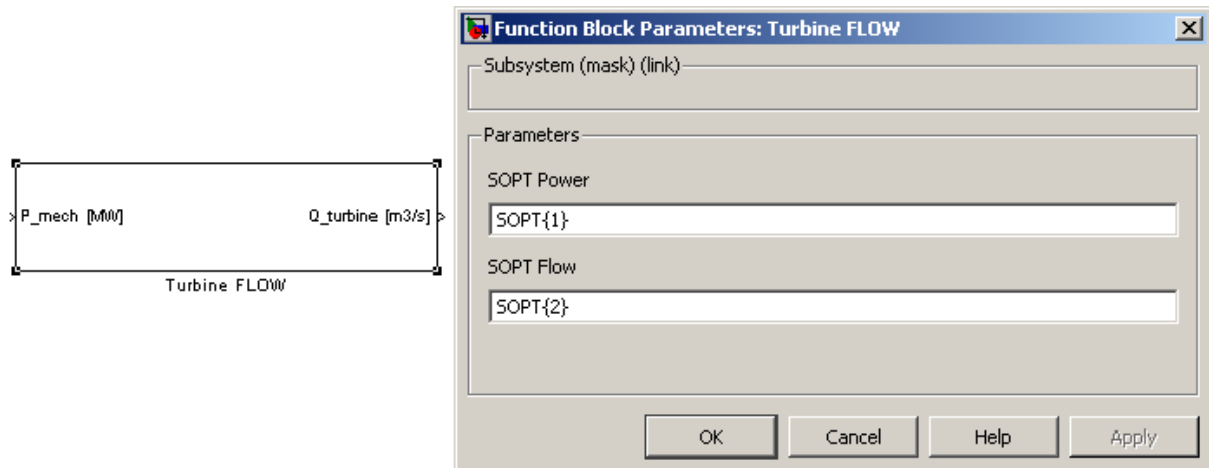


Figure 56: Turbine flow module, I/O and internal parameters

Input:

- P_{mech} [MW] – turbine mechanical power output

Output

- $Q_{turbine}$ [m³/s] – turbine flow

Internal variables:

- SOPT tables – set of values for correlating current flow ($Q_{turbine}$) to current power output (P_{mech})

A.6 LFC – distribution module

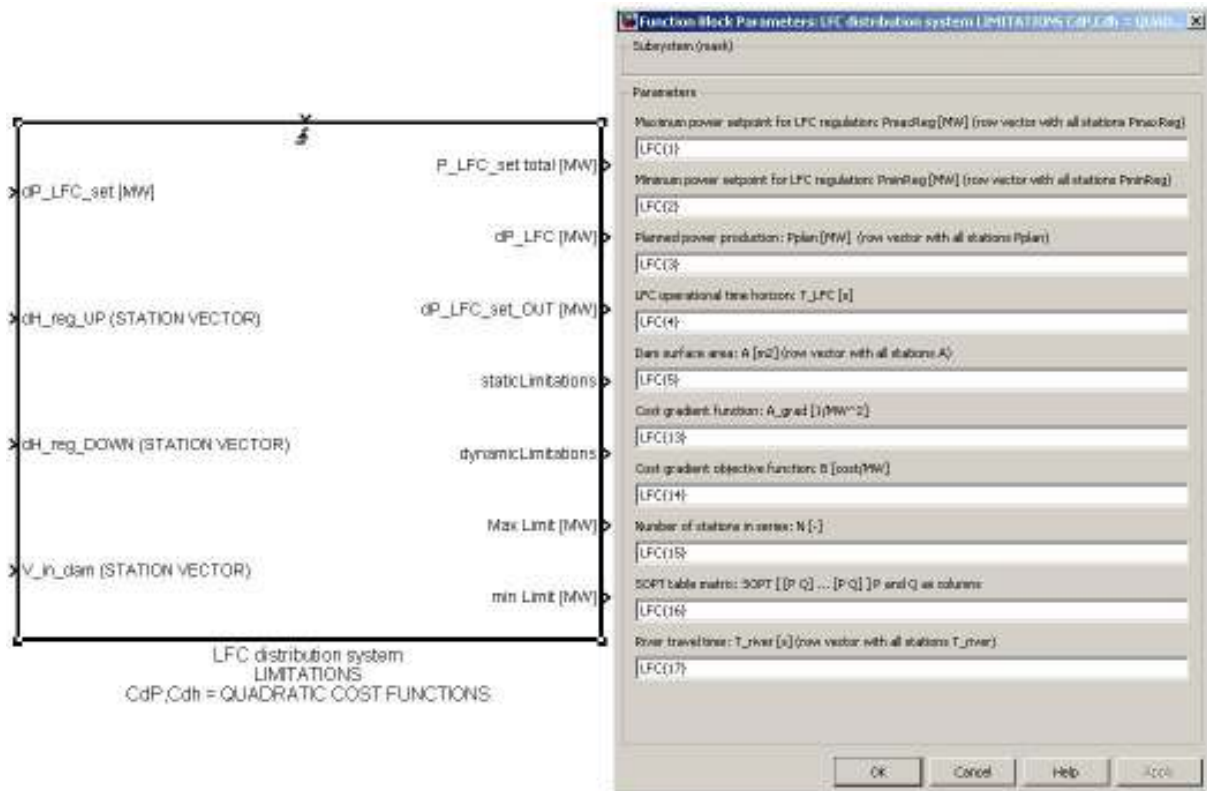


Figure 57: LFC distribution module, I/O and internal parameters

Input:

- dP_LFC_set [MW] – total LFC regulation demand from TSO SCADA systems
- dH_reg_UP [m] – vector containing all the reservoirs upwards regulations capacities
- dH_reg_DOWN [m] – vector containing all the reservoirs downwards regulations capacities
- V_in_dam [m³] – total storage within the river reach flowing towards the reservoir

Output

- P_LFC_set total [MW] – vector with each stations' power setpoint
- dP_LFC [MW] – vector with each stations' current LFC regulation
- $dP_LFC_set_OUT$ [MW] – incoming demand signal from TSO SCADA systems
- $staticLimitations$ [-] – Boolean indicating if the total static limitation is reached
- $dynamicLimitations$ [-] - Boolean indicating if the total dynamic limitation is reached
- max limit [MW] – vector with maximum LFC regulation for each station
- min limit [MW] - vector with minimum LFC regulation for each station

Internal variables:

- PmaxReg [MW] – vector with all stations maximum power setpoint for LFC regulation
- PminReg [MW] – vector with all stations minimum power setpoint for LFC regulation
- Pplan [MW] – vector with all stations planned power production
- T_LFC [s] – LFC operational time horizon
- A_dam [m²] – vector with all stations reservoir surface area
- A_grad [1/MW²] – cost gradient matrix
- B [cost/MW] – cost gradient objective function
- N [-] – number of stations
- SOPT [MW and m³/s] – power to flow vectors, see section 4.1.4
- T_river [s] – vector with all stations travel time for their respective river reach

Power deviation target function

The power deviation target function, eq. 74, is designed to minimize LFC frequency regulation at each station by penalizing a power deviation from the planned production:

$$\text{eq. 74} \quad C_{\Delta P} = \sum_{n=1}^N k_n \frac{(\Delta P_{LFC \text{ setpoint}})^2}{P_{base}^n}$$

Pbase = base power of current generation unit, used to normalize each generation unit's cost [MW]

k_n = weight factor [1]

eq. 74 can also be expressed as

$$\text{eq. 75} \quad C_{\Delta P} = \mathbf{X}_{\Delta P}^T \mathbf{K}_{\Delta P} \mathbf{X}_{\Delta P}$$

$$\mathbf{X}_{\Delta P} = \begin{bmatrix} \Delta P_{LFC \text{ setpoint}}^1 \\ \vdots \\ \Delta P_{LFC \text{ setpoint}}^{N-1} \\ \Delta P_{LFC \text{ demand}} - \sum_{n=1}^{N-1} \Delta P_{LFC \text{ setpoint}}^n \end{bmatrix}$$

$$\mathbf{K}_{\Delta P} = \begin{bmatrix} \frac{k_1}{P_{base}^1} & 0 & \dots & 0 \\ 0 & \ddots & & \vdots \\ \vdots & & \ddots & 0 \\ 0 & \dots & 0 & \frac{k_N}{P_{base}^N} \end{bmatrix} = \begin{bmatrix} q_{\Delta P}^1 & 0 & \dots & 0 \\ 0 & \ddots & & \vdots \\ \vdots & & \ddots & 0 \\ 0 & \dots & 0 & q_{\Delta P}^N \end{bmatrix}$$

q_{ΔP} = total weight factor [1]

With the target function being quadratic it is possible to analytically calculate its minimum point.

$$\text{Eq. 76} \quad \nabla C_{\Delta P} = \begin{bmatrix} dC_{\Delta P}/d\Delta P_{LFC \text{ setpoint}}^1 \\ \vdots \\ dC_{\Delta P}/d\Delta P_{LFC \text{ setpoint}}^{N-1} \end{bmatrix}^{N-1 \times 1} = \mathbf{0}$$

$$\text{eq. 77} \quad \left. \frac{dC_{\Delta P}}{d\Delta P_{LFC \text{ setpoint}}^n} \right|_{n < N} = 2 \left(\begin{bmatrix} \mathbf{0}_1 \\ \vdots \\ \mathbf{0}_{n-1} \\ \mathbf{1}_n \\ \mathbf{0}_{n+1} \\ \vdots \\ \mathbf{0}_{N-2} \\ [-\mathbf{1}_{N-1}] \end{bmatrix}^{N-1 \times 1} \right)^T \mathbf{K}_{\Delta P} \mathbf{X}_{\Delta P} = \mathbf{0}$$

Substituting Eq. 76 and eq. 78 into Eq. 53 gives

$$\text{eq. 78} \quad \nabla C_{\Delta P} = \begin{bmatrix} \mathbf{q}_{\Delta P}^1 + \mathbf{q}_{\Delta P}^N & \mathbf{q}_{\Delta P}^N & \dots & \mathbf{q}_{\Delta P}^N \\ \mathbf{q}_{\Delta P}^N & \ddots & \ddots & \vdots \\ \vdots & \ddots & \ddots & \mathbf{q}_{\Delta P}^N \\ \mathbf{q}_{\Delta P}^N & \ddots & \mathbf{q}_{\Delta P}^N & \mathbf{q}_{\Delta P}^{N-1} + \mathbf{q}_{\Delta P}^N \end{bmatrix} \begin{bmatrix} \Delta P_{LFC \text{ setpoint}}^1 \\ \vdots \\ \Delta P_{LFC \text{ setpoint}}^{N-1} \end{bmatrix} - \begin{bmatrix} \mathbf{q}_{\Delta P}^N \Delta P_{LFC \text{ demand}} \\ \vdots \\ \mathbf{q}_{\Delta P}^N \Delta P_{LFC \text{ demand}} \end{bmatrix} = \mathbf{0}$$

$$\text{or} \quad \nabla C_{\Delta P} = \mathbf{X}_{\Delta P}^{\text{grad}} \Delta P_{LFC \text{ setpoint}} - \mathbf{B}_{\Delta P} = \mathbf{0}$$

eq. 78 can be solved by

$$\text{eq. 79} \quad \Delta P_{LFC \text{ setpoint}}^{\text{minCost}} = \left(\mathbf{X}_{\Delta P}^{\text{grad}} \right)^{-1} \mathbf{B}_{\Delta P}$$

Surface level deviation target function

The surface level deviation target function, eq. 56, is designed to minimize the collection, or withdrawal, of water volumes more from one part of the river than the other, by penalizing deviations in flow between to stations connected in series.

$$\text{eq. 80} \quad C_{\Delta H} = \sum_{n=1}^N k_n \left(\frac{\Delta h_{LFC}^n}{\Delta H^n} \right)^2 = k_n \left(\frac{T_{LFC}}{A_{\text{reservoir}}^n \Delta H^n} \right)^2 (\Delta Q_{\text{turbine}}^{n-1} - \Delta Q_{\text{turbine}}^n)^2$$

ΔH = total regulation capacity within the reservoir [m]

Δh_{LFC} = reservoir surface level change from LFC governing [m]

k_n = weight factor [1]

$A_{\text{reservoir}}$ = reservoir surface area [m²]

Q_{turbine} = water discharge [m³/s]

The model does not have direct access to these flows but these can be derived from eq. 3.

$$\text{eq. 81} \quad Q_{\text{turbine}} = \frac{P}{\eta \rho H} = \alpha P$$

By linearization around a working point and setting this to zero, an expression for the flow deviation as a result of power regulation can be created.

$$\text{eq. 82} \quad \Delta Q_{\text{turbine}} = \alpha P_0 - Q_0 + \alpha \Delta P$$

$$\text{eq. 83} \quad \Delta Q_{\text{turbine}} = \alpha \Delta P$$

Using eq. 83 and expressing the cost function, eq. 74, as a matrix equation gives the following expression

$$\text{eq. 84} \quad \mathbf{C}_{\Delta P} = \mathbf{X}_{\Delta H}^T \mathbf{K}_{\Delta H} \mathbf{X}_{\Delta H}$$

$$\mathbf{X}_{\Delta H} = \begin{bmatrix} \Delta Q_0 - \alpha_1 \Delta P_{\text{LFC setpoint}}^1 \\ \alpha_1 \Delta P_{\text{LFC setpoint}}^1 - \alpha_2 \Delta P_{\text{LFC setpoint}}^2 \\ \vdots \\ \alpha_{N-2} \Delta P_{\text{LFC setpoint}}^{N-2} - \alpha_{N-1} \Delta P_{\text{LFC setpoint}}^{N-1} \\ \alpha_{N-1} \Delta P_{\text{LFC setpoint}}^{N-1} - \alpha_N (\Delta P_{\text{LFC demand}} - \sum_{n=1}^{N-1} \Delta P_{\text{LFC setpoint}}^n) \end{bmatrix}$$

$$\mathbf{K}_{\Delta P} = \begin{bmatrix} \mathbf{k}_1 \left(\frac{T_{\text{LFC}}}{A_{\text{reservoir}}^1 \Delta H_1} \right)^2 & 0 & \dots & 0 \\ 0 & \ddots & & \vdots \\ \vdots & \ddots & & 0 \\ 0 & \dots & 0 & \mathbf{k}_N \left(\frac{T_{\text{LFC}}}{A_{\text{reservoir}}^N \Delta H_N} \right)^2 \end{bmatrix} = \begin{bmatrix} q_{\Delta H}^1 & 0 & \dots & 0 \\ 0 & \ddots & & \vdots \\ \vdots & \ddots & & 0 \\ 0 & \dots & 0 & q_{\Delta H}^N \end{bmatrix}$$

Q_0 = inflow at the first power station [m³/s]

T_{LFC} = LFC operational time horizon [s]

The minimum point can again be found analytically.

$$\text{eq. 85} \quad \nabla \mathbf{C}_{\Delta P} = \begin{bmatrix} d\mathbf{C}_{\Delta P} / d\Delta P_{\text{LFC setpoint}}^1 \\ \vdots \\ d\mathbf{C}_{\Delta P} / d\Delta P_{\text{LFC setpoint}}^{N-1} \end{bmatrix}^{N-1 \times 1} = \mathbf{0}$$

$$\text{eq. 86} \quad \left. \frac{d\mathbf{C}_{\Delta H}}{d\Delta P_{\text{LFC setpoint}}^n} \right|_{n < N} = 2 \left(\begin{bmatrix} 0 \\ \vdots \\ 0 \\ -\alpha_n \\ \alpha_n \\ 0 \\ \vdots \\ 0 \end{bmatrix}^{N-1 \times 1} + \begin{bmatrix} 0 \\ \vdots \\ \vdots \\ \vdots \\ 0 \\ \alpha_N \end{bmatrix}^{N-1 \times 1} \right)^T \mathbf{K}_{\Delta H} \mathbf{X}_{\Delta H} = \mathbf{0}$$

The cost gradient can then be expressed as

$$\text{eq. 87} \quad \nabla \mathbf{C}_{\Delta H} = (\mathbf{X}_{\Delta H}^{\text{grad},1} + \mathbf{X}_{\Delta H}^{\text{grad},2}) \Delta \mathbf{P}_{\text{LFC setpoint}} - \mathbf{B}_{\Delta H} = \mathbf{0}$$

$$\begin{aligned}
\mathbf{X}_{\Delta H}^{\text{grad},1} &= \begin{bmatrix} \alpha_N^2 q_N & \dots & \alpha_N^2 q_N & \alpha_N(\alpha_{N-1} + \alpha_N)q_N \\ \vdots & \ddots & \vdots & \vdots \\ \alpha_N^2 q_N & \dots & \alpha_N^2 q_N & \alpha_N(\alpha_{N-1} + \alpha_N)q_N \\ \alpha_N(\alpha_{N-1} + \alpha_N)q_N & \dots & \alpha_N(\alpha_{N-1} + \alpha_N)q_N & (\alpha_{N-1} + \alpha_N)^2 q_N \end{bmatrix} \\
\mathbf{X}_{\Delta H}^{\text{grad},2} &= \begin{bmatrix} \alpha_1^2(q_1 + q_1) & -\alpha_1\alpha_2q_2 & 0 & 0 \\ -\alpha_2\alpha_1q_2 & \ddots & \vdots & \vdots \\ 0 & 0 & 0 & 0 \\ \vdots & \vdots & \alpha_{N-2}^2(q_{N-2} + q_{N-1}) & -\alpha_{N-2}\alpha_{N-1}q_{N-1} \\ 0 & 0 & -\alpha_{N-1}\alpha_{N-2}q_{N-1} & \alpha_{N-1}^2q_{N-1} \end{bmatrix} \\
\mathbf{B}_{\Delta H} &= \begin{bmatrix} \alpha_N^2 q_N \Delta P_{\text{LFC demand}} \\ \vdots \\ \vdots \\ \alpha_N^2 q_N \Delta P_{\text{LFC demand}} \\ 0 \end{bmatrix}^{N-1 \times 1} + \begin{bmatrix} \alpha_1 q_1 \Delta Q_0 \\ 0 \\ \vdots \\ 0 \\ \alpha_N(\alpha_{N-1} + \alpha_N)q_N \Delta P_{\text{LFC demand}} \end{bmatrix}^{N-1 \times 1}
\end{aligned}$$

eq. 87 can then be solved by

$$\text{eq. 88} \quad \Delta \mathbf{P}_{\Delta H, \text{LFC setpoint}}^{\text{minCost}} = \left(\mathbf{X}_{\Delta H}^{\text{grad},1} + \mathbf{X}_{\Delta H}^{\text{grad},2} \right)^{-1} \mathbf{B}_{\Delta H}$$

B - Initiation files/values

B.1 Jämtkraft

To create the static water discharge for each simulation the planned discharge for those days were retrieved from Jämtkraft and can be seen in Figure 58. For May 3rd and August 2nd the maximum discharge plan for the days were used as the static plan within the simulation. For December 6th on the other hand the simulated discharge needed be lowered some to give the LFC regulation and interval to work within, otherwise Hissmofors would not have *any* upwards regulation capacity according to our calculations.

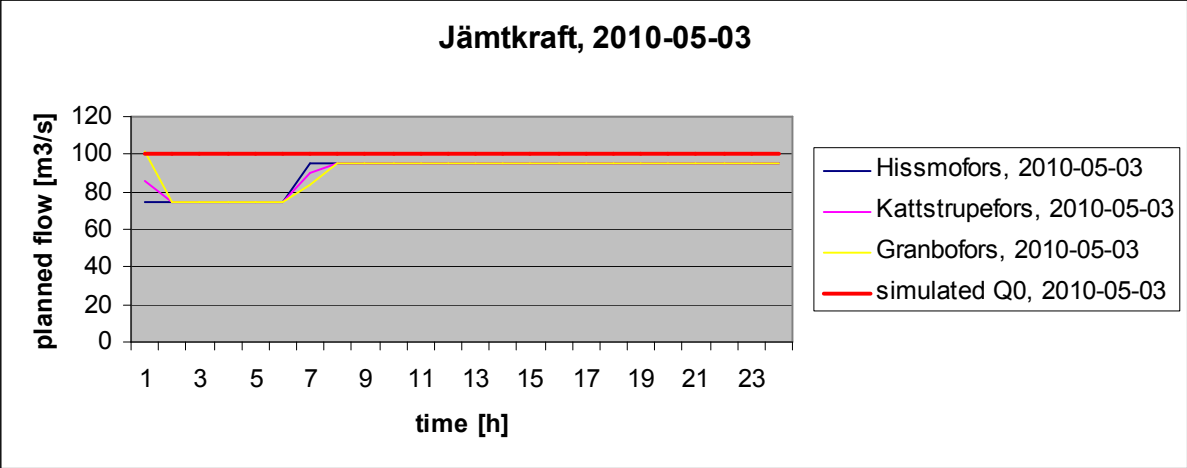


Figure 58: Planned discharges for the Jämtkraft reach on May 3rd 2010

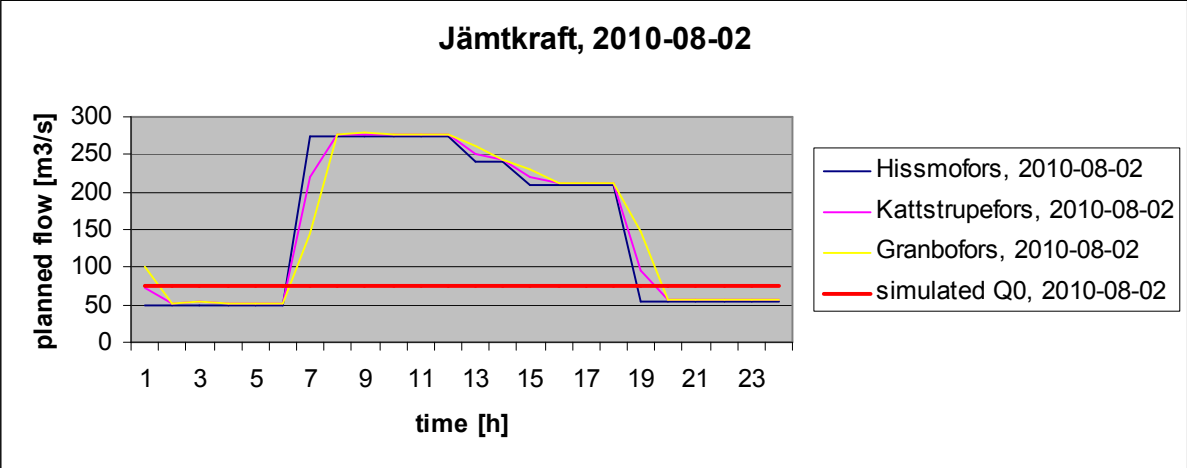


Figure 59: Planned discharges for the Jämtkraft reach on August 2nd 2010

The discharge for the august simulation was chosen as a low load plan to try and analyse the reach’s possibilities to maintain frequency reserves at low load conditions. The simulated discharge was chosen as a little higher than the absolute minimum *to be able to regulate* some.

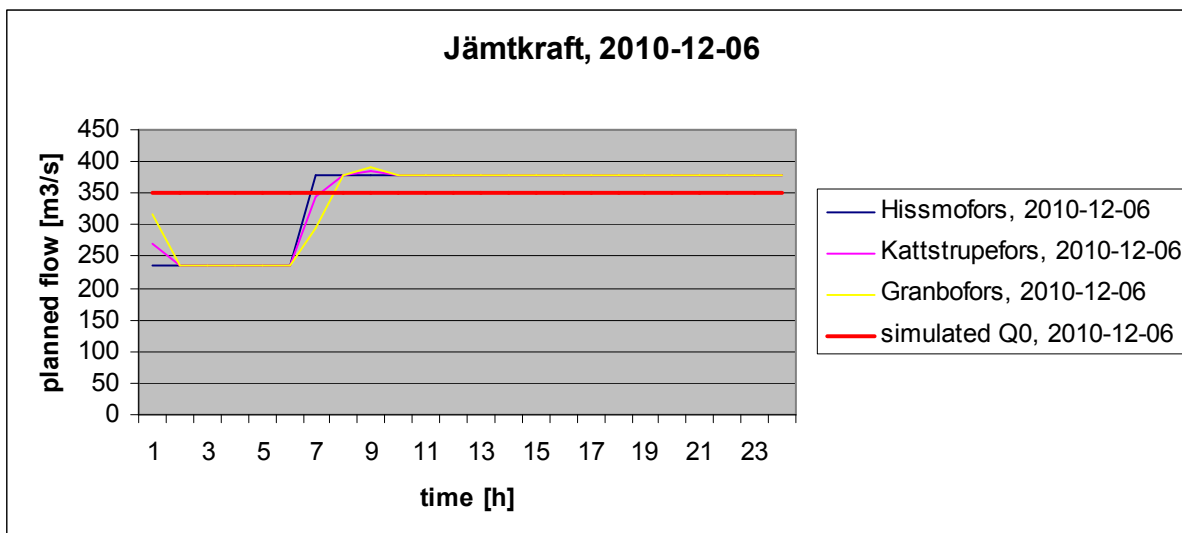


Figure 60: Planned discharges for the Jämtkraft reach on December 6th 2010

The simulations for Jämtkraft were setup as stated in Table 4.

Table 4: Initiation setups for the Jämtkraft simulations, all min/max regulation capacities refer to reserved FNR regulation.

Jämtkraft	2010-05-03			2010-12-06		
	Hissmorfors	Kattstrupefors	Granbofors	Hissmorfors	Kattstrupefors	Granbofors
Q0 [m ³ /s]	180	180	180	350	350	350
h0 setpoint [m]	2.25	0.1	0.1	2.25	0.1	0.1
ep [p.u.]	0.1	1,0	1,0	0.04	1,0	1,0
Pmin [MW]	8.13	3.55	1.3	35.6	35.6	29,0
PminReg [MW]	8.8	3.8	1.3	39,0	37,0	30.2
Pplan [MW]	16.25	11.4	4.7	60.6	50.1	18.7
PmaxReg [MW]	32.3	14.5	13.3	65.3	59.4	23.1
Pmax [MW]	33,0	14.8	13.3	68.7	60.6	23.1
Regulation limit	FDR	FDR	-	FDR	FDR	-
	2010-08-02					
	Hissmorfors	Kattstrupefors	Granbofors			
Q0 [m ³ /s]	280	280	280			
h0 setpoint [m]	2.25	0.1	0.1			
ep [p.u.]	0.1	1,0	1,0			
Pmin [MW]	8.13	3.55	1.3			
PminReg [MW]	8.8	3.8	1.3			
Pplan [MW]	12.7	7.6	3.1			
PmaxReg [MW]	32.4	14.5	13.3			
Pmax [MW]	33	14.8	13.3			
Regulation limit	FNR	FNR	-			

B.3 Vattenfall

For the Vattenfall reach simulations were made for all three different dates of May 3rd, August 2nd and December 6th of 2010. The original discharge plans were retrieved from Vattenfall and from these a static discharge plan was created, see Figure 61, Figure 62 and Figure 63.

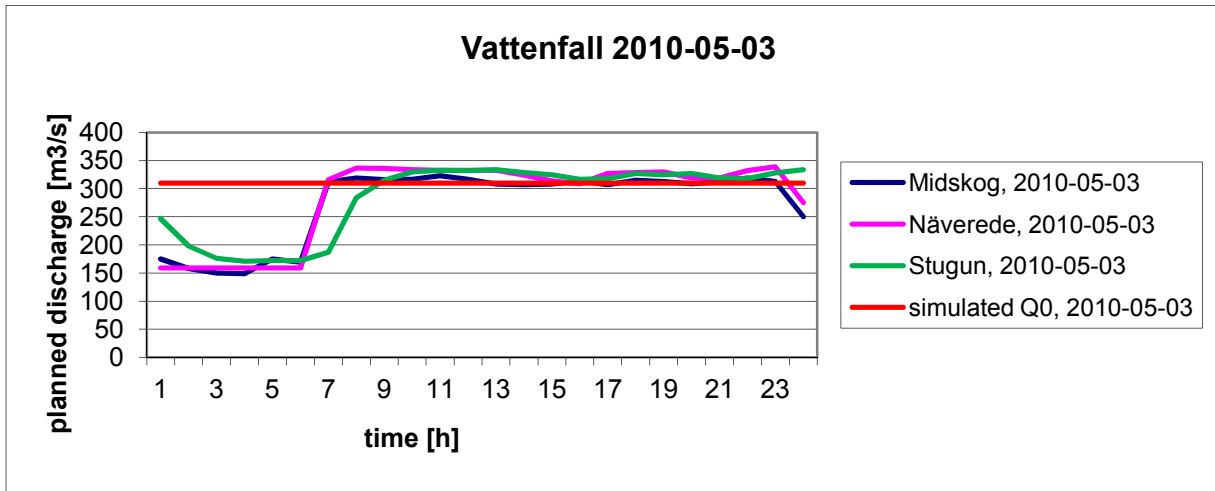


Figure 61: Discharge plan for Vattenfall on May 3rd 2010

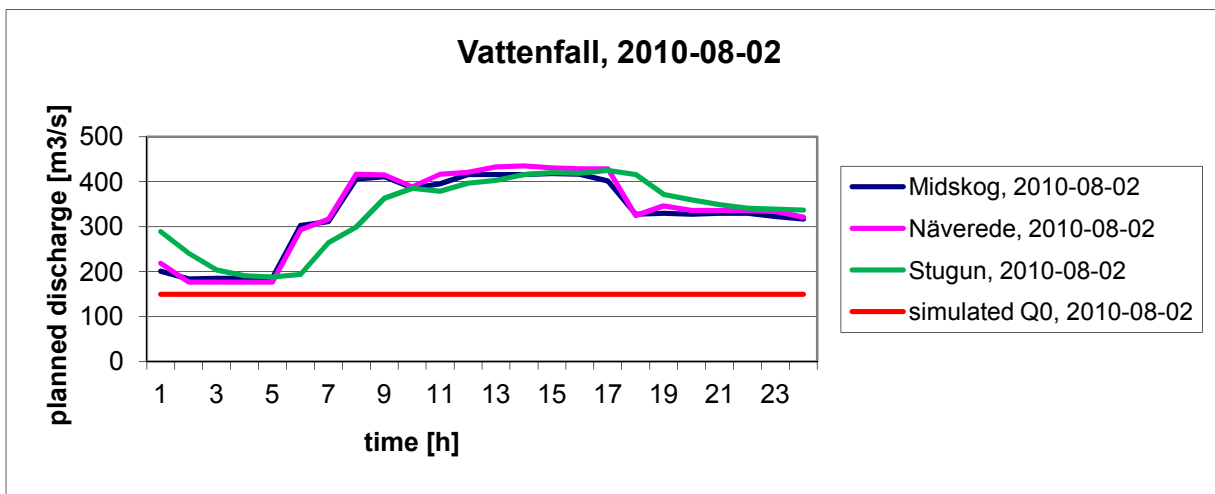


Figure 62: Discharge plan for Vattenfall on August 2nd 2010

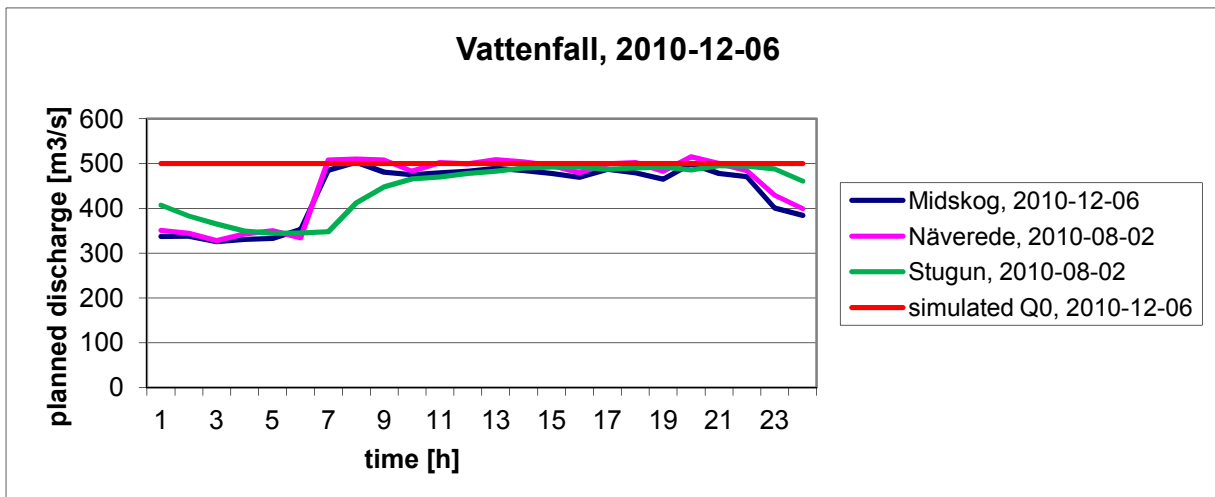


Figure 63: Discharge plan for Vattenfall on December 6th 2010

The discharge for simulation for August 2nd has been chosen at the lower end of the discharge plan and then lowered some more. This was done to analyse the river reach's possibility to maintain the

reserves during low load operation, see 1.1 Project aim. The lowest plan for the day was roughly 180 m³/s but at this level Midskog would have no possibilities for downwards regulation and according to (Damgren 2011) a typical low load discharge for this reach is roughly 150 m³/s and it was therefore chosen.

The simulations for Vattenfall were setup as stated in Table 5.

Table 5: Initiation setup for the Vattenfall simulations, all min/max regulation capacities refer to reserved FNR regulation.

VATTENFALL	2010-05-03			2010-12-06		
	Midskog	Näverede	Stugun	Midskog	Näverede	Stugun
Q0 [m ³ /s]	310	310	310	500	310	310
h0 setpoint [m]	0.5	0.05	0.05	0.5	0.05	0.05
ep [p.u.]	0.1	1,0	1,0	0.1	1,0	1,0
Pmin [MW]	56.95	10.7	24.09	99.87	36.6	24.09
PminReg [MW]	62.25	10.7	24.10	103.07	36.6	24.10
Pplan [MW]	74.31	33.9	24.1	118.8	53.1	38.33
PmaxReg [MW]	92.1	35.7	47.93	152.13	66.6	47.93
Pmax [MW]	97.4	35.7	47.93	155.33	66.6	47.93
Regulation limit	FNR	-	-	FNR	-	-
	2010-08-02					
	Midskog	Näverede	Stugun			
Q0 [m ³ /s]	390	310	310			
h0 setpoint [m]	0.5	0.05	0.05			
ep [p.u.]	0.1	1,0	1,0			
Pmin [MW]	56.95	36.6	24.09			
PminReg [MW]	59.15	36.6	24.10			
Pplan [MW]	92.92	42,0	30.56			
PmaxReg [MW]	95.2	66.6	47.93			
Pmax [MW]	97.4	66.6	47.93			
Regulation limit	FNR	-	-			

B.3 Fortum

From Fortum only one simulation was made, the one from 2010-12-06. This was decided after analysing their discharge plans for the respective days where it was found that the individual station discharge plans differ too much from each other se (Figure 117, Figure 118 and Figure 119) in order for this model to be able to create a static discharge plan for each station.

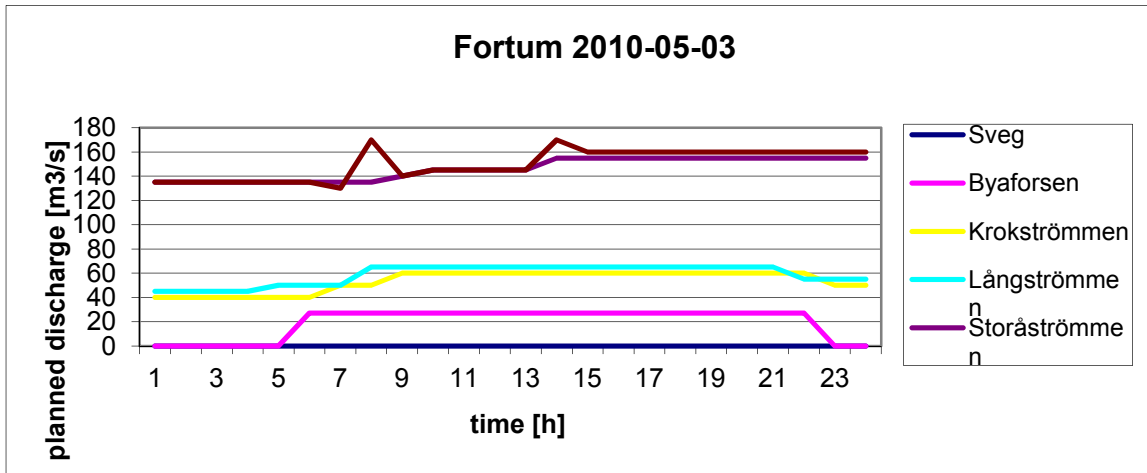


Figure 64: Discharge plan for the Fortum reach on May 3rd 2010.

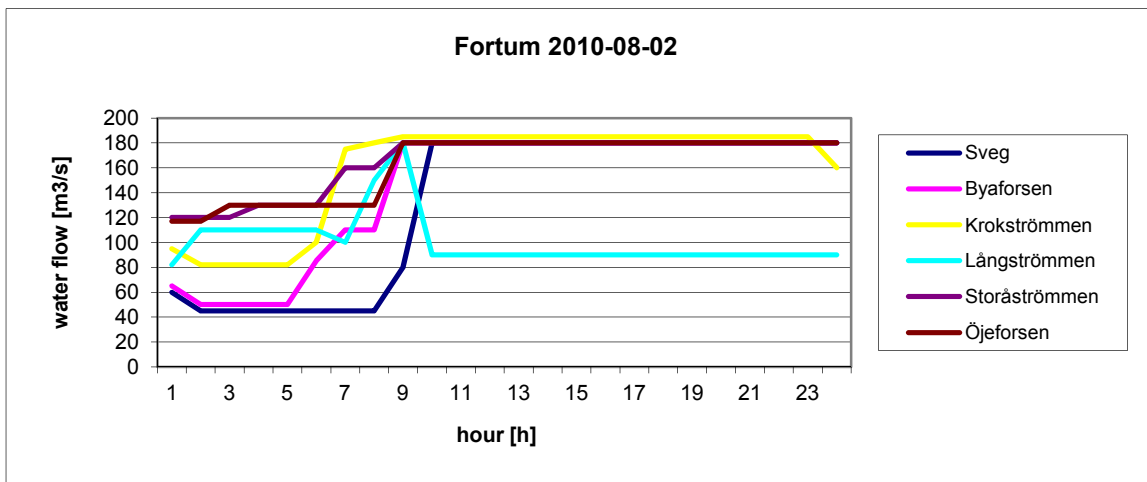


Figure 65: Discharge plan for the Fortum reach on August 2nd 2010

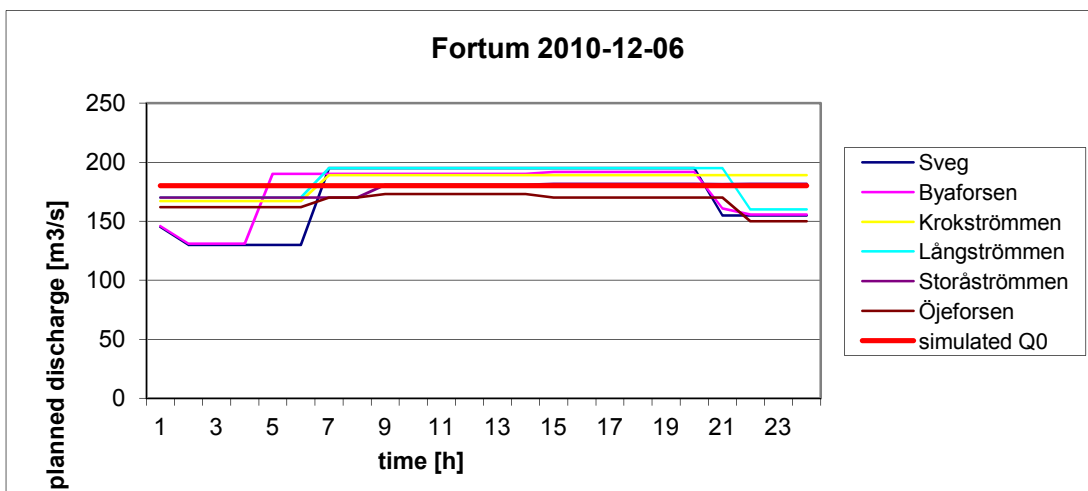


Figure 66: Discharge plan for the Fortum reach on December 6th 2010 including the static discharge plan Q0 used for the simulation

The simulation for Fortum was setup in accordance with Table 6.

Table 6: Initiation setup for the Fortum simulation, all min/max regulation capacities refer to reserved FNR regulation.

Fortum	2010-12-06		
	Sveg	Byaforsen	Krokströmmen
Q0 [m3/s]	180	180	180
h0 setpoint [m]	10	0.5	0.4
ep [p.u.]	1	1	0.06
Pmin [MW]	1.2	1.6	62.3
PminReg [MW]	1.3	1.6	65.6
Pplan [MW]	30.4	15.5	89
PmaxReg [MW]	34.3	17.3	96.7
Pmax [MW]	34.5	17.3	100
Regulation limitation	-	-	FNR

	2010-12-06		
	Långströmmen	Storåströmmen	Öjeforsen
Q0 [m3/s]	180	180	180
h0 setpoint [m]	0.25	0.3	0.4
ep [p.u.]	1	0.1	0.1
Pmin [MW]	38.5	14.4	9
PminReg [MW]	38.6	14.9	9.58
Pplan [MW]	50.4	25.6	28
PmaxReg [MW]	56.2	26.3	28.7
Pmax [MW]	56.3	26.8	29,3
Regulation limitation	FNR	-	FNR

C – Simulation results

C.1 Jämkraft

May 3rd 2010

For this simulation to produce a stable solution for the developments of the reservoir surfaces the weights for the optimization needed to be changed. This was done by setting the weight for power deviation (eq. 4.9) to the identity matrix and the weight for surface level deviation (eq. 4.18) to zero. The results can be seen in the following graphs.

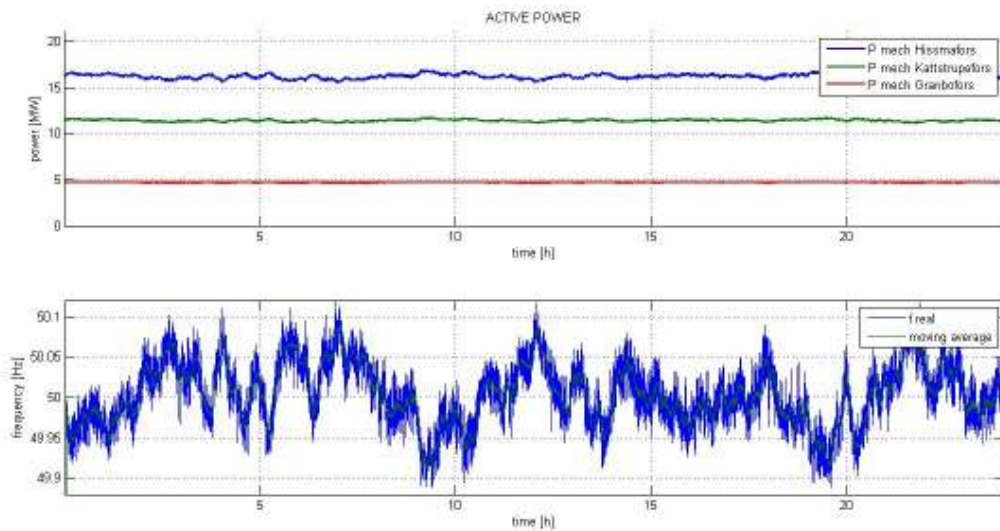


Figure 67: LFC = OFF, 2010-05-03 simulation, Mechanical power delivered by Hissmofors, Kattstrupefors and Granbofors displayed with the resulting grid frequency.

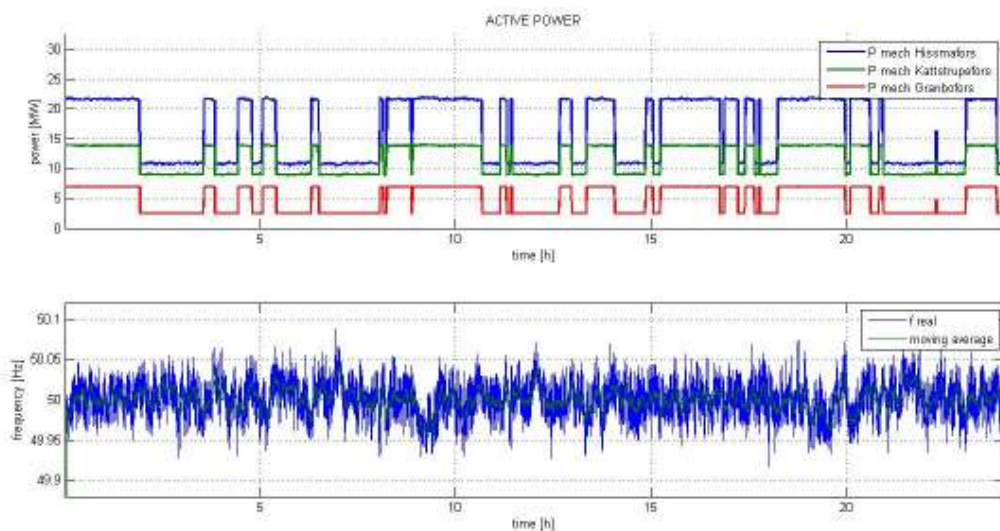


Figure 68: LFC = ON, 2010-05-03 simulation, Mechanical power delivered by Hissmofors, Kattstrupefors and Granbofors displayed with the resulting grid frequency.

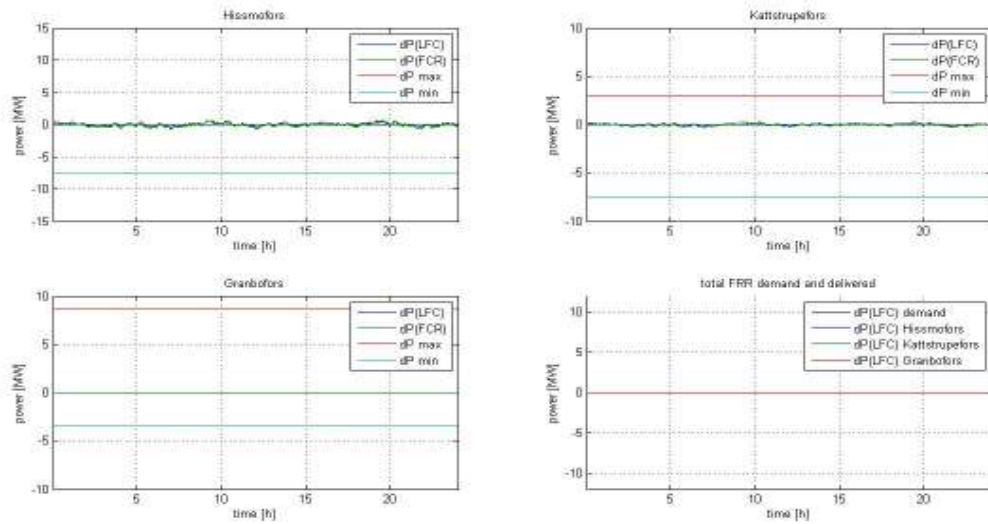


Figure 69: LFC = OFF, 2010-05-03 simulation, Active mechanical power regulation delivered by Hissmofors, Kattstrupefors and Granbofors.

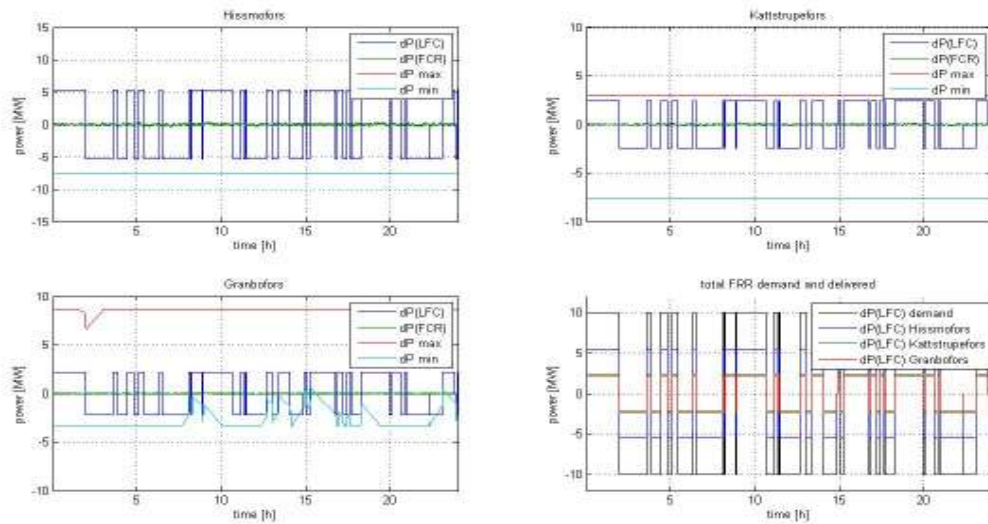


Figure 70: LFC = ON, 2010-05-03 simulation, Active mechanical power regulation delivered by Hissmofors, Kattstrupefors and Granbofors. The sum of all LFC regulation is also displayed.¹⁵

¹⁵ As you can see here the active regulation for Granbofors is not limited by the minimum regulation. This is fault within the distribution algorithm and discussed in section 6.1.

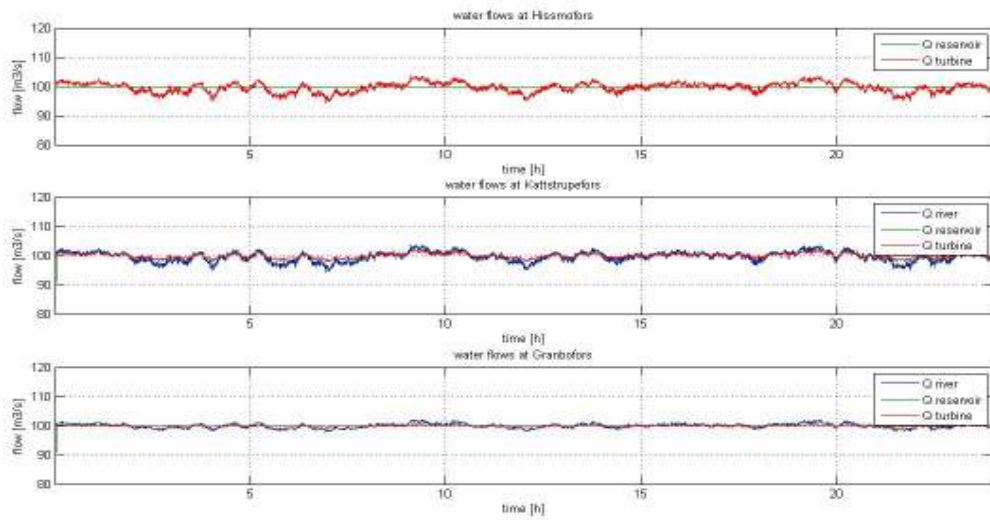


Figure 71: LFC = OFF, 2010-05-03 simulation, Resulting water flows entering the river (except Hissmofors where the reservoir is taken to be the initial point), entering the reservoir and flow used by the turbine to provide mechanical power.

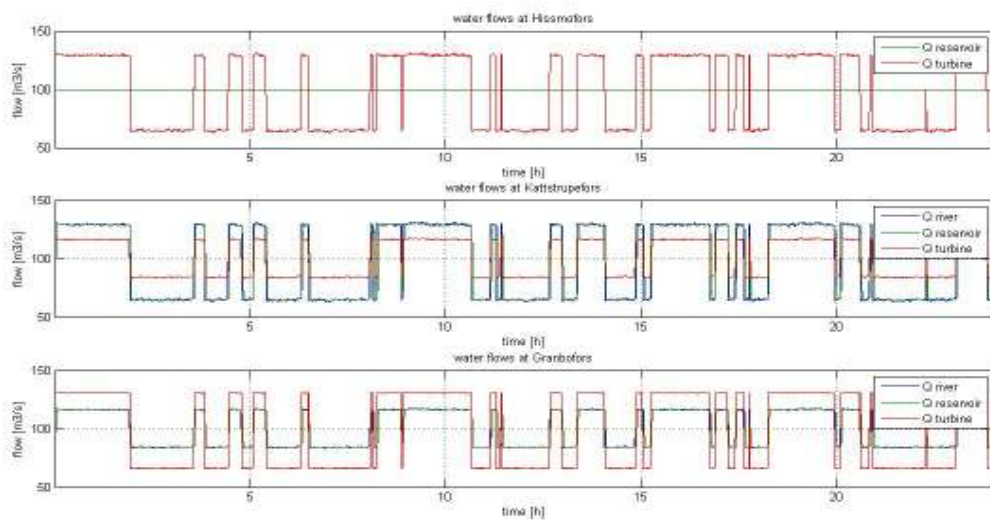


Figure 72: LFC = ON, 2010-05-03 simulation, Resulting water flows entering the river (except Hissmofors where the reservoir is taken to be the initial geographical point of the simulation), entering the reservoir and flow used by the turbine to provide mechanical power.

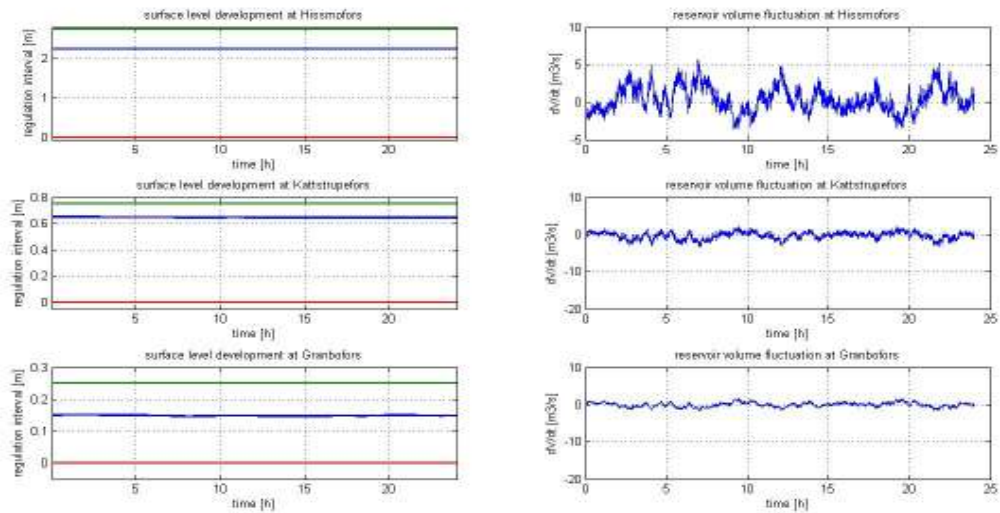


Figure 73: LFC = OFF, 2010-05-03 simulation, Resulting water levels in the reservoirs of Hissmofors, Kattstrupefors and Granbofors. The derivative of the reservoir volume fluctuation is also shown.

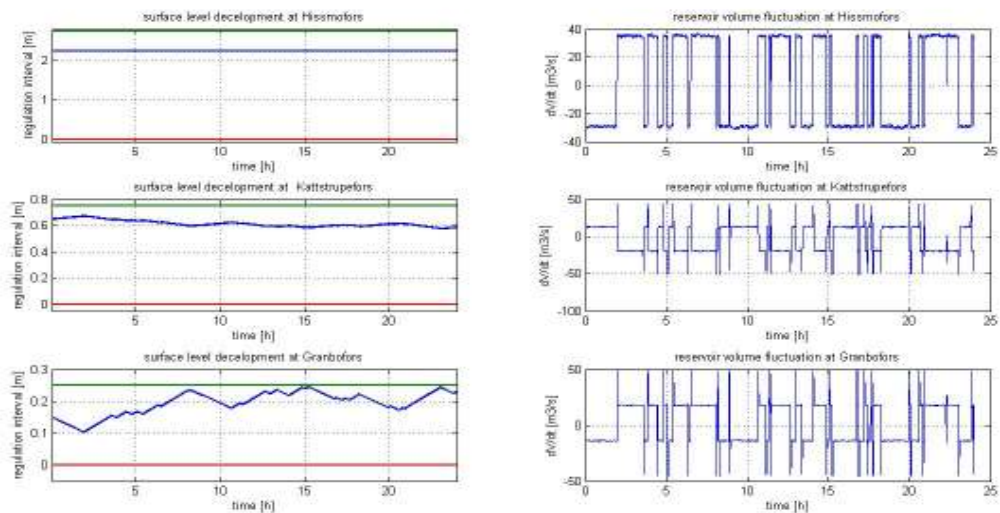


Figure 74: LFC = ON, 2010-05-03 simulation, Resulting water levels in the reservoirs of Hissmofors, Kattstrupefors and Granbofors. The derivative of the reservoir volume fluctuation is also shown.

August 2nd 2010

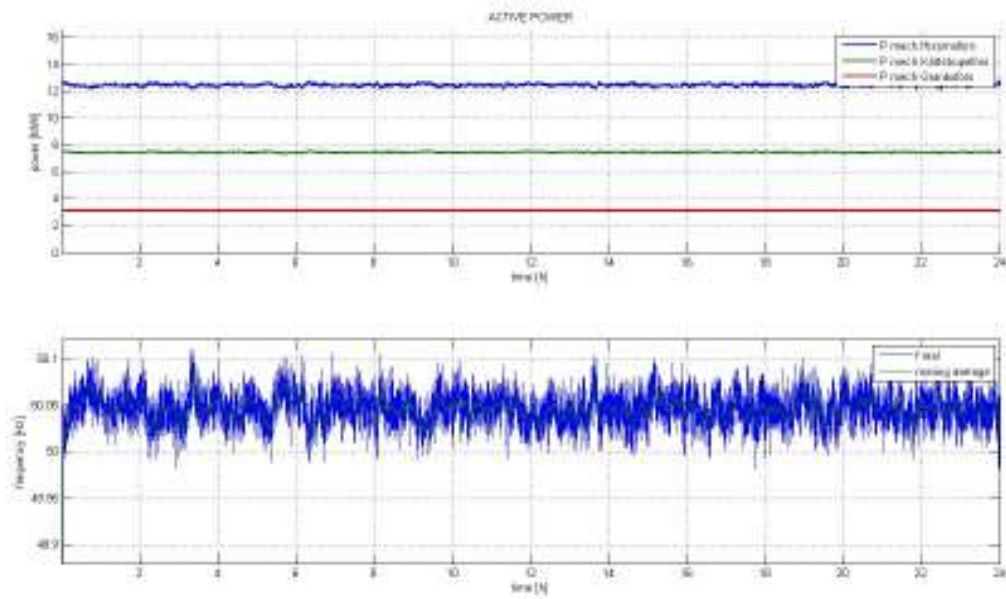


Figure 75: LFC = OFF, 2010-08-02 simulation, Mechanical power delivered by Hissmofors, Kattstrupefors and Granbofors displayed with the resulting grid frequency.

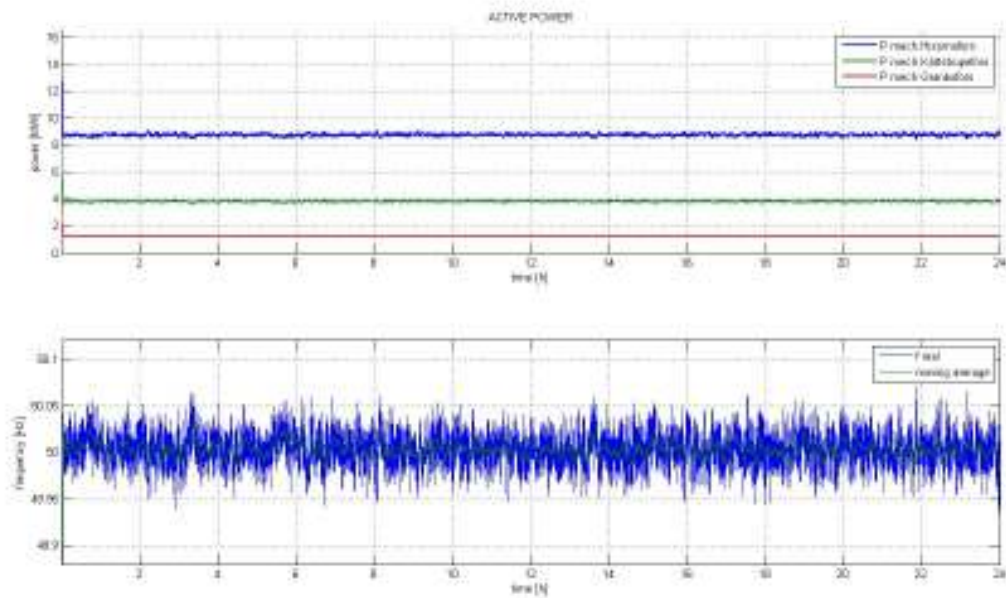


Figure 76: LFC = ON, 2010-08-02 simulation, Mechanical power delivered by Hissmofors, Kattstrupefors and Granbofors displayed with the resulting grid frequency.¹⁶

¹⁶ At roughly $t=16$ hours you can clearly see that the numerical solutions fails to stabilize, this is discussed in section 6.1.

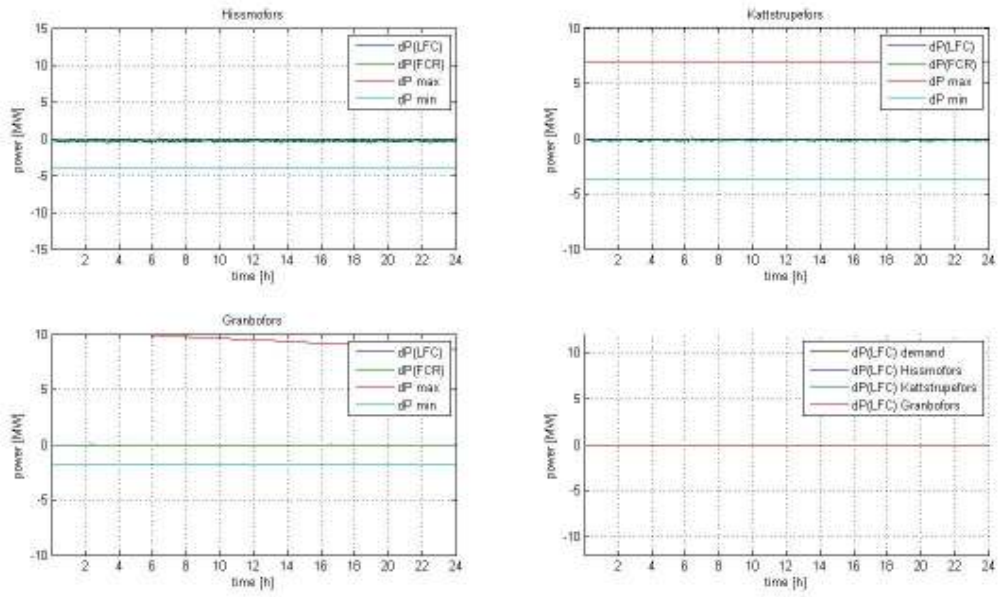


Figure 77: LFC = OFF, 2010-08-02 simulation, Active mechanical power regulation delivered by Hissmofors, Kattstrupefors and Granbofors.

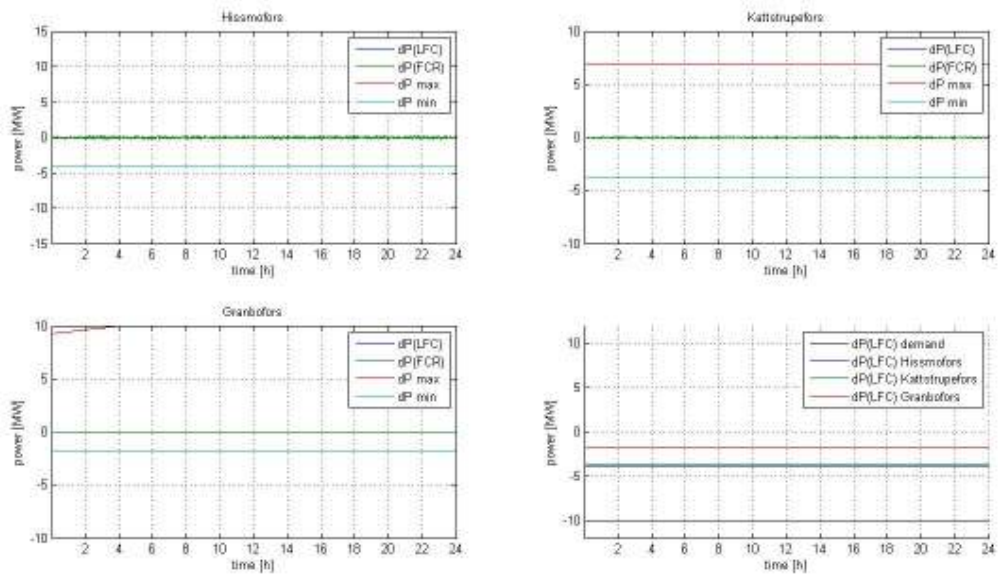


Figure 78: LFC = ON, 2010-08-02 simulation, Active mechanical power regulation delivered by Hissmofors, Kattstrupefors and Granbofors. The sum of all LFC regulation is also displayed.¹⁷

¹⁷ As you can see here the active regulation for Granbofors is not limited by the minimum regulation. This is fault within the distribution algorithm and discussed in section 6.1.

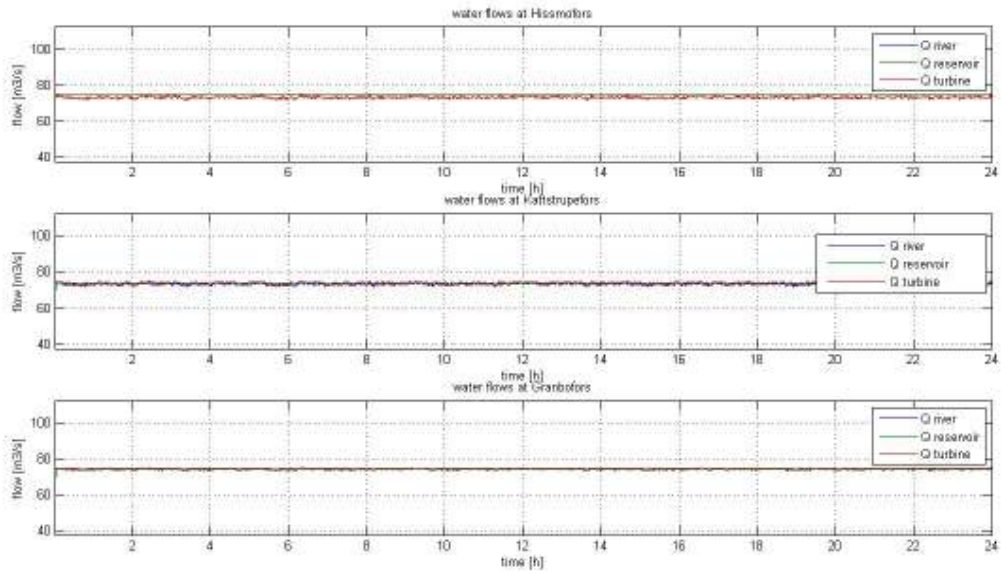


Figure 79: LFC = OFF, 2010-08-02 simulation, Resulting water flows entering the river (except Hissmofors where the reservoir is taken to be the initial point), entering the reservoir and flow used by the turbine to provide mechanical power.

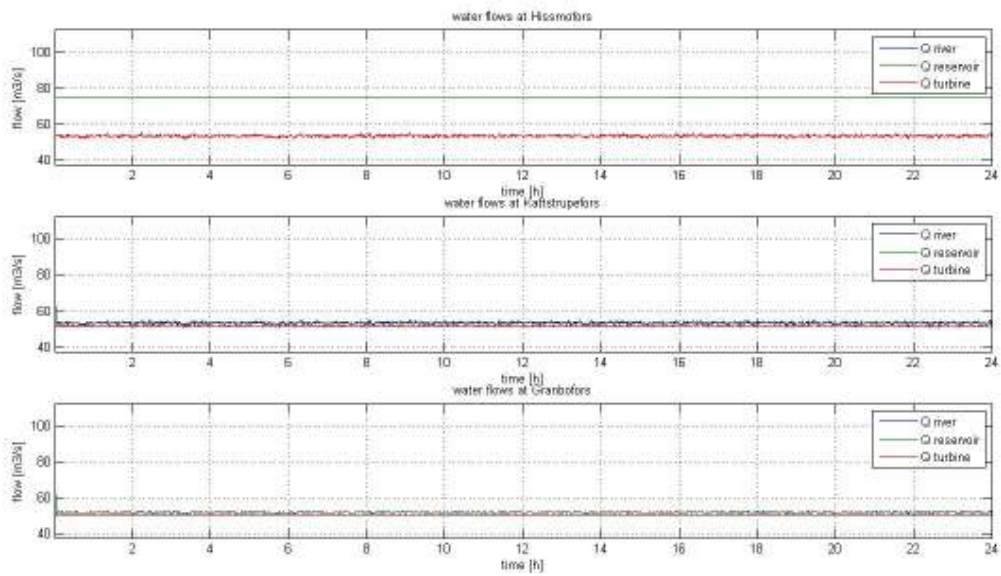


Figure 80: LFC = ON, 2010-08-02 simulation, Resulting water flows entering the river (except Hissmofors where the reservoir is taken to be the initial geographical point of the simulation), entering the reservoir and flow used by the turbine to provide mechanical power.

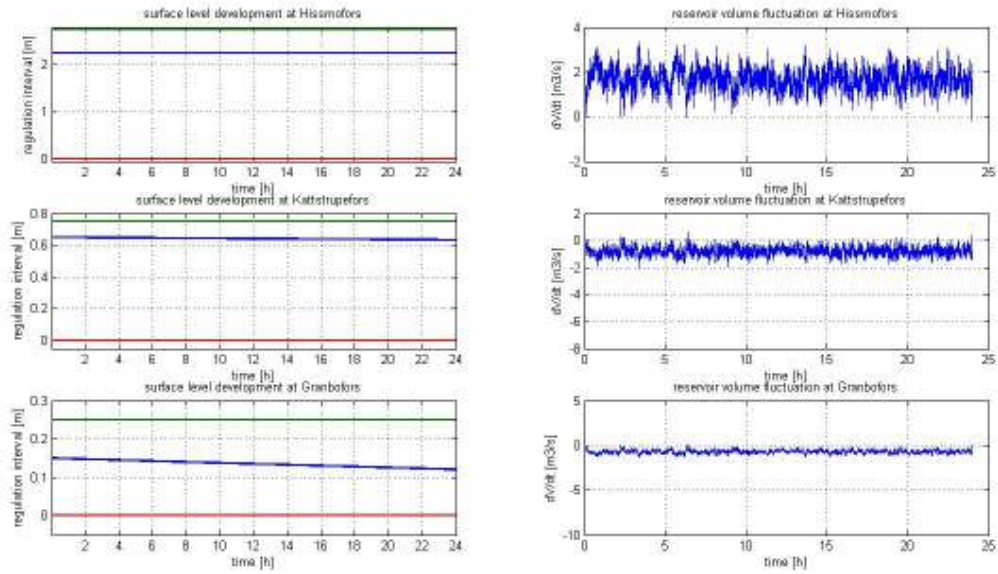


Figure 81: LFC = OFF, 2010-08-02 simulation, Resulting water levels in the reservoirs of Hissmofors, Kattstrupefors and Granbofors. The derivative of the reservoir volume fluctuation is also shown.

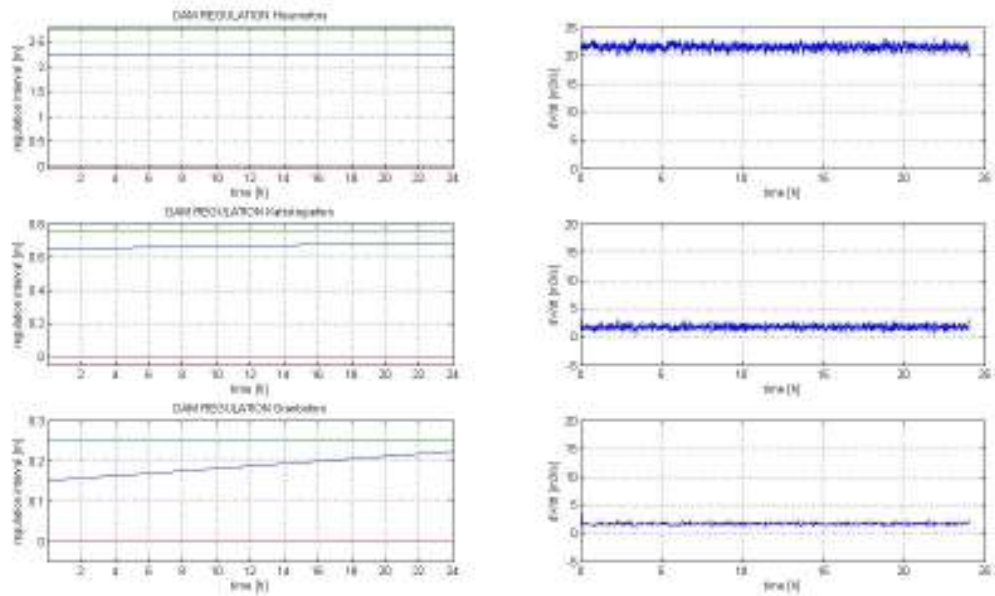


Figure 82: LFC = ON, 2010-08-02 simulation, Resulting water levels in the reservoirs of Hissmofors, Kattstrupefors and Granbofors. The derivative of the reservoir volume fluctuation is also shown.

December 6th 2010

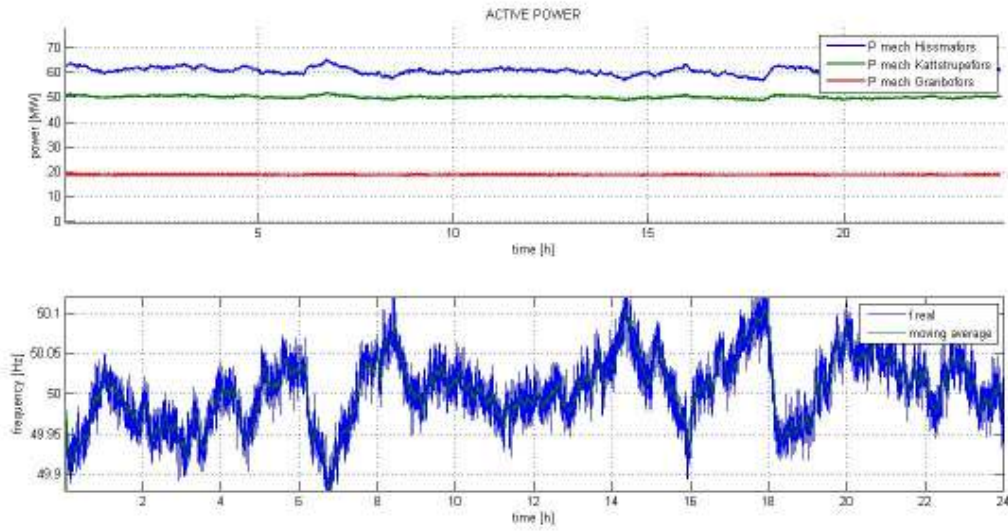


Figure 83: LFC = OFF, 2010-12-06 simulation, Mechanical power delivered by Hissmofors, Kattstrupefors and Granbofors displayed with the resulting grid frequency.

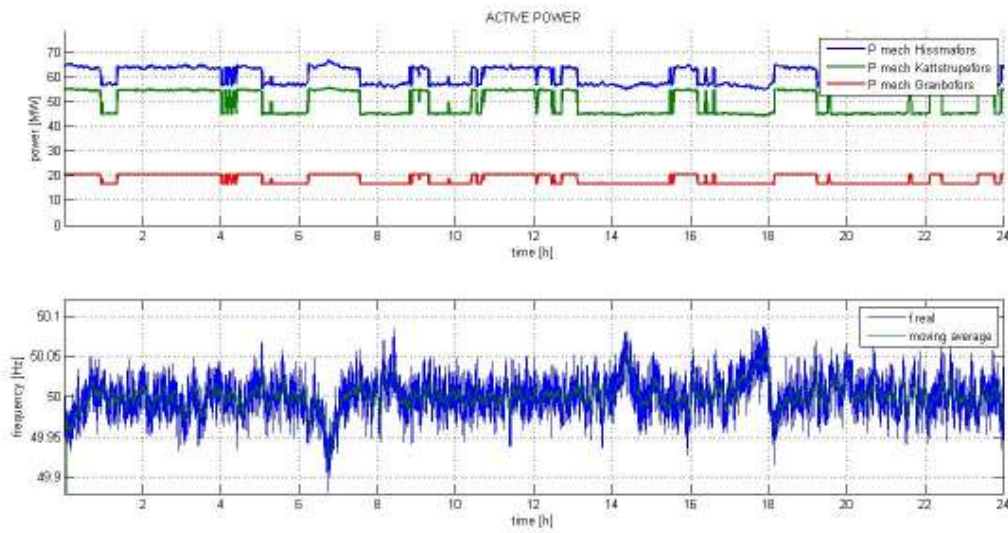


Figure 84: LFC = ON, 2010-12-06 simulation, Mechanical power delivered by Hissmofors, Kattstrupefors and Granbofors displayed with the resulting grid frequency.

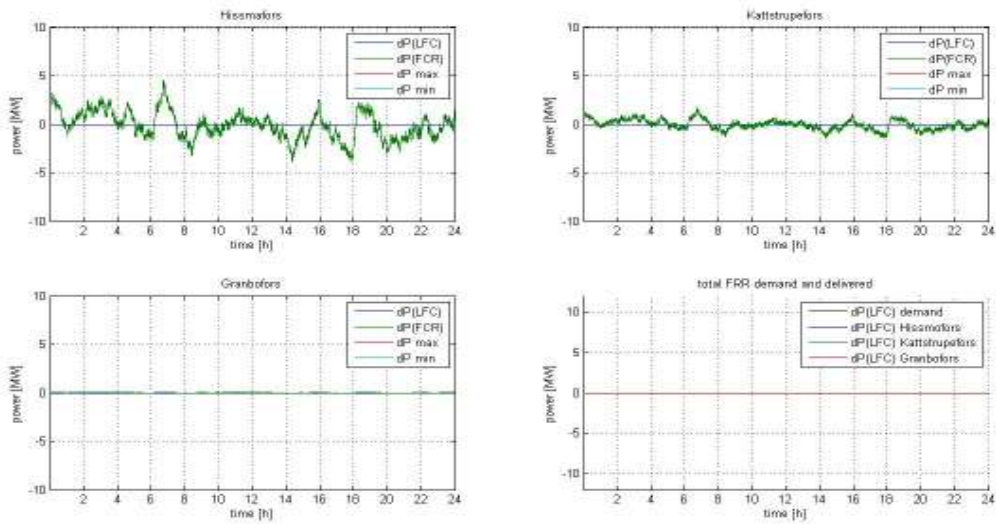


Figure 85: LFC = OFF, 2010-12-06 simulation, Active mechanical power regulation delivered by Hissmofors, Kattstrupefors and Granbofors.

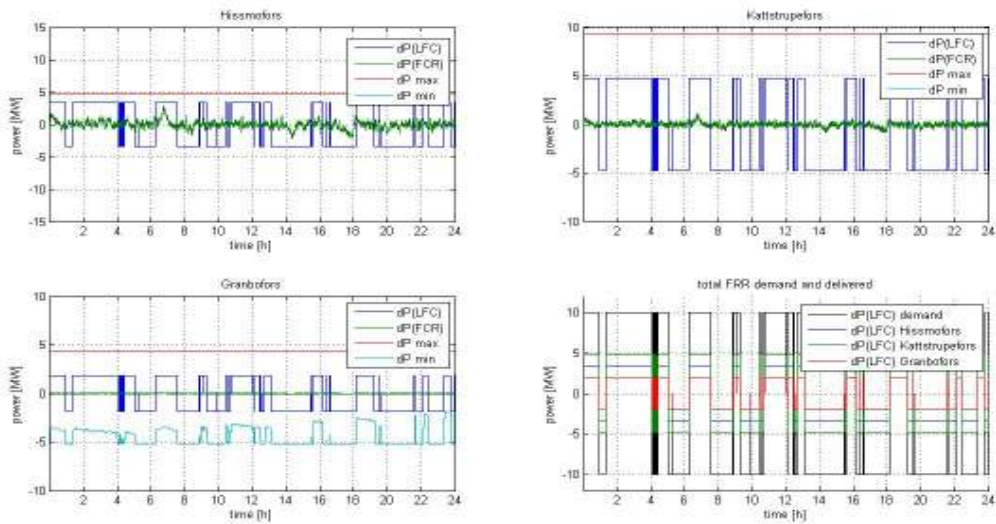


Figure 86: LFC = ON, 2010-12-06 simulation, Active mechanical power regulation delivered by Hissmofors, Kattstrupefors and Granbofors. The sum of all LFC regulation is also displayed.

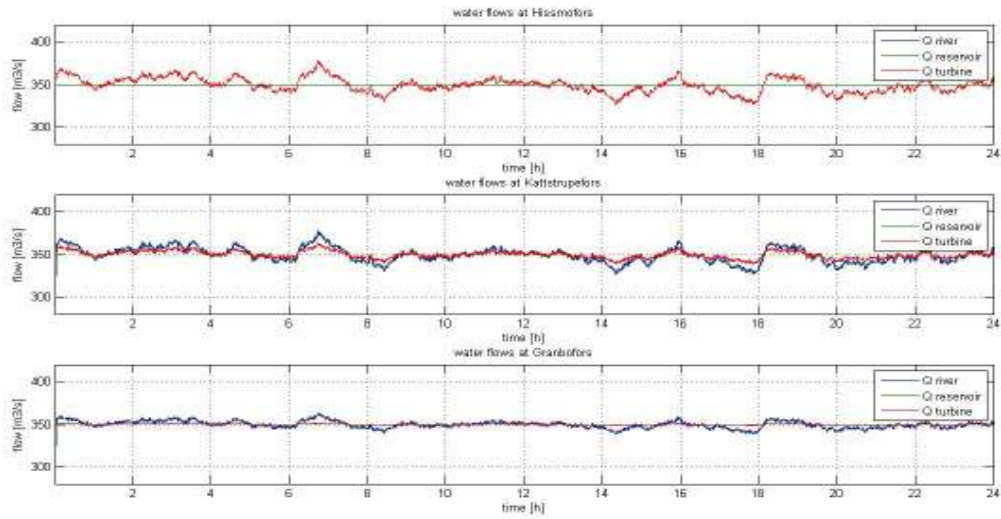


Figure 87: LFC = OFF, 2010-12-06 simulation, Resulting water flows entering the river (except Hissmofors where the reservoir is taken to be the initial point), entering the reservoir and flow used by the turbine to provide mechanical power.

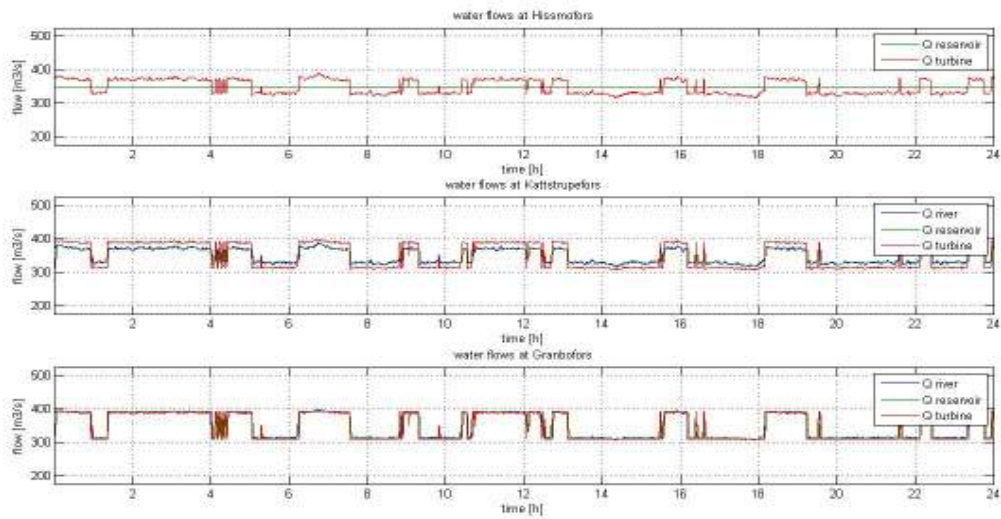


Figure 88: LFC = ON, 2010-12-06 simulation, Resulting water flows entering the river (except Hissmofors where the reservoir is taken to be the initial geographical point of the simulation), entering the reservoir and flow used by the turbine to provide mechanical power.

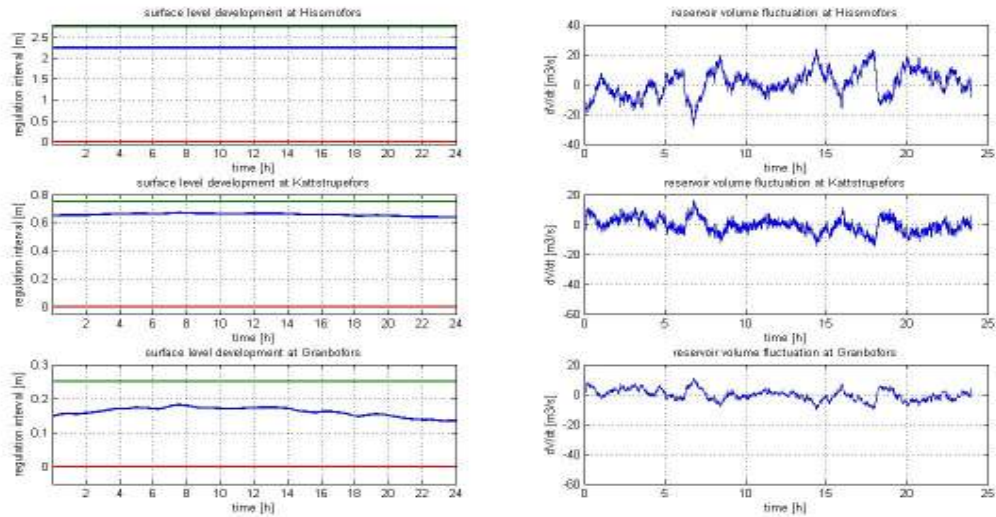


Figure 89: LFC = OFF, 2010-12-06 simulation, Resulting water levels in the reservoirs of Hissmofors, Kattstrupefors and Granbofors. The derivative of the reservoir volume fluctuation is also shown.

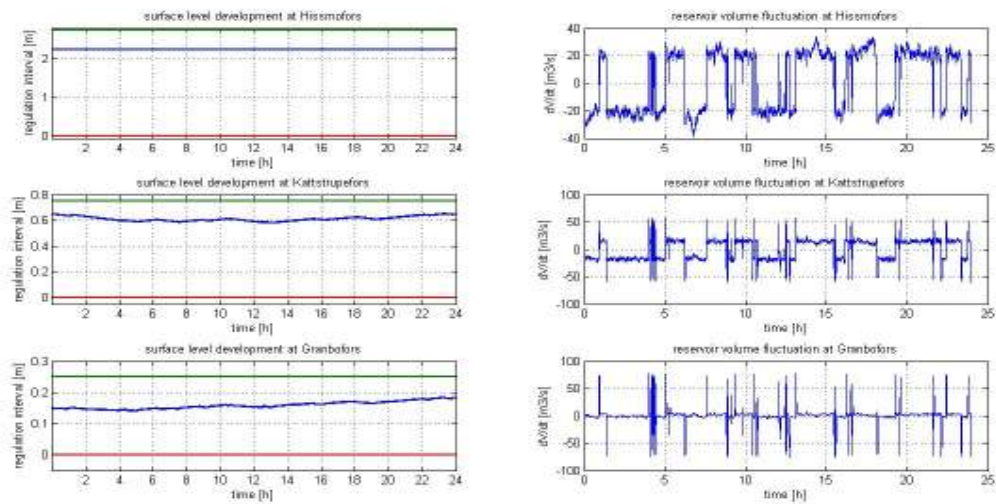


Figure 90: LFC = ON, 2010-12-06 simulation, Resulting water levels in the reservoirs of Hissmofors, Kattstrupefors and Granbofors. The derivative of the reservoir volume fluctuation is also shown.

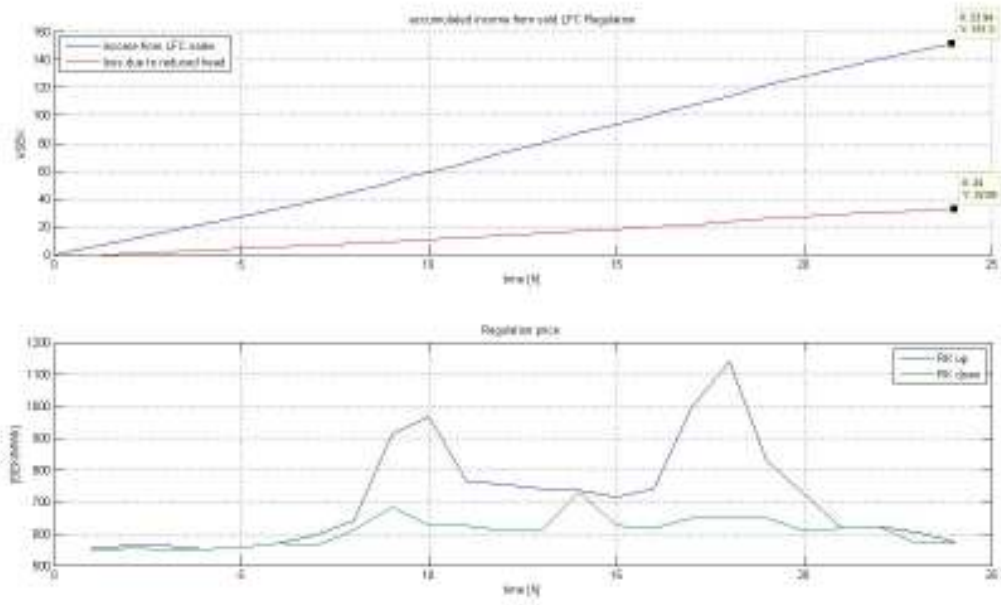


Figure 91: Accumulated income from sales of LFC with losses due to lowered surface levels in combination with the price at hand during the day for sale of regulation.

C.2 Vattenfall

May 3rd 2010

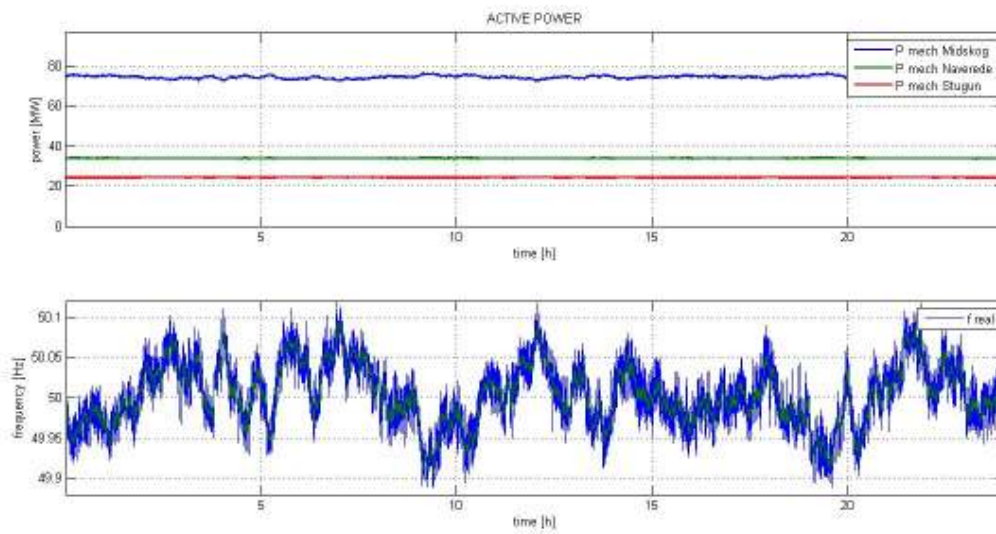


Figure 92: LFC = OFF, 2010-05-03 simulation, Mechanical power delivered by Midskog, Näverede and Stugun displayed with the resulting grid frequency.

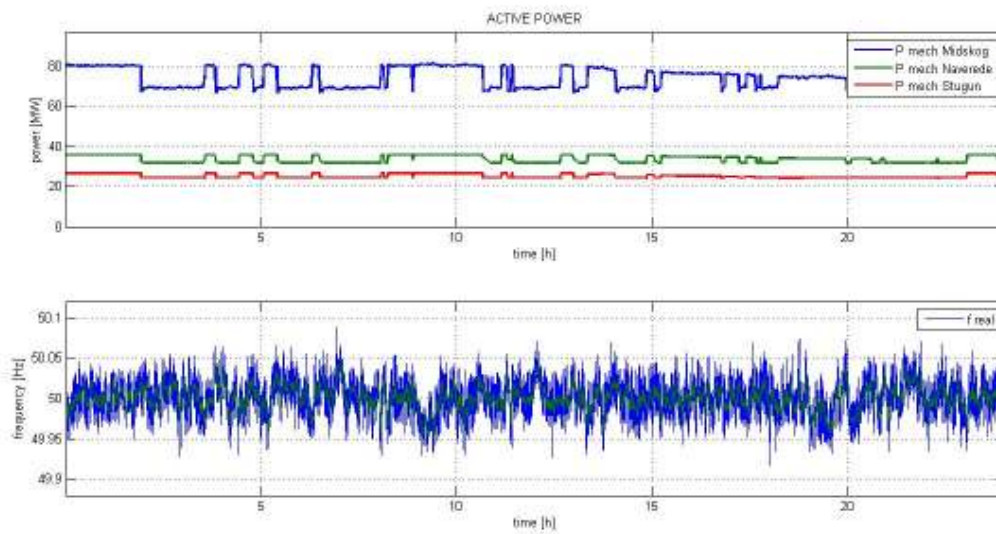


Figure 93: LFC = ON, 2010-05-03 simulation, Mechanical power delivered by Midskog, Näverede and Stugun displayed with the resulting grid frequency.

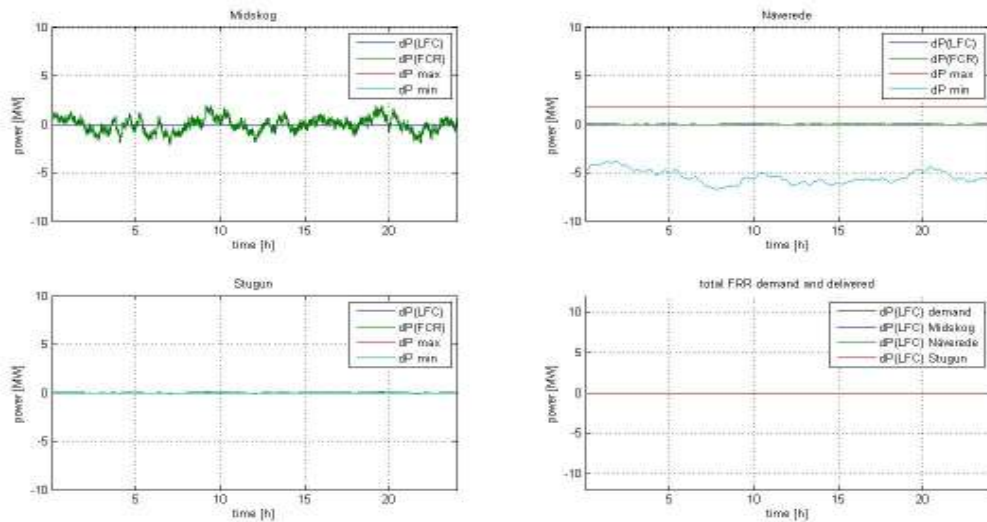


Figure 94: LFC = OFF, 2010-05-03 simulation, Active mechanical power regulation delivered by Midskog, Näverede and Stugun.

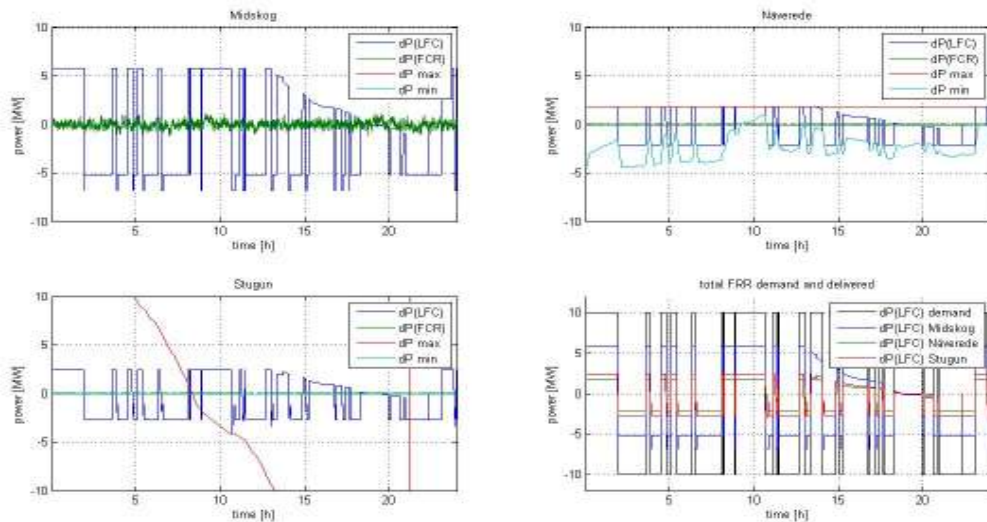


Figure 95: LFC = ON, 2010-05-03 simulation, Active mechanical power regulation delivered by Midskog, Näverede and Stugun. The sum of all LFC regulation is also displayed.¹⁸

¹⁸ As you can see here the active regulation for Stugun is not limited by the minimum regulation. For some unknown reason the max/min limits for Stugun also behaved radically irrational and is probably related some manual initiation fault. This is a fault within the distribution algorithm and is discussed in section 6.1.

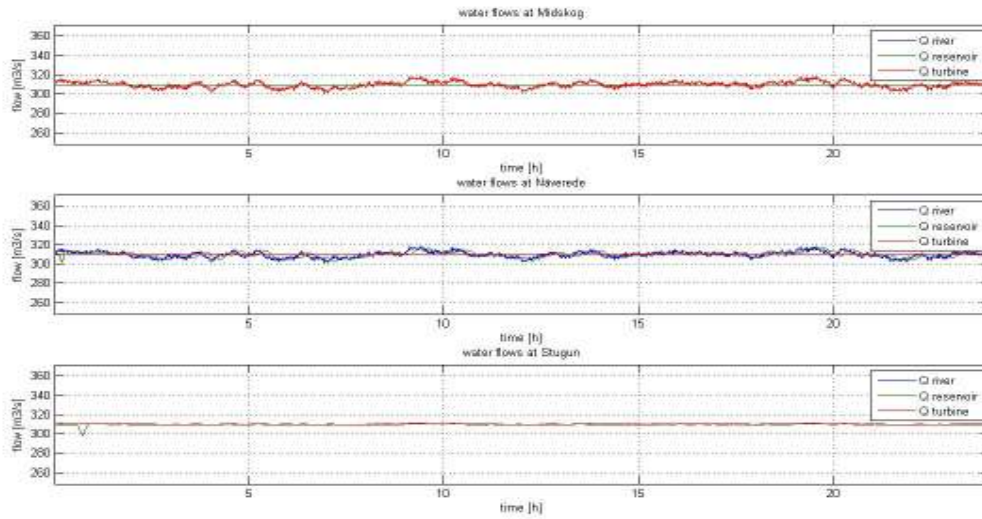


Figure 96: LFC = OFF, 2010-05-03 simulation. Resulting water flows entering the river (for Midskog, the flow entering and exiting the river is the same since this is kept as constant), entering the reservoir and discharge used by the turbine to provide mechanical power.

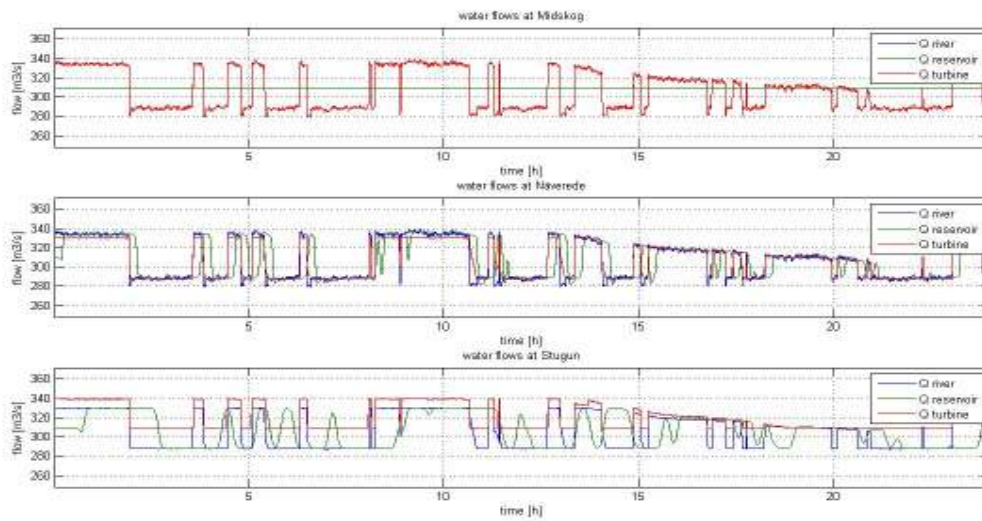


Figure 97: LFC = ON, 2010-05-03 simulation. Resulting water flows entering the river (for Midskog, the flow entering and exiting the river is the same since this is kept as constant), entering the reservoir and discharge used by the turbine to provide mechanical power.

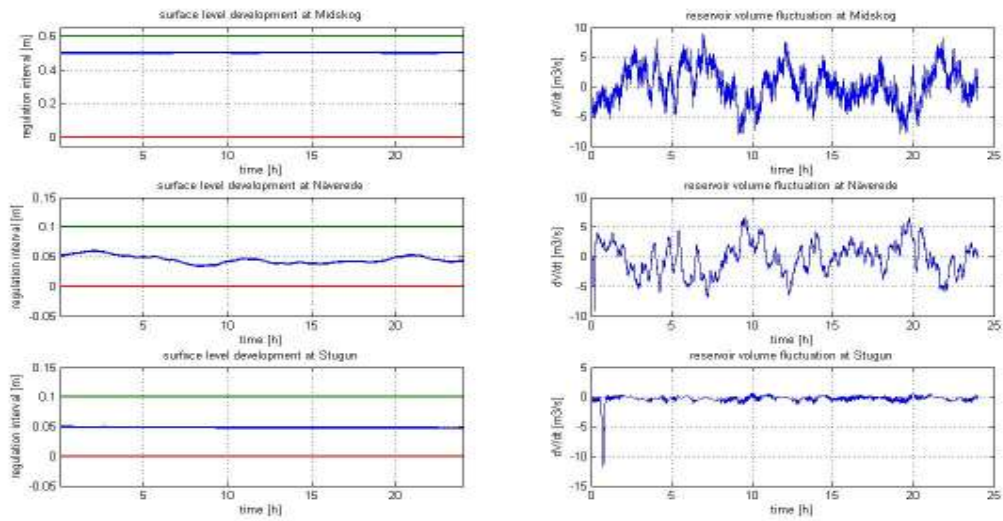


Figure 98: LFC = OFF, 2010-05-03 simulation, Resulting water levels in the reservoirs of Midskog, Näverede and Stugun. The derivative of the reservoir volume fluctuation is also shown.

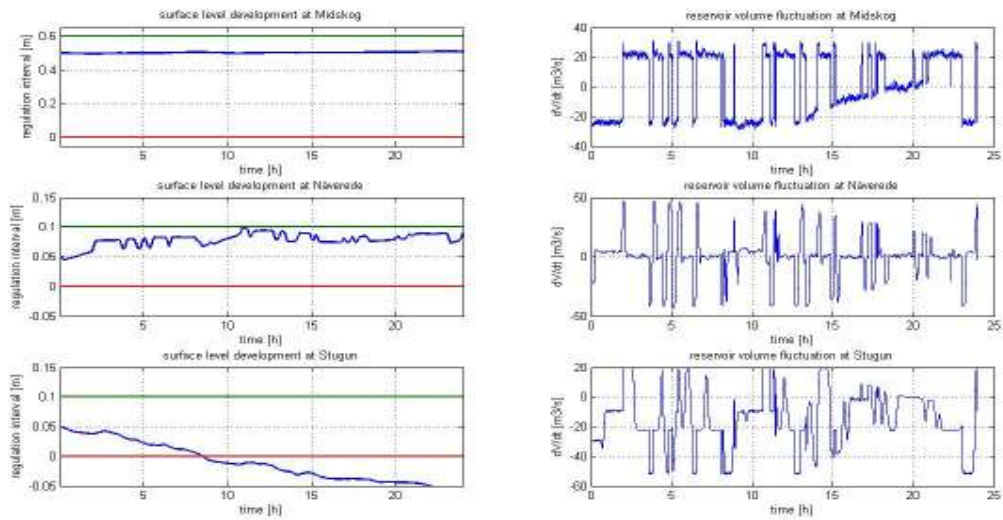


Figure 99: LFC = ON, 2010-05-03 simulation, Resulting water levels in the reservoirs of Midskog, Näverede and Stugun. The derivative of the reservoir volume fluctuation is also shown.

August 2nd 2010

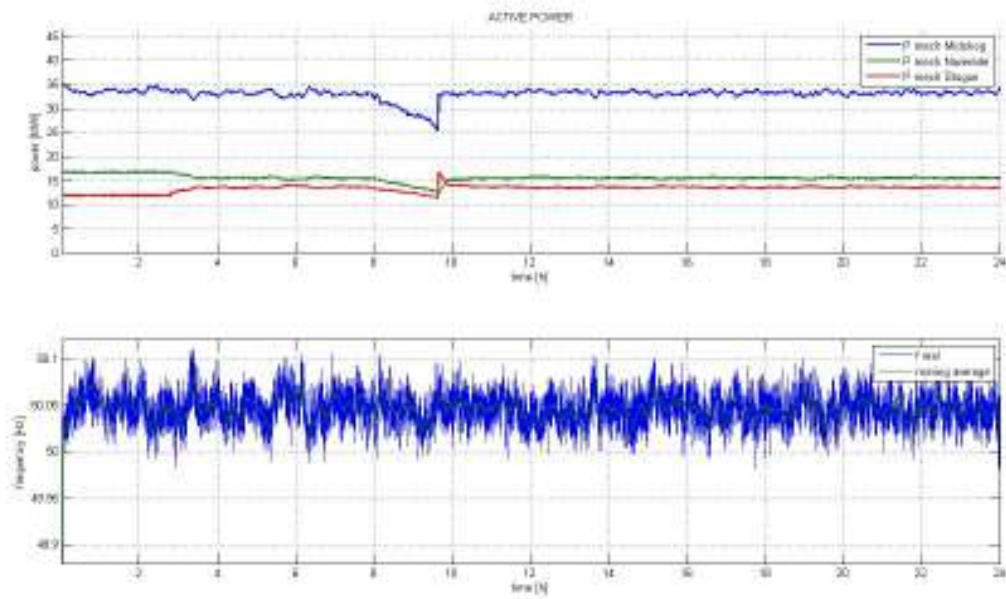


Figure 100: LFC = OFF, 2010-08-02 simulation, Mechanical power delivered by Hissmofors Midskog, Näverede and Stugun displayed with the resulting grid frequency.

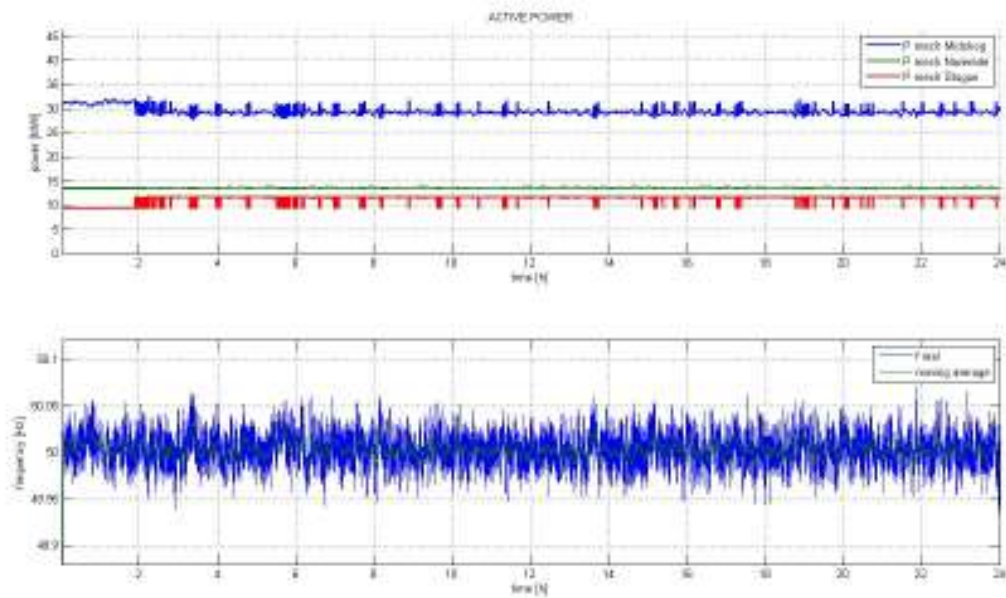


Figure 101: LFC = ON, 2010-08-02 simulation, Mechanical power delivered by Midskog, Näverede and Stugun displayed with the resulting grid frequency.¹⁹

¹⁹ At roughly t=4 hours you can clearly see that the numerical solutions fails to stabilize, this is discussed in section 6.1.

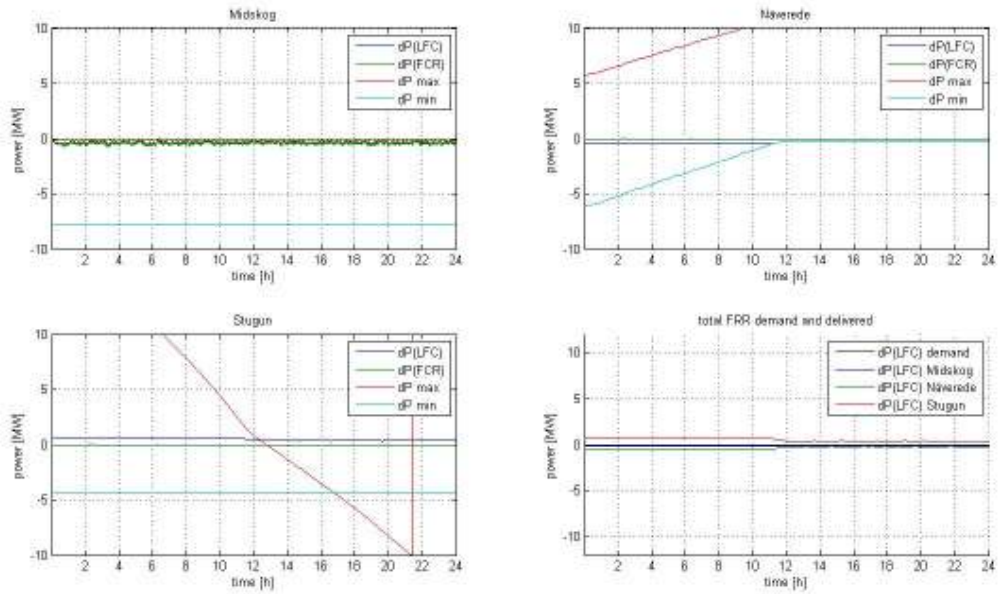


Figure 102: LFC = OFF, 2010-08-02 simulation, Active mechanical power regulation delivered by Midskog, Näverede and Stugun.²⁰

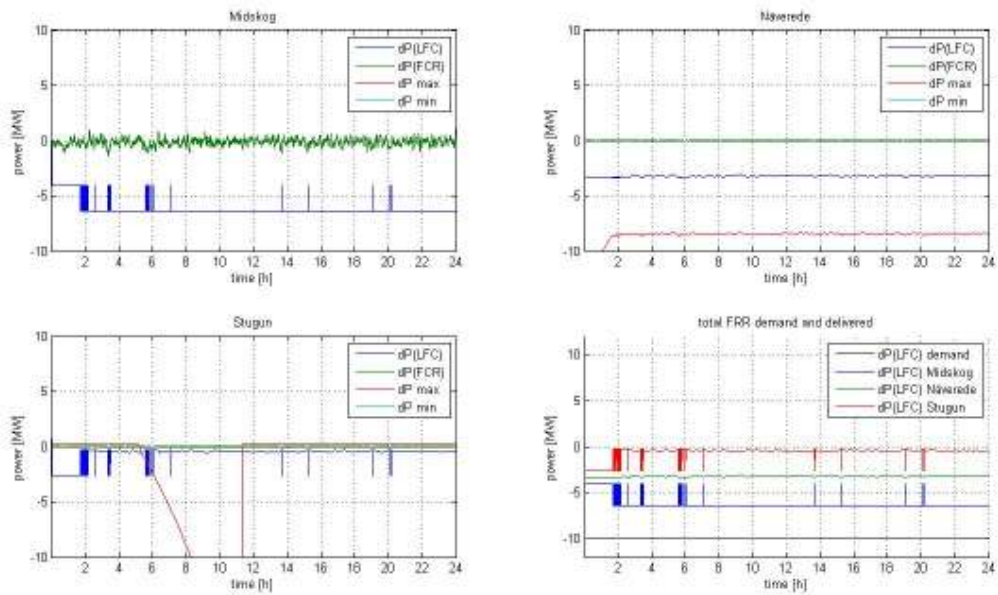


Figure 103: LFC = ON, 2010-08-02 simulation, Active mechanical power regulation delivered by Midskog, Näverede and Stugun. The sum of all LFC regulation is also displayed.

²⁰ As you can see here the active regulation for Stugun is not limited by the minimum regulation. For some unknown reason the max/min limits for Stugun also behaved radically irrational and is probably related some manual initiation fault. This is a fault within the distribution algorithm and is discussed in section 6.1.

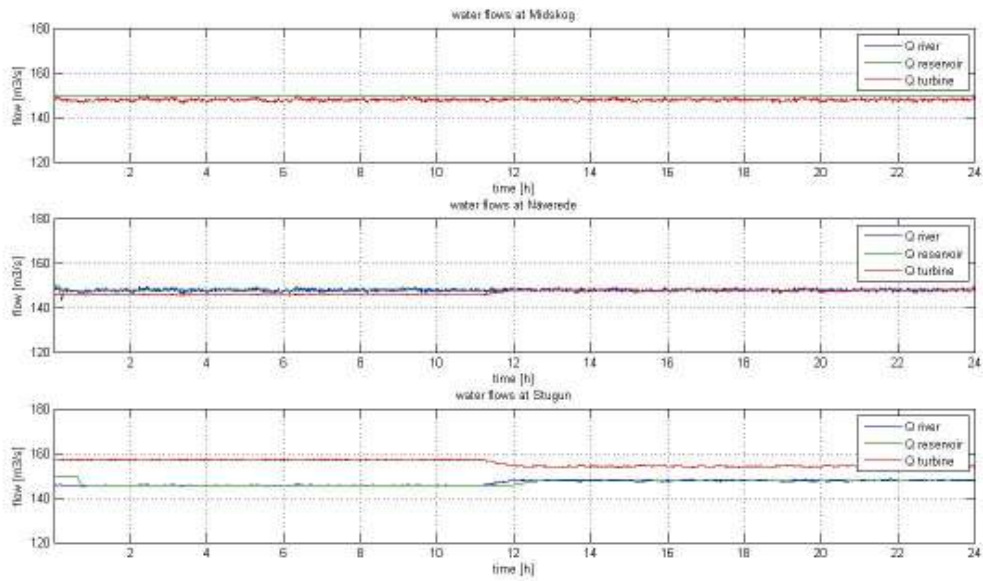


Figure 104: LFC = OFF, 2010-08-02 simulation. Resulting water flows entering the river (for Midskog, the flow entering and exiting the river is the same since this is kept as constant), entering the reservoir and discharge used by the turbine to provide mechanical power.

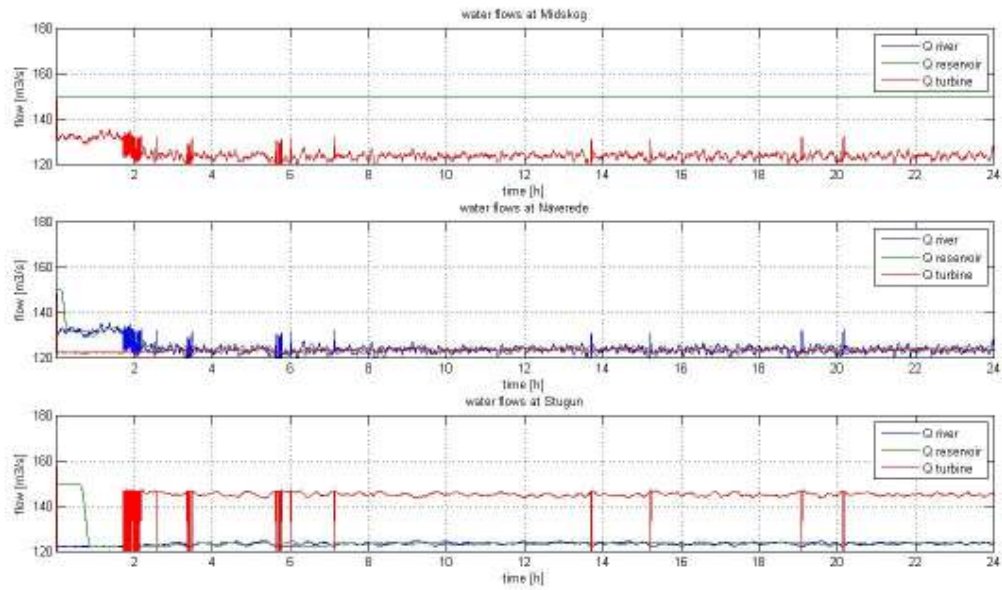


Figure 105: LFC = ON, 2010-08-02 simulation. Resulting water flows entering the river (for Midskog, the flow entering and exiting the river is the same since this is kept as constant), entering the reservoir and discharge used by the turbine to provide mechanical power.

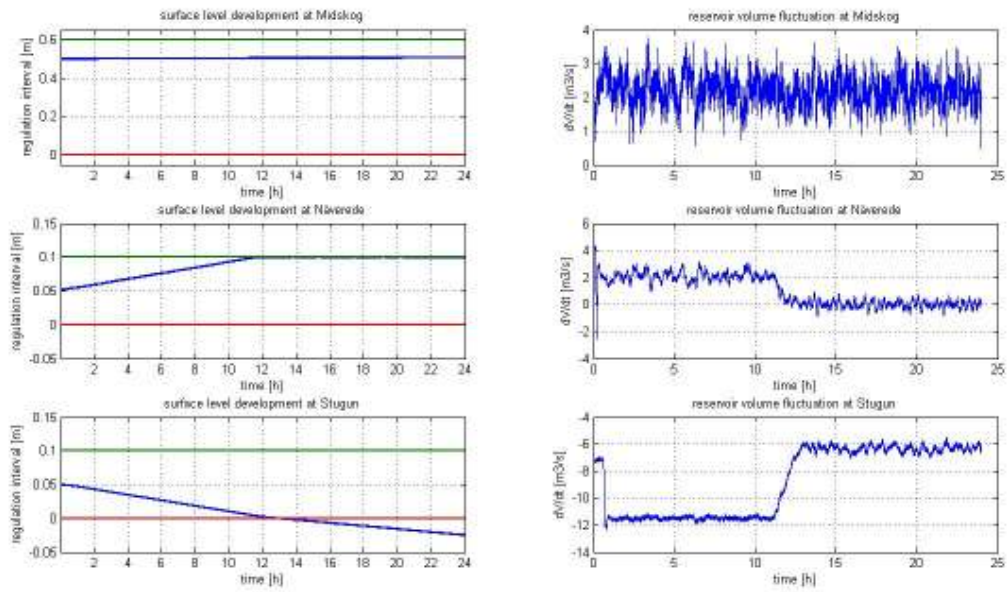


Figure 106: LFC = OFF, 2010-08-02 simulation, Resulting water levels in the reservoirs of Midskog, Näverede and Stugun. The derivative of the reservoir volume fluctuation is also shown.

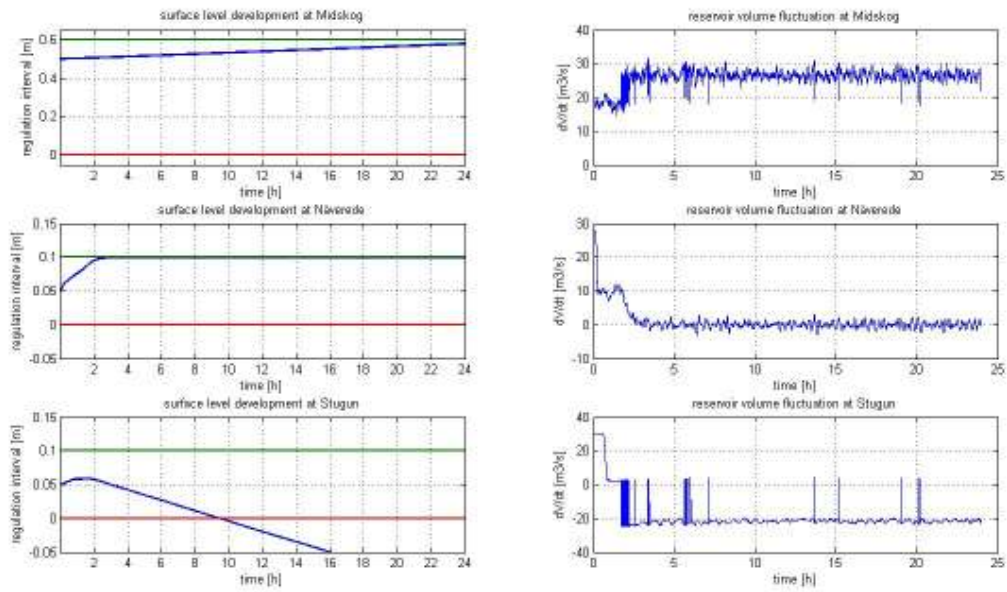


Figure 107: LFC = ON, 2010-08-02 simulation, Resulting water levels in the reservoirs of Midskog, Näverede and Stugun. The derivative of the reservoir volume fluctuation is also shown.

December 6th 2010

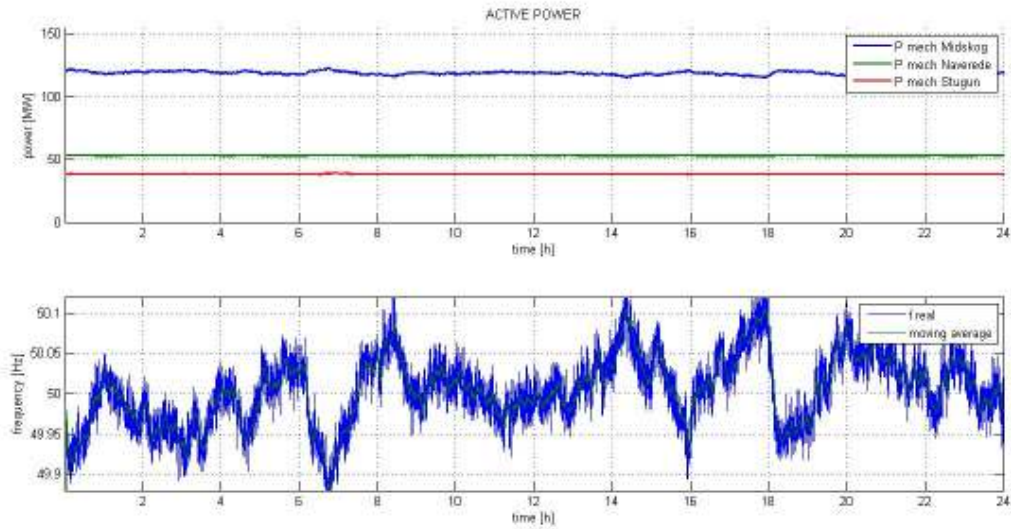


Figure 108: LFC = OFF, 2010-12-06 simulation, Mechanical power delivered by Hissmofors Midskog, Näverede and Stugun displayed with the resulting grid frequency.

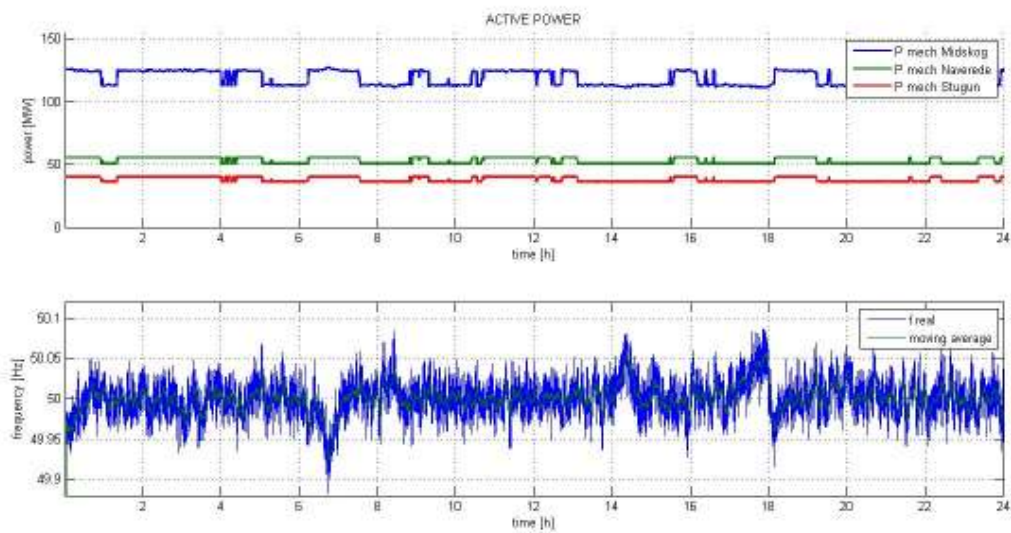


Figure 109: LFC = ON, 2010-12-06 simulation, Mechanical power delivered by Midskog, Näverede and Stugun displayed with the resulting grid frequency.

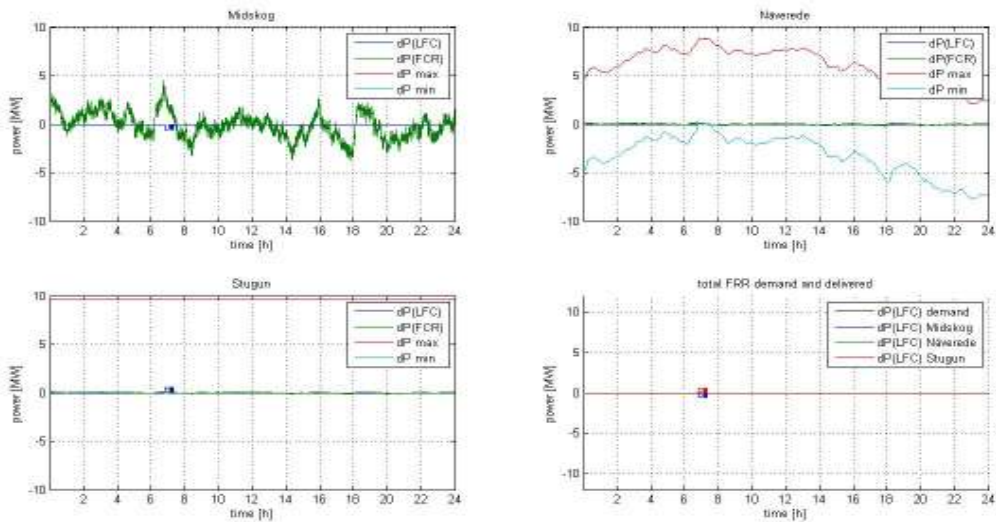


Figure 110: LFC = OFF, 2010-12-06 simulation, Active mechanical power regulation delivered by Midskog, Näverede and Stugun.

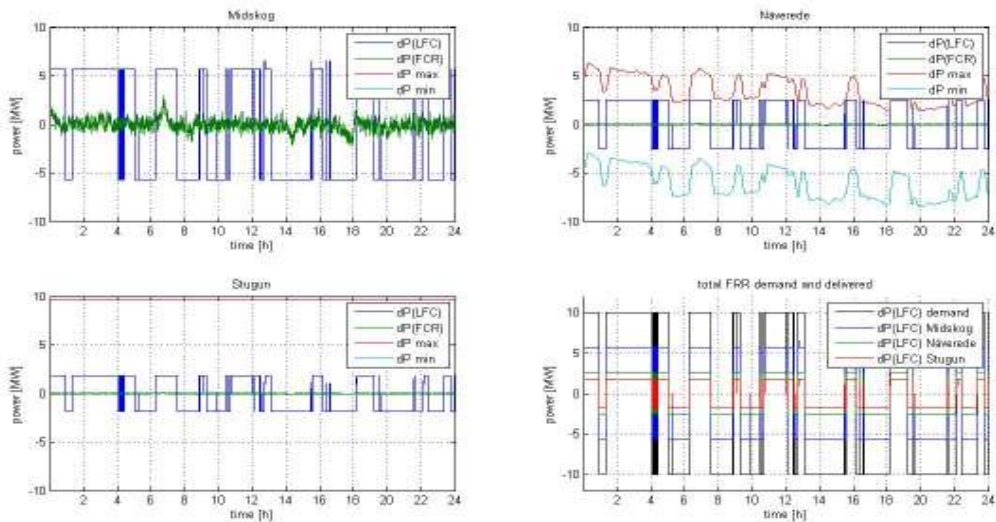


Figure 111: LFC = ON, 2010-12-06 simulation, Active mechanical power regulation delivered by Midskog, Näverede and Stugun. The sum of all LFC regulation is also displayed.

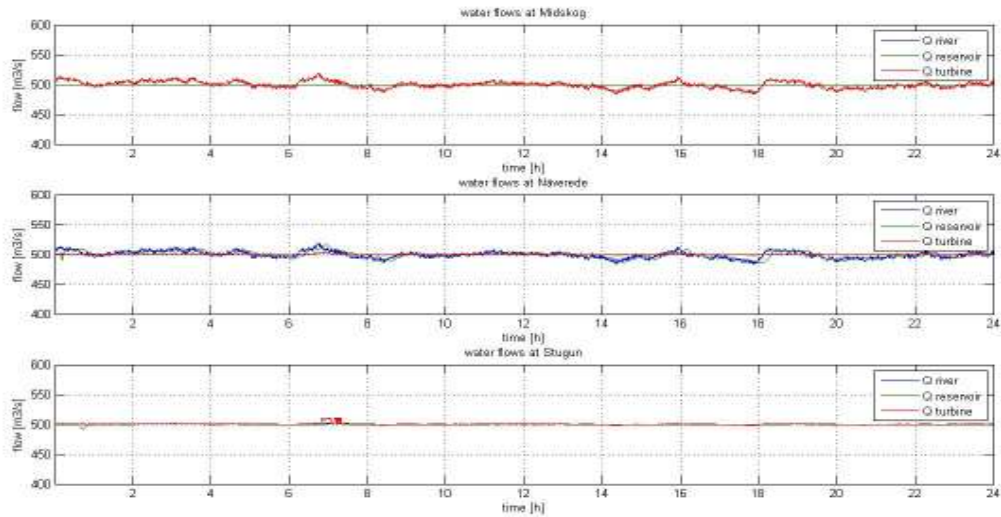


Figure 112: LFC = OFF, 2010-12-06 simulation. Resulting water flows entering the river (for Midskog, the flow entering and exiting the river is the same since this is kept as constant), entering the reservoir and discharge used by the turbine to provide mechanical power.

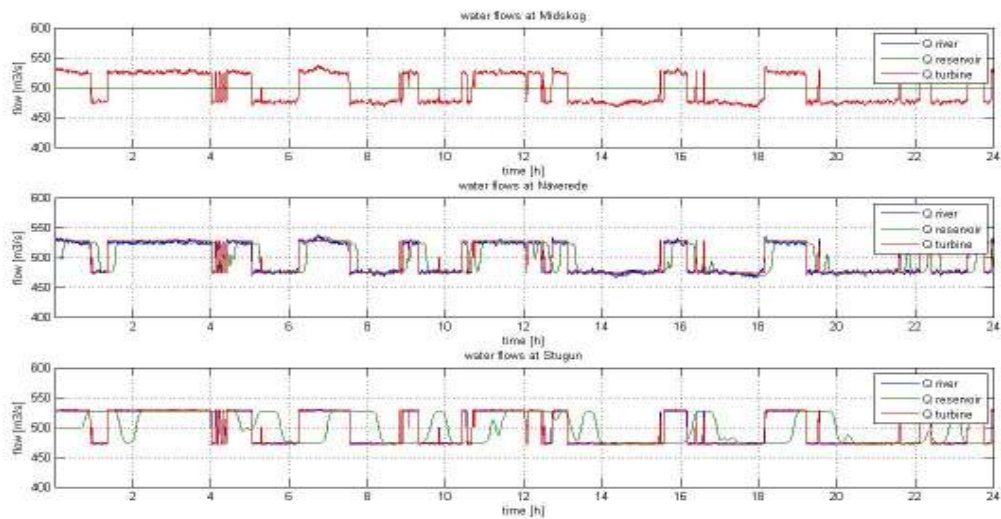


Figure 113: LFC = ON, 2010-12-06 simulation. Resulting water flows entering the river (for Midskog, the flow entering and exiting the river is the same since this is kept as constant), entering the reservoir and discharge used by the turbine to provide mechanical power.

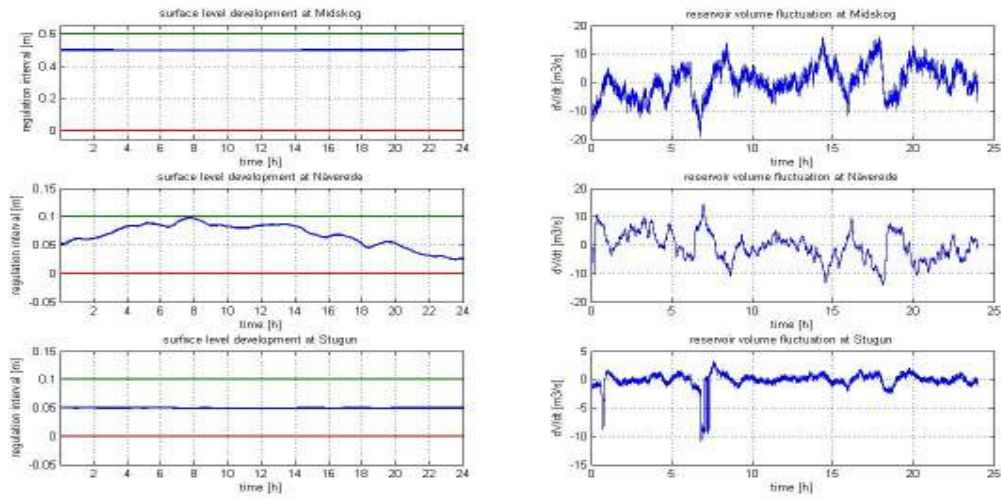


Figure 114: LFC = OFF, 2010-12-06 simulation, Resulting water levels in the reservoirs of Midskog, Näverede and Stugun. The derivative of the reservoir volume fluctuation is also shown.

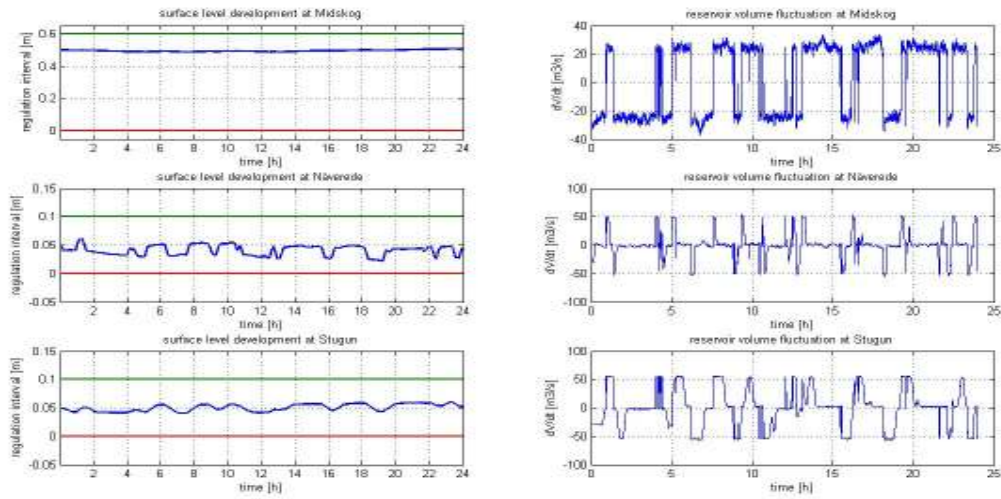


Figure 115: LFC = ON, 2010-12-06 simulation, Resulting water levels in the reservoirs of Midskog, Näverede and Stugun. The derivative of the reservoir volume fluctuation is also shown.

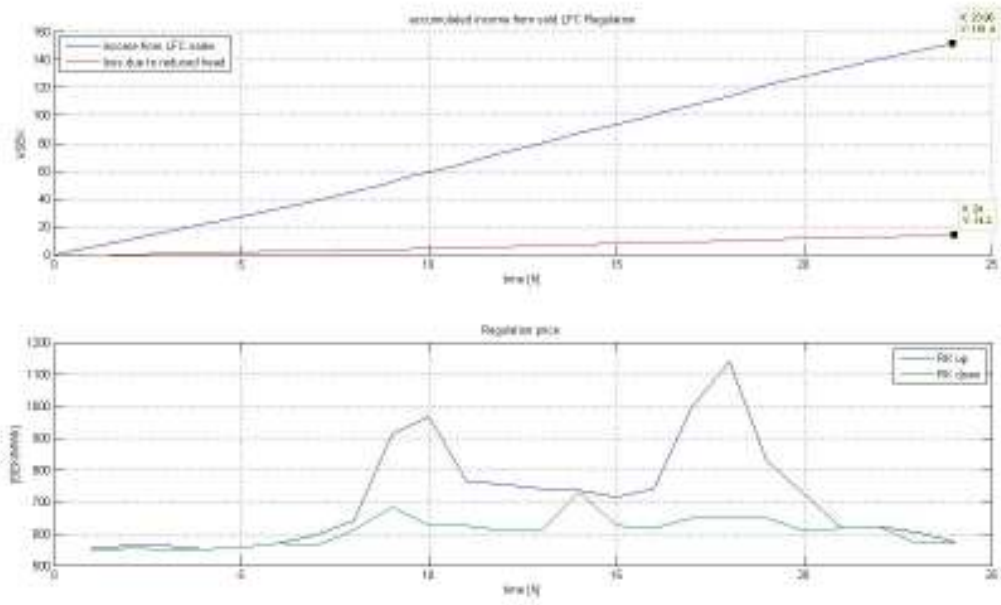


Figure 116: Accumulated income from sales of LFC with losses due to lowered surface levels in combination with the price at hand during the day for sale of regulation.

C.3 Fortum

From Fortum only one simulation was made, the one from 2010-12-06. This was decided after analysing their discharge plans for the respective days where it was found that the individual station discharge plans differ too much from each other se (Figure 117, Figure 118 and Figure 119) in order for this model to be able to create a static discharge plan for each station.

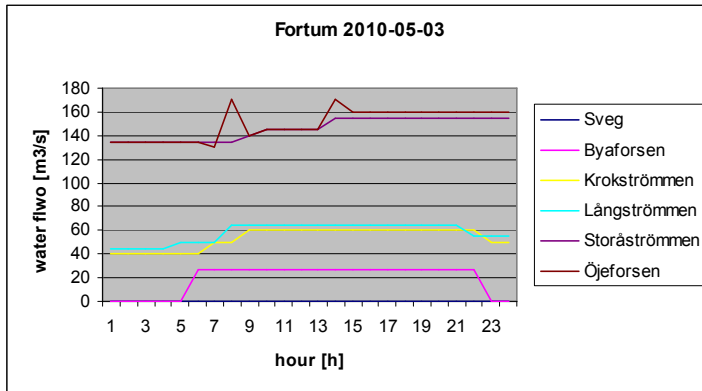


Figure 117: Discharge plan for the Fortum reach on May 3rd 2010.

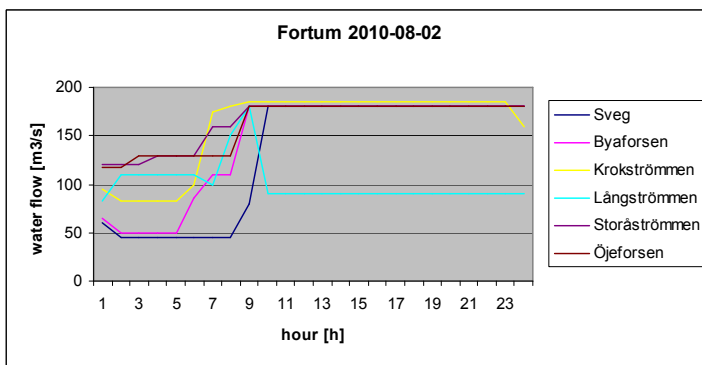


Figure 118: Discharge plan for the Fortum reach on August 2nd 2010

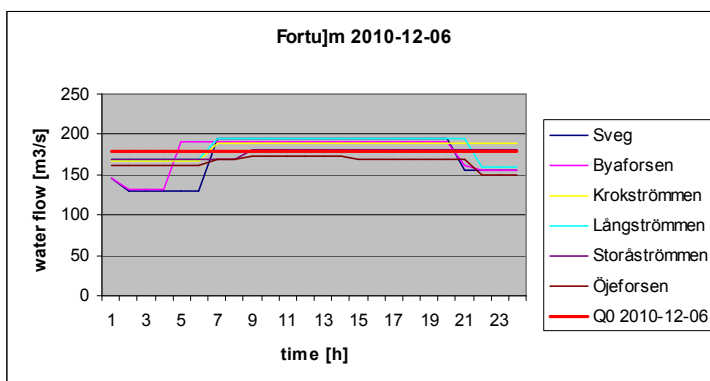


Figure 119: Discharge plan for the Fortum reach on December 6th 2010 including the static discharge plan Q0 used for the simulation

December 6th 2010

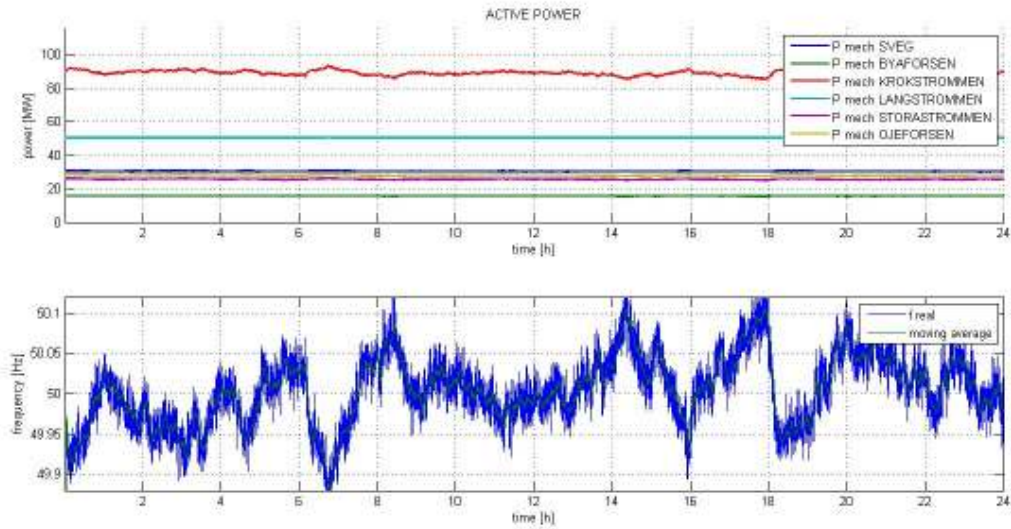


Figure 120: LFC = OFF, 2010-12-06 simulation, Mechanical power delivered by Sveg, Byaforsen, Kattstrupeforsen, Långströmmen, Storåströmmen and Öjeforsen displayed with the resulting grid frequency.

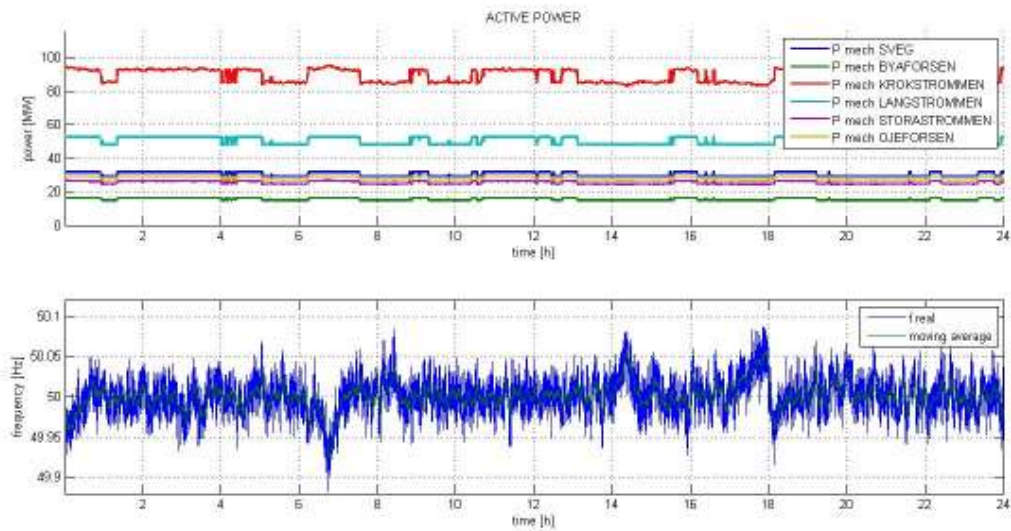


Figure 121: LFC = ON, 2010-12-06 simulation, Mechanical power delivered by Hissmofors Sveg, Byaforsen, Kattstrupeforsen, Långströmmen, Storåströmmen and Öjeforsen displayed with the resulting grid frequency.

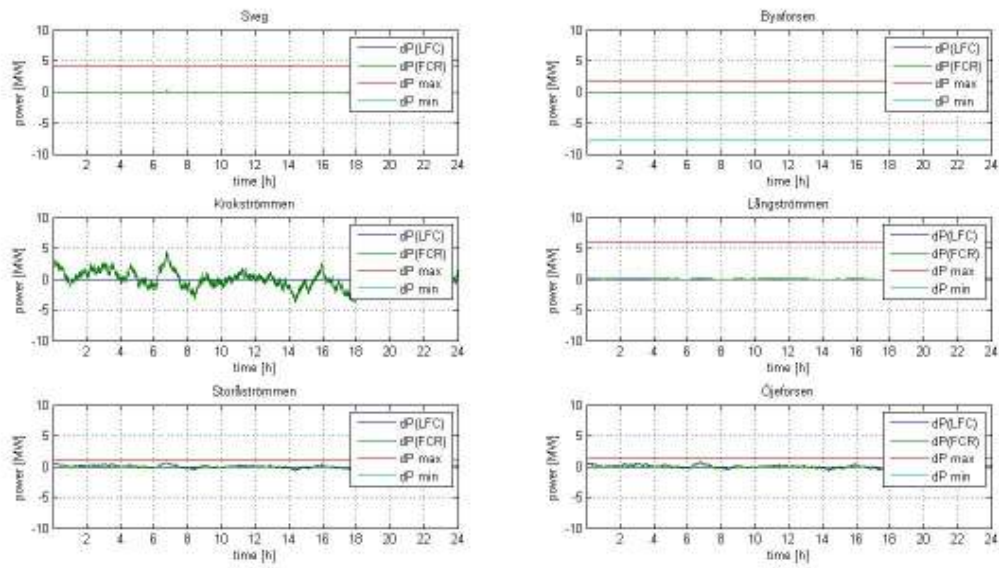


Figure 122: LFC = OFF, 2010-12-06 simulation, Active mechanical power regulation delivered Sveg, Byaforsen, Kattstrupeforsen, Långströmmen, Storåströmmen and Öjeforsen.

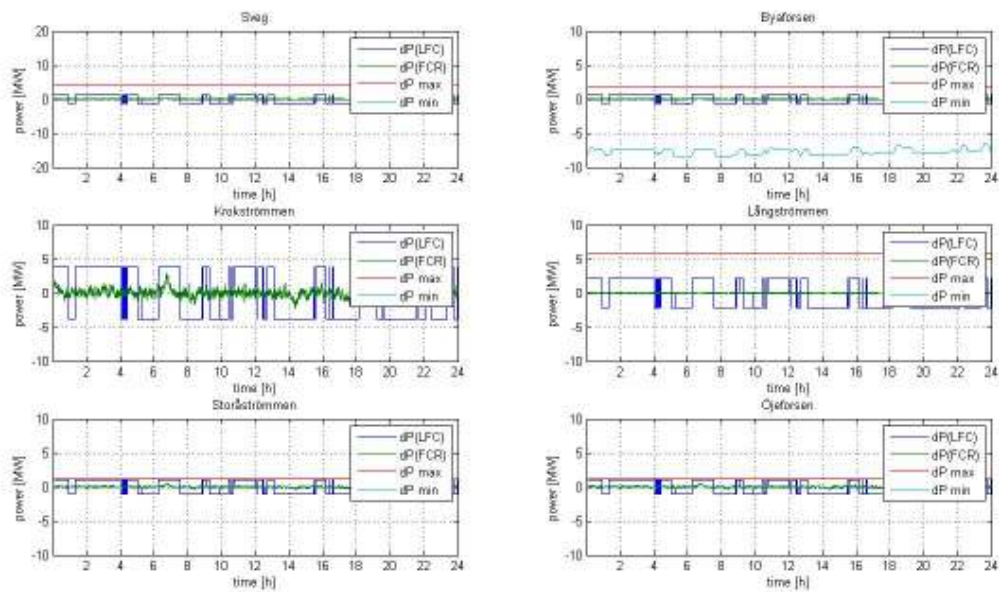


Figure 123: LFC = ON, 2010-12-06 simulation, Active mechanical power regulation delivered by Sveg, Byaforsen, Kattstrupeforsen, Långströmmen, Storåströmmen and Öjeforsen. The sum of all LFC regulation is also displayed.

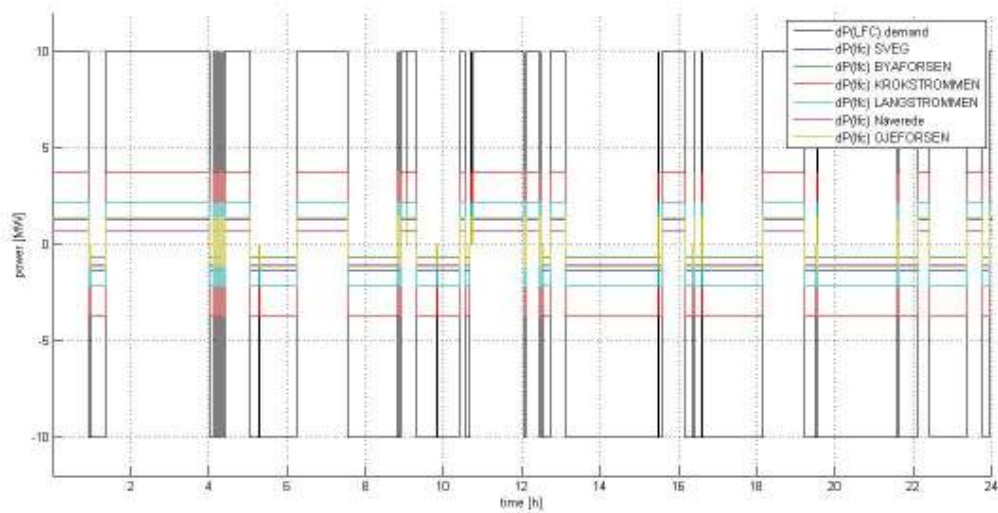


Figure 124: Total LFC regulation provided by the Fortum reach. The graph displays what the individual stations provide by themselves in contrast to what the incoming demand signal is.

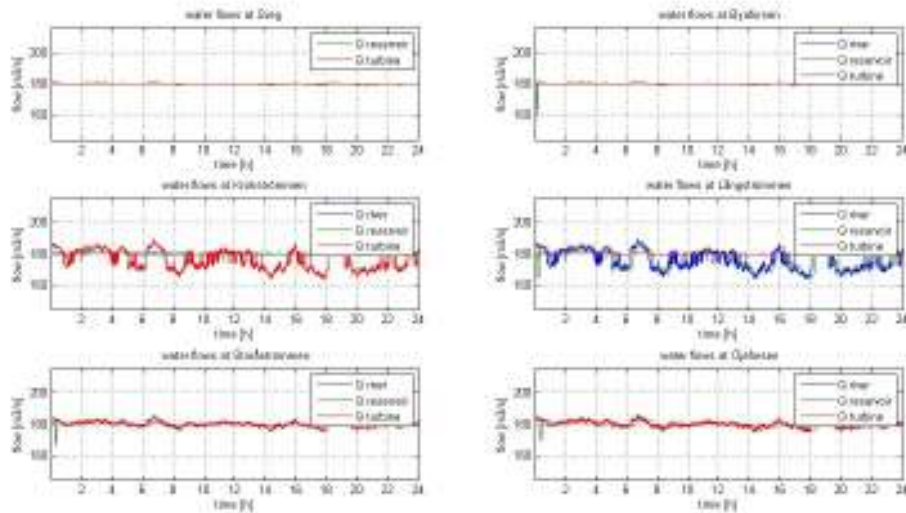


Figure 125: LFC = OFF, 2010-12-06 simulation, Resulting water flows entering the river (except Sveg where the reservoir is taken to be the initial point), entering the reservoir and flow used by the turbine to provide mechanical power.

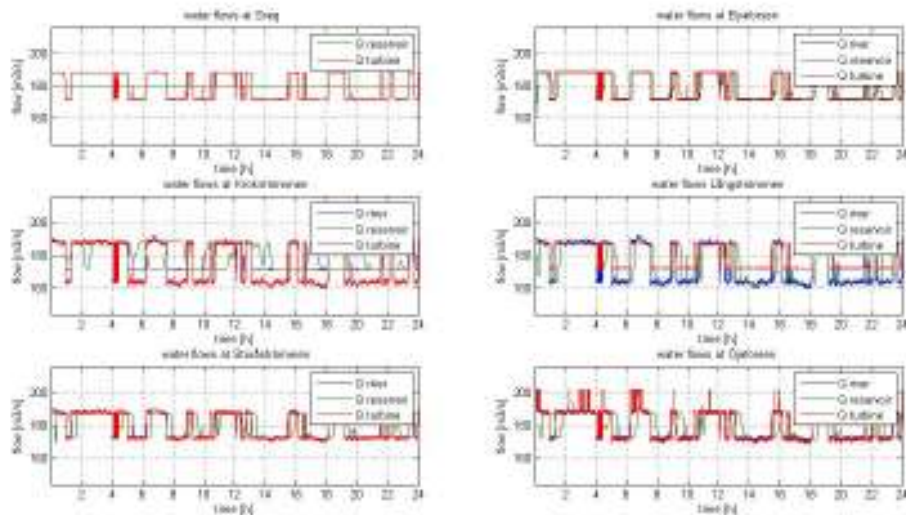


Figure 126: LFC = ON, 2010-12-06 simulation, Resulting water flows entering the river (except Sveg where the reservoir is taken to be the initial geographical point of the simulation), entering the reservoir and flow used by the turbine to provide mechanical power.

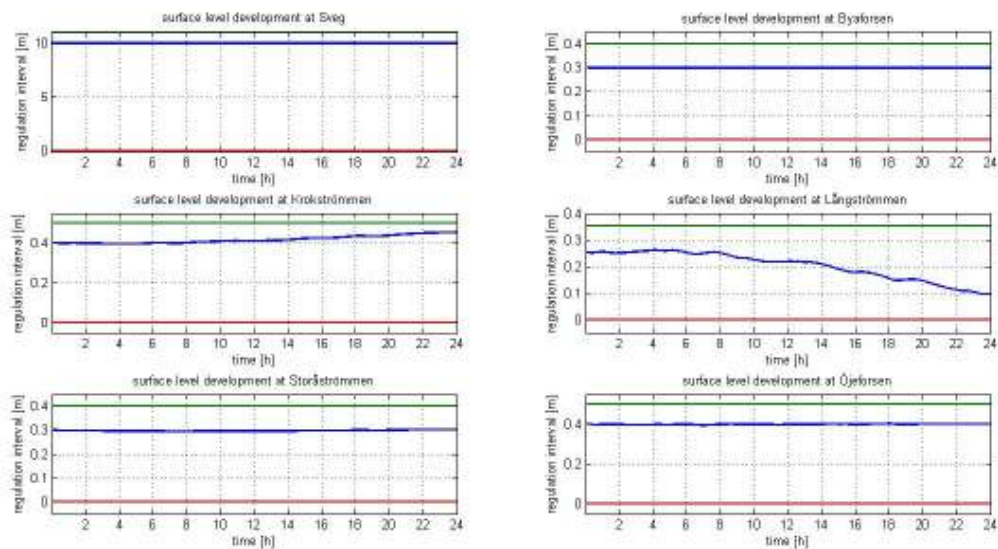


Figure 127: LFC = OFF, 2010-12-06 simulation, Resulting water levels in the reservoirs of Sveg, Byaforsen, Kattstrupeforsen, Långströmmen, Storåströmmen and Öjeforsen. The derivative of the reservoir volume fluctuation is also shown.

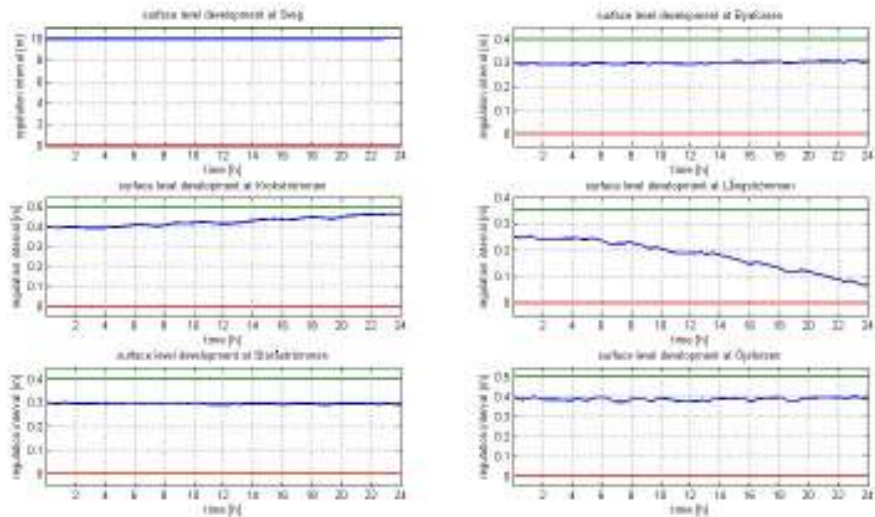


Figure 128: LFC = ON, 2010-12-06 simulation, Resulting water levels in the reservoirs of Sveg, Byaforsen, Kattstrupeforsen, Långströmmen, Storåströmmen and Öjeforsen. The derivative of the reservoir volume fluctuation is also shown.

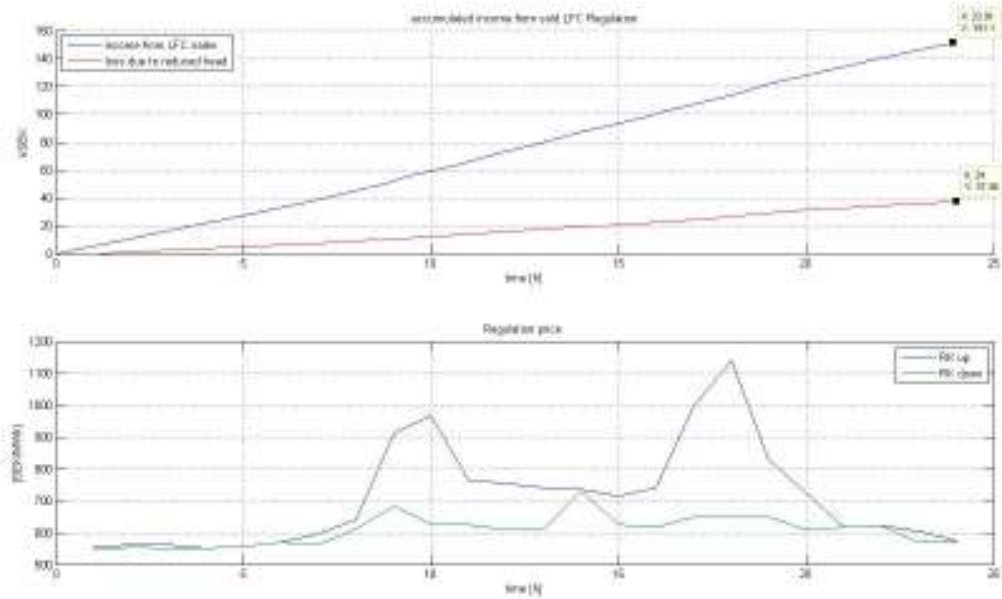


Figure 129: Accumulated income from sales of LFC with losses due to lowered surface levels in combination with the price at hand during the day for sale of regulation.

D – Contacts

The method and results of this thesis would not have been possible without the help from people at Svenska Kraftnät, Statnett, Vattenfall, Fortum and Jämtkraft and I thank them for their help and support. For future development of this model or plainly the development of the LFC system these contacts will now be summed.

Svenska Kraftnät

Christer Bäck; Operational Department – Balance service / ancillary service

Statnett

Eivind Lindeberg; Control systems, IKT-division

Vattenfall

Niklas Dahlbäck; Vattenfall Projects

Katarina Boman; Vattenfall RnD

Jonas Persson; Vattenfall RnD

Reinhard Kaisingern; Vattenfall RnD

Roger Hugosson; Vattenfall Hyrdopower

Joakim Allenmark; Vattenfall Asset Optimization - Nordic

Fortum

Erik Byström; Fortum Generation

Jämtkraft

Magnus Jämting; Elproduktion Drift

Andreas Wiklander; Elproduktion Drift